**Composite Polymeric Delivery for Use as a Single Dose Vaccine**

by

Prachi Pravin Sangle

A dissertation submitted to the Graduate Faculty of
Auburn University
in partial fulfillment of the
requirements for the Degree of
Doctor of Philosophy

Auburn, Alabama
August 4, 2018

Keywords: Polymeric Particles, PLGA, Chitosan, Viral Vectors



Approved by

Allan E David, Chair, Assistant Professor of Chemical Engineering
Maria Auad, Professor of Chemical Engineering
Robert Pantazes, Assistant Professor of Chemical Engineering
Aime Johnson, Associate Professor of Clinical Sciences
M Scot Roberts, Chief Scientific Officer of Altimmune, Inc.

## Abstract

Vaccinology in the 21st century is characterized by refinement of Jenner's principle of protection using less pathogenic organisms with natural or induced reduction of virulence. The approach to the treatment of the new diseases as well as stopping the pandemic from known diseases has generally been reactive, and specific medical interventions have not been available in time to make a substantial impact. Developing better ways to anticipate and modulate the ongoing microbial challenge will be critical for achieving the ability to prevent the spread of diseases. Technical advances in the field of vaccines and understanding the molecular mechanisms of the immune system have provided tools that have made a more proactive approach feasible. There is a necessity for rapid diagnosis, the definition of transmission pathways, availability of antimicrobial agents and predominantly the delivery of these antimicrobial agents to battle the diseases.

Traditional vaccines are effective for disease prevention, but they still face various limitations like the requirement of repeated administration to boost immune response, the potential side effects of inflammation and difficulty in the administration to patients which has motivated the use of nanomedicine for vaccine delivery. Nanomedicine can help achieve the long-lasting controlled burst release of vaccines, the capability of co-encapsulating adjuvants or immune modulators for enhanced immune response and targeting to a group of immune cells. New and powerful vaccine technologies, combined with nanotechnologies, could revolutionize vaccines. Controlled drug delivery for small molecule drugs has advanced tremendously in the past few decades that we no longer depend only on the conventional pharmaceutical formulations. The ease of manufacture and the ability to modify the properties of these controlled drug delivery devices will provide an excellent opportunity to use these novel approaches for the delivery of vaccines.

The primary goal of this work is to develop a controlled pulsed delivery system which can be utilized as a single dose vaccine, which will help avoid the need for the repeated administration to achieve full and sustained protection. Vaccine release from these devices mainly depends on the way it is incorporated within the delivery device, i.e., encapsulated/entrapped into or merely adsorbed /associated onto the device and the choice of the delivery device (liposomes, polymeric delivery). Biodegradable polymeric nanoparticles are preferred devices for controlled release because of ease of manufacturing, high encapsulation efficiencies, tunable properties, and long-term stability. The advantage of nanoparticle formulations against conventional systems is that they might increase the efficacy of treatment as well as reduce side effects due to their specific targeting action.

There have been a variety of biodegradable delivery devices that are being studied currently including biodegradable polymers such as poly-(D, L-lactic-co-glycolic) acid (PLGA) and polysaccharides such as alginate and chitosan. PLGA has emerged as a promising candidate and is FDA approved for use in sutures in humans for controlled drug delivery. A composite polymeric delivery approach with PLGA and chitosan is used in this work to achieve a pulsed delivery system.

In the present work, adenoviral vectors are used as model vaccines which are encapsulated inside biodegradable and biocompatible composite polymeric delivery device produced with PLGA and chitosan. These composite particles are produced using a modified double emulsion solvent evaporation process. Varying process conditions achieve modulation of size and surface properties of these particles. It is possible to modulate the size of the particles in a range of 300nm to 4.5 μm along with changing the distribution of chitosan in the particle. It is demonstrated that adenoviral vector (Ad-eGFP) retained its activity after the encapsulation process. The particles demonstrated a controlled delivery of Ad-eGFP, and it is possible to vary the release kinetics by varying various process parameters. Furthermore, Ad-flu is encapsulated in these composite particles and in vitro and in vivo release behavior is observed. In vivo immune response in mice is checked using the HAI assay. Mechanism of release kinetics is explained using some of the established models. It is observed that the release of the viral vectors from these composites

follows Non-Fickian diffusion kinetics. The composite polymeric delivery device developed using PLGA and chitosan shows a promising controlled delivery device for vaccine delivery; they could be further explored by tailoring their properties to achieve a pulsed delivery system. These composite particles can be used as potential candidates to encapsulate various macromolecules like proteins, peptides, and cancer vaccines for the future generation of controlled delivery devices.

Acknowledgments

First, I would first like to thank my advisor Dr. Allan E. David for his motivation and mentorship throughout my Ph.D. project and in the preparation of this dissertation. Without his encouragement and guidance, this dissertation would not have been possible. I would like to acknowledge my committee members Dr. M Scot Roberts, Dr. Aime Johnson, Dr. Maria Auad and Dr. Robert Pantazes for their willingness to serve on my committee. I would also like to thank Dr. Dean Schwartz for undertaking the role of the university reader for my dissertation.

I would like to thank Dr. Henry Baker for his insightful comments and support during my entire research. I would like to thank Dr. Dean Schwartz and Cristine Robinson for their immense help and letting me use the RT-qPCR. I would like to thank Dr. Michael Miller for his help with the scanning electron microscope, Dr. Sushil Adhikari and Avanti Kulkarni for the help with thermogravimetric analysis. My sincere thanks to Jianfeng Zhang and Altimmune, Inc. for their expertise with the HAI assay utilized in this study.

I would like to thank current and past members of the David Lab that include: Dr. Young Suk Choi, Dr. Alexander Kelly, Dr. Xin Fan, Dr. Barry Yeh, Dr. Tareq Anani, Camille Hanot, Richard Cullum, Alan Hanley, Chelsea Harris, Marjan Azadi, Ricky Whitener, Nayer Sultana and Braden Hahn. I would also like to thank David Hall, undergraduate I had a chance to work with and for the opportunity to mentor. I would also like to acknowledge the help from Dr. Mario Eden, Karen Cochran, Naomi Gehling and Elaine Manning from Chemical Engineering department for the help in various matters.

Finally, this work would not have been possible without the continued support from my mother, Anita Sangle who has been a constant source of inspiration and encouragement throughout my endeavors. I would like to thank Pravin Sangle and Pratik Sangle who have always supported me. I would like to express my immense gratitude to Raj Thakur for being an invaluable support system. Finally, I would also like to thank Vinit Singh, Micah Bowden, Aditya Agarwal, Mikhail Zade, Gayatri Nayak, Shubham Garg, Amey Rane, Ajit Chavan, Niranjana Nayak, and countless others who made my time at Auburn memorable.

Table of Contents

List of Tables

List of Figures

List of Abbreviations

| | |
|---|---|
| DD | Degree of deacetylation |
| FFU | Fluorescent focus unit |
| FITC | Fluorescein-isothiocyanate |
| HEK | Human embryonic kidney cells |
| HPMA | Hydroxyl-poly-methyl-acrylate |
| NPs | Nanoparticles |
| PLA | Poly-lactic acid |
| PLGA | Poly-lactic-*co*-glycolic-acid |
| PMA | Poly-methyl-acrylate |
| $T_g$ | Glass transition temperature |
| DCM | Dichloromethane |
| AA | Acetic Acid |
| ACN | Acetonitrile |
| LC | Loading Capacity |
| Ad-flu | Adenoviral vector for influenza |
| Ad-eGFP | GFP-expressing adenoviral vector |

| | |
|---|---|
| APC | Antigen presenting cells |
| DC | Dendritic cells |
| HEK | Human Embryonic Kidney Cells |
| HAI | Hemagglutination Inhibition |
| RBC | Red Blood Cells |
| RDE | Receptor Destroying Enzyme I |

# Chapter 1: Introduction

## 1.1 Introduction to Nanomedicine

Nanomedicine is usually defined as technology that uses molecular tools and knowledge of the human body for medical diagnosis and treatments or it can also be described as the use of nanoscale or nanostructured materials in medicine that according to their structure have unique medical effects, like the ability to cross biological barriers or the passive targeting of tissues[1]. Nanomedicine encompasses the vast field of nanotechnology and its applications in healthcare therapeutics as well as diagnostics. Nanotechnology started developing after the 1959 annual meeting of American Physical Society, where Richard Feynman provided a dream where he developed the vision of modulating things on a small scale[2]. New opportunities, in the field of nanotechnology, have been realized in virtually all branches of technology like medicine, optical systems, electronic, chemical, automotive industries, and environmental engineering. "Smart" surface coatings, original nanoscale materials, faster electronics, unprecedented optics, biosensors, and nanomotors are just a few examples from this transdisciplinary area. Since the 1950s, in the field of medicine, the first generation of nanoparticles[3,4] used were primarily based on liposomes, and polymer-drug conjugates and the first FDA approved nanoparticle-based therapeutic was in 1989[5]. Several therapeutics based on nanomedicine have been successfully introduced for the treatment of cancer, pain and infectious diseases[5]. Since then there has been tremendous research in this field which has revolutionized the field of drug delivery.

The advantage of nanoparticle formulations as opposed to conventional systems is that they could increase the efficacy of treatment as well as reduce side effects due to their specific targeting action[5,6]. This targeting action of the nanoparticles depends on the physical and chemical characteristics of nanoparticles. Small molecule drug delivery has advanced tremendously in the past few decades that we no longer depend only on the conventional pharmaceutical formulation to treat diseases like diabetes, cancer, infectious diseases[7–16], with the recent focus shifting towards macromolecular therapeutics like peptides[17,18], proteins[19,20], enzymes, monoclonal antibodies[21–23], and viral vectors[4,17]. Depending on the application

envisioned to target, there are many drug delivery devices available that are used for nanomedicine research, like solid particles[1] (silica, gold, iron oxide), polymeric particles[27] (polyesters, polycaprolactones, polyamides, chitosan, alginate), liposomal delivery[28], and dendrimers[27].

## 1.2 Introduction to Vaccines

Vaccines are one of medicine's most significant accomplishments. They have saved more lives and prevented more human and animal suffering than any other single medical intervention. A vaccine can be described as a biological agent that delivers active developed immunity to a particular disease. It stimulates the body's immune system to recognize it as peril, destroy it, and retain a record of it, and any such successive related infection can be more definitely known by the immune system and destroyed[29]. Vaccines work by mimicking disease agents and stimulating the immune system to build up defenses against them. They are administered as an initial dose which is then usually followed by a booster dose. Over the period of time, the body's memory to fight against the disease decreases and the booster dose re-exposes the body to the immunizing antigen increasing the immunity against the disease[30,31].

Vaccines protect a projected 8 million lives yearly and are broadly acknowledged to be the most effective medical treatment for preventing various diseases[16]. Diseases such as measles, mumps, rubella, diphtheria, tetanus, pertussis, *Haemophilus influenzae* type b (Hib) disease, polio, and yellow fever are now under control due to vaccination[29]. Smallpox has been eradicated[29,32] and polio is on the brink of elimination[33], due to aggressive vaccination campaigns. Other diseases, including hepatitis B virus (HBV), foot and mouth disease in cattle and pneumococcal infection are better confined due to vaccines, but there is still much that needs to be done to eradicate such diseases, even in the developed world[29]. While the World Health Organization's (WHO) Expanded Program on Immunization (EPI) has been immensely successful in raising global vaccination rates from just 5% in 1974 to 84% today, one in six infants stay under-immunized each year ensuing 1.5 million deaths[16]. Vaccinating animals routinely is often more affordable than paying for the treatment of sick animals, and it reduces transmission of microorganisms in the animal population reducing animal suffering.

### 1.3 Delivery of Vaccines

Major entities in global health such as the World Health Organization (WHO) and the Center for Disease Control and Prevention (CDC) have claimed the need to invest research efforts in developing advanced delivery technologies, which might streamline immunization schedules[34]. Current vaccination schedules involve multiple visits to a healthcare provider; this epitomizes a significant logistical barrier to immunization — especially in the developing world. The multi-bolus regimens of vaccine administration are unfeasible in case of animals as well as human beings. A single dose composition to eliminate the need for reimmunization will help transform traditional vaccines to achieve full and sustained protection. If a single-dose vaccination method is established for presently available vaccines with no other changes to patient access or infrastructure, it could save hundreds of thousands of lives annually[16]. Despite considerable work towards developing single-dose vaccines, this method has yet to be efficaciously commercialized. Most research in this field has focused on developing injectable devices that release antigen over the course of months. Single dose vaccines provide tremendous opportunities for improving healthcare while concurrently reducing cost. This approach is exciting because it reduces risk factors like failure to vaccinate and allergic reactions. While the advent of specialized single-use syringes, the occurrence of unsafe practices have lowered, single-injection vaccines could further reduce transmission by minimizing the number of both injections and syringes required. From a patient's perspective, single dose vaccines would help reduce pain and improve convenience as fewer injections and healthcare visits are needed.

Moreover, state of the art delivery devices are being developed for drug delivery whereas delivery of vaccines have lagged behind these essential new technological advances as we still depend on traditional dosage systems since the 1900s in humans as well as animals[16,30,35]. With the ability to control size, shape, composition and surface properties, nanotechnology offers tremendous potential in the biomedical field. In recent years, billions of dollars have been invested in the global market of nanoparticles in life sciences, especially in the area of drug delivery system, which accounts for 76% of nanotechnology research

publications in 2014[36]. Rational approaches to vaccine design based on the thorough understanding of the molecular mechanisms of the immune system could eventually allow one to induce a specific adaptive immune response and the preferred effector mechanism without additional damage to the host tissues[37]. Spectacular advances in immunology and the advent of molecular medicine will give us remarkable opportunities to develop delivery systems that can help us gain full potential of vaccines.

The idea of using controlled release delivery devices to deliver drugs/vaccines efficaciously is first proposed by Preis and Langer[38]. After a few decades of work in this field it has become clear that antigen release mainly depends on the way it is incorporated within the delivery carrier, i.e., encapsulated/entrapped into or simply adsorbed/associated onto the polymer and the choice of the delivery device (liposomes, polymeric delivery). Biodegradable polymeric nanoparticles are preferred devices for controlled release because of ease of manufacture, high encapsulation efficiencies, tunable properties, long-term stability[16,39,40]. Such nanoparticles deliver controlled/sustained release property, subcellular size and biocompatibility with tissue and cells[6]. Therapeutic devices such as temporary prostheses, three-dimensional porous structures as scaffolds for tissue engineering and as controlled/sustained release drug delivery devices are usually developed using biodegradable polymers. Each of these applications demands materials with specific physical, chemical, biological, and biomechanical properties to deliver effective therapy. These formulations might also protect the encapsulated vaccine from degradation inside the body and maintain its therapeutic activity[5,6].

### 1.4 Summary of Chapters

Chapter 2 explains the overall background and motivation for the development of the composite particle starting with an introduction to vaccine immunology, benefits of nanomedicine for vaccine delivery, use of composite polymeric delivery followed by materials chosen for this particular application and the mechanism of release for the encapsulated vaccine. Chapter 3 explains the experimental development of the composite particles, modulating the size, and inherent composition followed by their affects the *in vitro* release of the adenoviral vector encapsulated. Chapter 4 elucidates on the preservation

of the activity of the adenovirus encapsulated. The encapsulation and *in vitro* release of the adenoviral-based vaccine for influenza from the composite particles are analyzed along with *in vivo* studies conducted with CD1 mice to validate the antibody response in Chapter 5. Mechanism of release of the encapsulated vaccine is compared to existing theoretical models to substantiate the process of how the particles degrade and the vaccine is released *in vitro* to modulate the release in future is summarized in Chapter 6. Finally, Chapter 7 gives an idea on some of the future avenues that can be explored to optimize the release kinetics followed by Chapter 8, which is the summary of the entire project.

# Chapter 2: Background

## 2.1 Vaccine Immunology

The immune system is a host defense system comprising of many biological assemblies and processes in an organism that shields against various diseases. The immune system in vertebrates consists of two parts: the innate immune system and the adaptive immune system (**Figure 2-1**). An immune system detects a wide variety of organisms like pathogens, viruses, parasitic worms, separating them from the organism's own healthy tissue. Long-term immunity is conferred by the maintenance of antigen-specific immune effectors and/or by the immune memory cells, that may be efficient and rapidly reactivated into immune effectors in case of pathogen exposure[35]. Long-term protection entails generation of vaccine antibodies and immune memory cells capable of efficient reactivation upon consequent microbial exposure. The determinants of immune memory induction, as well as the relative contribution of persisting antibodies and of immune memory to protect against specific diseases, are thus essential parameters of long-term vaccine efficacy[35].

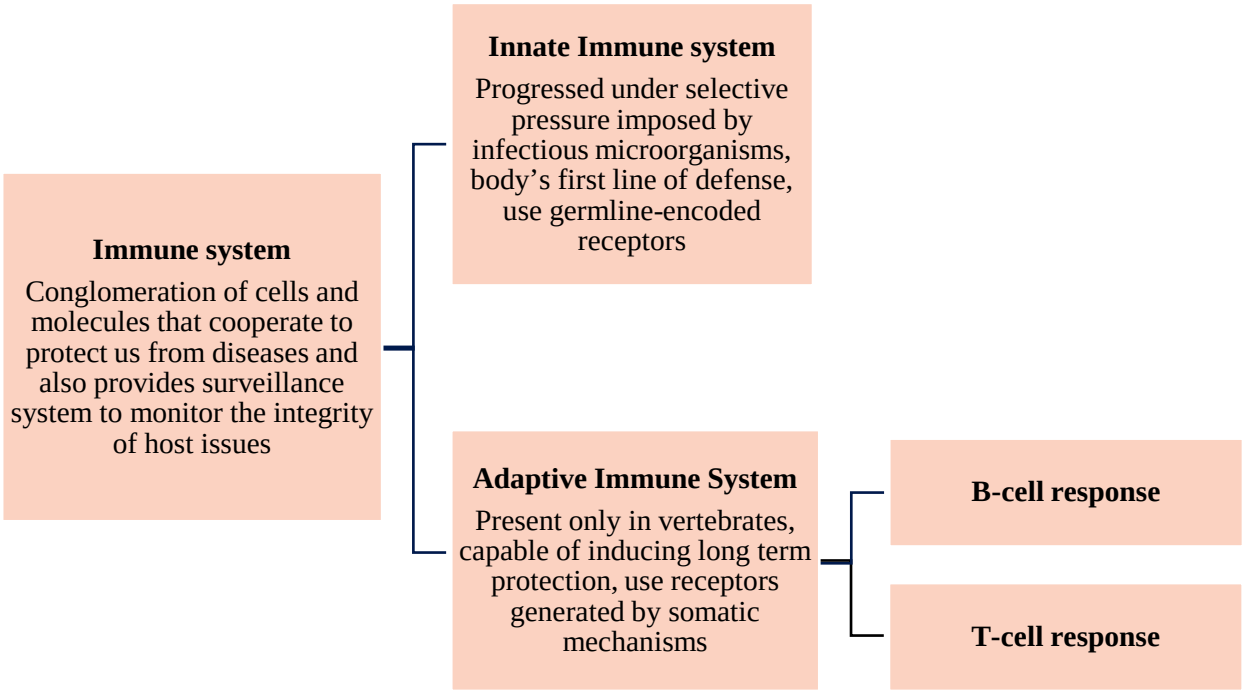


**Figure 2-1:** Brief description of Immune System

### 2.1.1 Innate Immune system

Innate immune responses have been found in both vertebrates and invertebrates. These cells respond to pathogens non-specifically and do not provide long-lasting immunity when compared to the adaptive immune system, as they do not have memory. Innate immune responses depend on a group of proteins and phagocytic cells found in all microorganisms, and it is quickly activated to help destroy invaders[30]. The innate immune system consists of anatomical barriers like skin, GI tract, mucous membranes which prevent the entry of many foreign organisms. There are also physiological barriers like interferon, mucus, surfactant proteins, tears which contain lysozyme. Inflammation is the body's next response if there is tissue damage or microbial invasion[30,37].

Cells of the innate immune system exhibit pattern recognition receptors (PRRs) to identify two classes of molecules: pathogen-associated molecular patterns (PAMPs), which are associated with microbial pathogens, and damage-associated molecular patterns (DAMPs), associated with cell components released during cell damage or death[37]. This strategy allows a limited number of germline-encoded receptors to recognize a great variety of molecular structures associated with pathogens. Functionally, PRRs are divided into three types: humoral proteins circulating in the plasma, endocytic receptors expressed on the cell surface, and signaling receptors expressed either on the cell surface or intracellularly[37]. The innate immune system consists of cells like mast cells, phagocytes, neutrophils, macrophages, basophils, eosinophils, natural killer cells, and dendritic cells. The main function of the innate immune system is to contain the pathogen until adaptive immunity can be induced. If the innate immune response is not able to eradicate the pathogen, it stimulates the adaptive immune system to engage in the additional immune response. Dendritic cells play a vital role as a link between the innate and adaptive systems[41].

### 2.1.2 Adaptive Immune System

Control and elimination of diseases require the generation of protective immunity in an ample amount of the population best achieved by immunization programs capable of inducing long-term protection[35]. This is a trademark of adaptive immunity that contrasts the sharp but short-lasting innate immune responses. The adaptive immune system is made of systemic cells and processes that eliminate pathogens or prevents their growth. It is highly specific to a particular pathogen which makes it slower than the innate immune response[30]. The adaptive immune response is mainly carried out by white blood cells called the lymphocytes. Lymphocytes consist of 3 types of cells mainly: B-cells, T-cells and Natural Killer (NK) cells. The responses by the B-cells and T-cells start simultaneously when an adaptive immune response is elicited by any antigen.

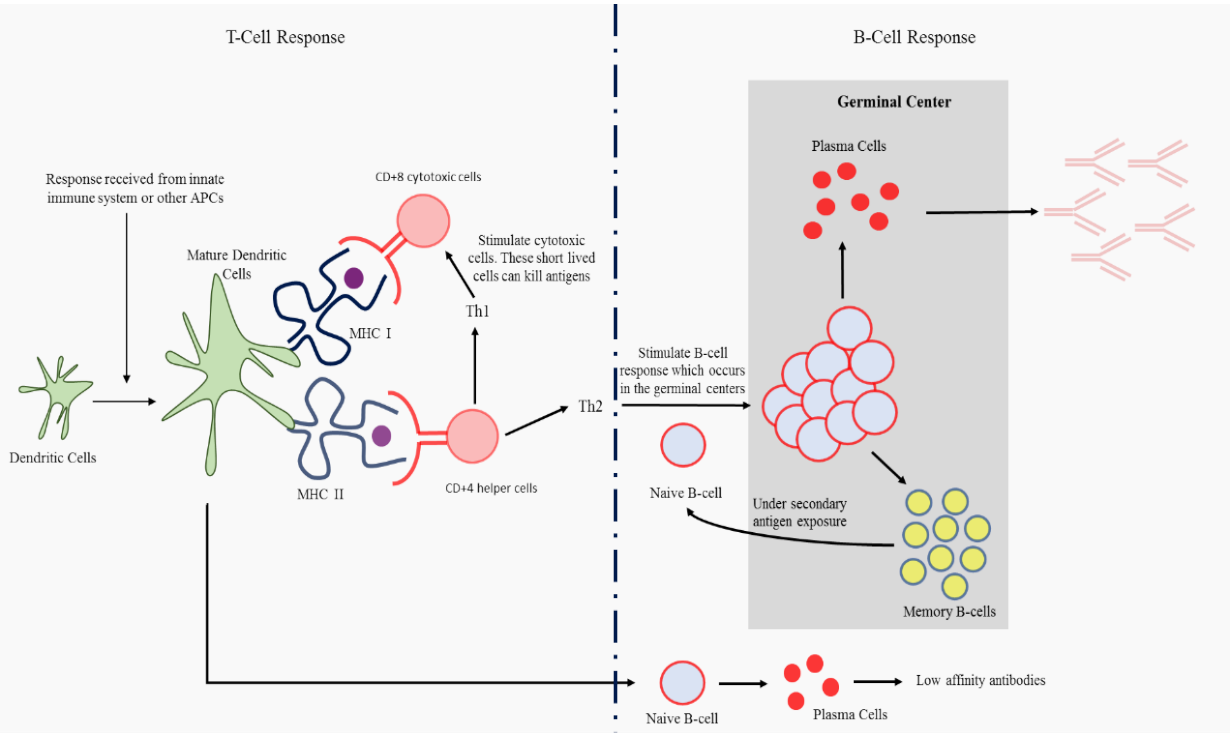


**Figure 2-2:** Illustration of Adaptive Immune System

When the innate immune response cannot process an antigen, the dendritic cells (DCs) (a type of antigen presenting cells (APCs)) are stimulated for further response. DCs take up vaccine antigens, and these start migrating to drain the lymph nodes. During this migration, DCs mature and break the antigen

into small fragments which are displayed on the surface of the cells in the groves of major histocompatibility complex (MHC) molecules. The major histocompatibility complex (MHC) is a set of cell surface proteins essential for the adaptive immune system to identify alien molecules. The key function of MHC molecules is to attach to antigens derived from pathogens subsequently displaying them on the cell surface for recognition by the appropriate T-cells[42]. The MHC molecules are divided into two types as MHC I (peptide presentation from antigens produced within infected cells) and MHC II (present phagocytosed antigens). The T-cells identify these proteins displayed on the surface of the DCs. MHC I stimulates the cytotoxic T-cells, and MHC II stimulates the helper T-cells[41]. The T-cells bound to the MHC II peptides further differentiate into Th1 and Th2. Th1 stimulates the cytotoxic cells, and Th2 further activates the B-cells. This differentiation depends on various determinants like a dose of antigen (lower vaccine doses being classically associated with preferential Th1 responses), route of administration, and type of DC activation by the innate system[35]. Consequently, T-cell responses are highly variable within a population. These T-cell epitopes may be generated from any area of the vaccine antigens, irrespective of the peptide sequence located within or at the surface of the proteins[30].

B-cell recognition is opposite to this process, which remains essentially limited to conformational determinants constituted by amino acids at the antigen surface[35]. Antigen-specific B-cells that are activated proliferate in specialized structures called germinal centers (GCs) and undergo somatic hyper mutation[16,35]. These matured B-cells, in a stochastic process, further differentiate into plasma cells (short-lived) which secrete large amounts of antigen-specific antibodies and memory B-cells which migrate towards the bone marrow where they may produce vaccine antigens during extended periods. These memory B-cells do not protect by producing antibodies but upon re-exposure to the antigen differentiate into plasma cells producing higher affinity antibodies than the primary plasma cells produced during the initial response. Re-exposure, the so-called “boost” doses, is required to re-challenge the immune system and form stronger immunological memory against the same antigen. These doses are most effective when administered after circulating antibody titers have decreased to minimize binding competition between B cells and antibodies

that would hinder the formation of immune memory[30]. As a result, most vaccines are administered as a primary-booster dose to generate long term immunity.

### 2.1.3 Advances in Different Types of Vaccines

A vaccine typically consists of a disease-causative microorganism which is often prepared from killed or inactivated forms of the microbe, its toxins (referred to as toxoids) or one of its surface proteins[40]. Most of the vaccines used today are of the type of whole inactivated, live attenuated, subunit vaccines as shown in **Figure 2-3**[43]. A vaccine containing virus particles, bacteria, or pathogens grown in culture and then killed using heat or chemical treatment of formaldehyde are called whole inactivated vaccines. Subunit

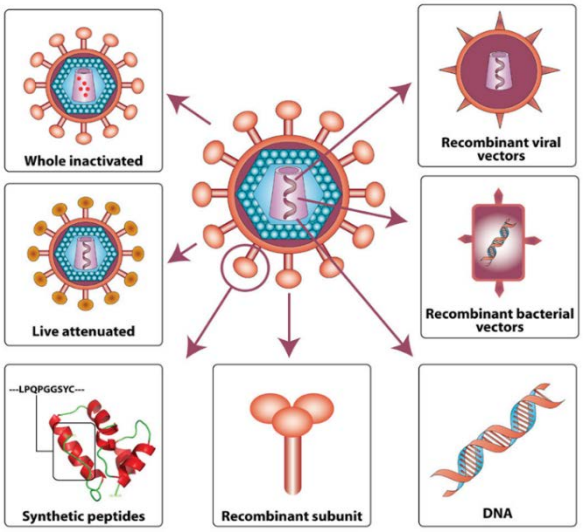


**Figure 2-3:** Examples of different types of vaccines[43]

vaccines are manufactured by purifying out the antigens that stimulate the immune system to mount a response to the virus while eliminating other components necessary for the virus to replicate or survive or that can cause adverse reactions. Both of these vaccines generate a weak immune response as compared to live attenuated vaccines. Due to this, these vaccines require multiple booster injections as well as adjuvants to produce required immunity. An adjuvant is by definition any molecule or macromolecule structure or system capable of augmenting an immune response against specific antigen[44]. Live attenuated vaccines prompt a strong T-cell response, have a higher strength of innate responses as compared to other vaccines available and can produce both humoral and cellular immunity[34,35,40]. The major drawback with these live

vaccines is the danger of reverting back to their virulent form, intrinsic instability, cannot be administered to people with the weakened immune system, the chance of secondary mutation, and pose logistical problems when it comes to transport and delivery[16,34,35,40].

Currently, the main challenges for vaccinologists comprise of improving vaccines against yet undefeated pathogens, rapid identification and response to evolving diseases and successful intervention in chronic diseases in which ongoing immune responses are insufficient. Recent approaches have focused on utilizing technologies such as recombinant DNA methods to develop DNA, subunit vaccines and conjugate vaccines (a weak antigen is linked to a stronger immunogen such as a protein or membrane complex) as well as the use of new adjuvants, using particulate nature of the vaccine as compared to solution of the antigen, direct stimulation of immune system through enriched cytokine production[4,8,10,14,15–18]. With the advent of new technologies like modeling genome sequences, Clustered Regularly Interspaced Short Palindromic Repeats (CRISPR), and gene modification, it is possible to develop novel vaccines. Some examples of recent developments in the different types of vaccines as well as delivery systems are viral vectored vaccines, virosomes, virus-like particles (VLPs), polymeric delivery devices, liposomes, immunostimulating complexes[16,28,34,36,40,49].

Modern vaccine development is increasingly seeking novel adjuvants and delivery systems to boost immunogenicity. Adenoviruses (Ads) are non-enveloped DNA viruses consisting of a linear, double-stranded DNA genome of approximately 30 - 40 kbp. More than 51 different human adenoviruses (Ad) serotypes have been identified of which serotypes 2 (Ad2) and 5 (Ad5) have been extensively characterized genetically and biochemically. Advantages of Ad-vectors include: (1) the safety and relative ease of vector development[26], (2) ability to infect a wide variety of actively dividing and non-dividing mammalian cells and to induce a high-level of transgene expression[50], (3) minimum risk of integration into the host genome[51], (4) capacity to be grown to very high titers in tissue culture[52], (5) availability of certified cell lines and technology for large-scale purification[51], (6) inherent property of serving as an adjuvant by activating innate immunity and the development of strong cellular and humoral immune responses[51]. Viral vaccine vectors,

deployed in heterologous prime-boost regimes, have been developed to induce T cell responses targeting intracellular pathogens[53].

Immune responses by viral vectored vaccines are stronger when a prime-boost regimen is employed[43,53,54]. These vectors are themselves immunostimulatory, and they are safe for the patient, operators and the environment. This type of delivery system has advantages like ease of production, a good safety profile, and potential for nasal and mucosal immunization[25,55,56]. Adenovirus has provided vector platform for various vaccines like influenza[56], tetanus[55], HIV based vaccines[25,40]. The prime-boost regimen induces strong T cell responses which has lead to its current status as a promising technology. This vector system has been shown to induce innate immunity, has effective immunological memory, provides a natural presentation of immunogens and has a broad host tropism[10,24,41].

### 2.2 Nanomedicine for Vaccine Delivery

Traditional vaccines are effective for disease prevention, but they still face various limitations like the requirement of repeated administration to generate long term immunity, the potential side effects of inflammation, and difficulty in the administration to patients which has motivated for the use of nanomedicine for vaccine delivery. Nanomedicine can help achieve the long-lasting controlled burst release of vaccines, the capability of co-encapsulating adjuvants or immune modulators for enhanced immune response and targeting to a group of immune cells[48,57,58]. Antigen itself sometimes is less immunogenic, hence an adjuvant is used to intensify immune response. Adjuvants are also included in vaccines to guide the type of immune response generated[59,60]. Adjuvants and delivery devices have also been shown to protect antigens from degradation, although this generally depends on the nature of adjuvant and delivery device. For example, while chitosan-alginate nanoparticles were found to stabilize ovalbumin[61], other studies have shown that model protein antigens are actually destabilized by traditional aluminum salt adjuvant[62,63].

Particulate systems offer several advantages for vaccine delivery. They protect the associated antigen from adverse physiologic conditions such as enzyme degradation or non-specific interaction with other

molecules in the extracellular matrix and provide a prolonged release profile, more similar to a real infection[34]. Uptake of the particles by immune representing cells (APCs, DCs, MHC) depends on the relative characteristic of the delivery system like size and surface characteristics[57]. It is found that particles of less than 10 μm diameter are effectively phagocytosed by various macrophage populations which can allow delivery of entrapped vaccines intracellularly to the cells responsible for immune response initiation[64,65,66]. This property can be used to improve the cellular uptake of antigens, hence increasing the efficacy of antigen recognition and presentation. Size plays a very important role in the uptake by immune cells which also determines their intracellular outcome; though the optimal size required for the uptake by these cells is still debatable[57,67–69]. As the immune system is equipped to deal with a range of antigens like viruses (20 – 100 nm) to bacteria and cells (in micrometer range) it is difficult to find an optimal size for targeting immune cells.

Various nanocarriers that can be used for delivery of vaccines include liposomes[40,70,71], emulsions[72], biodegradable polymeric particles[40,73], non-biodegradable solid particles like carbon, silica, gold, and iron oxide[74,72]. Polymeric delivery devices are particularly interesting because of the ease of formulation[8,75–77], protection to the antigen entrapped or encapsulated[78–80], modify the release rate of vaccine using various characteristics like composition, size and surface properties[78,81]. The short half-lives of many of the modern therapeutics, in addition to the nonspecific distribution and toxicity of previously identified small molecule drugs, has been a major driving force for the development of polymeric drug delivery platforms. We have integrated two of the above promising technologies, i.e., the adenoviral vectored vaccines and polymeric delivery devices to create a single dose formulation**.**

### 2.3 Polymeric Delivery Devices

Polymers, the most versatile class of materials, have changed our day-to-day lives over the past several decades. Polymeric drug delivery devices have advanced enormously over the past few years to modulate drug release of macromolecules to get a continuous, pulsed or burst release depending on the application[27,82–84]. Some of the delivery devices used for vaccines are listed in **Table 2-1**.

**Table 2-1:** Examples of the release of vaccines from polymeric devices

| Vaccine | Polymer | Size of the particles | Release profile | Ref |
|---|---|---|---|---|
| Influenza | PLGA | 6 µm | Release up to 1 month | [85] |
| | Chitosan | 850nm | Low amount of titers at 3 months | [86] |
| Inactivated rabies virus | PLGA | < 1 µm | 28 days | [87] |
| Malaria synthetic peptide SPF66 | PLGA | 1.4 µm | 45 days | [88] |
| Hep B | PLGA | 2.97 µm | Continuous release for 30 days | [89] |
| | PLGA | 7.3 µm | Continuous release for 30 days | [90] |
| Ovalbumin | PVM/MA | 239 nm | 48 day release | [91] |
| Diphtheria toxoid | PEGylated chitosan | <500 nm | Titers detected at 60 days | [92] |
| | poly-(e-caprolactone) | 267 nm | Low amount of titers at 2 months | [93] |
| PVM/MA: poly(methyl vinyl ether-co-maleic anhydride) | | | | |
| PLGA: poly-(lactic-glycolic acid) | | | | |

Delivery of macromolecules poses a greater challenge than small molecule drugs as maintaining the therapeutic activity of macromolecules is challenging. Macromolecules are prone to protein aggregation, deamidation, hydrolysis, enzymatic degradation, and loss of structural integrity[16]. Hence, delivery devices play an essential role in their delivery. Significant research has been conducted on delivery by biodegradable polymeric devices, subsequent to the market entrance of bioresorbable surgical sutures about two decades ago[94]. Drug delivery research utilizes many polymers for effective delivery of drugs to target sites. These same polymers can be used for macromolecular delivery, in this case, Ad-vectors with modifying the properties of the devices like size and surface charge. The optimal release of the adenoviral vectors with minimum side effects and low toxicity are some of the goals of these delivery devices.

Over the last couple of decades, there has been a nonstop increase in the amount of publications regarding antigen delivery devices. The dramatic increase in the use of nanoparticles as antigen delivery

carriers is predominantly significant[34]. Polymers are broadly classified as natural and synthetic polymers. Natural polymers have the advantage of the intrinsic property of environmental responsiveness via degradation and remodeling cell secreted enzymes[95]. They have been used for a wide variety of applications like gene delivery, tissue engineering, nanoparticles, and three-dimensional scaffolds[27,39,40,80,96]. There is an inherent batch-to-batch variability and fewer ways to tune material characteristics in order to achieve the desired release kinetics. However, these materials, which can be extracted rather than synthesized, are far less expensive than synthetic materials and still exhibit the beneficial effects of immune response due to extended antigen release. Synthetic polymers are available in a wide variety of compositions with custom properties, but this also makes them expensive. Some examples include natural polymers like chitosan, alginate, dextran, collagen, HPMA and synthetic polymers like poly (amides), poly (amino acids), poly (alkyl-a-cyano acrylates), poly (esters), poly (orthoesters), poly (urethanes), and poly (acrylamides).

## 2.4 Composite Polymeric Delivery Devices

Surface adsorbed therapeutic (Ad-vector) on the polymeric particle usually gives a burst release whereas when we have an Ad-vector encapsulated in the polymeric particle (depending on the type of polymer), gives a controlled release over a period of time (**Figure 2-4)**.

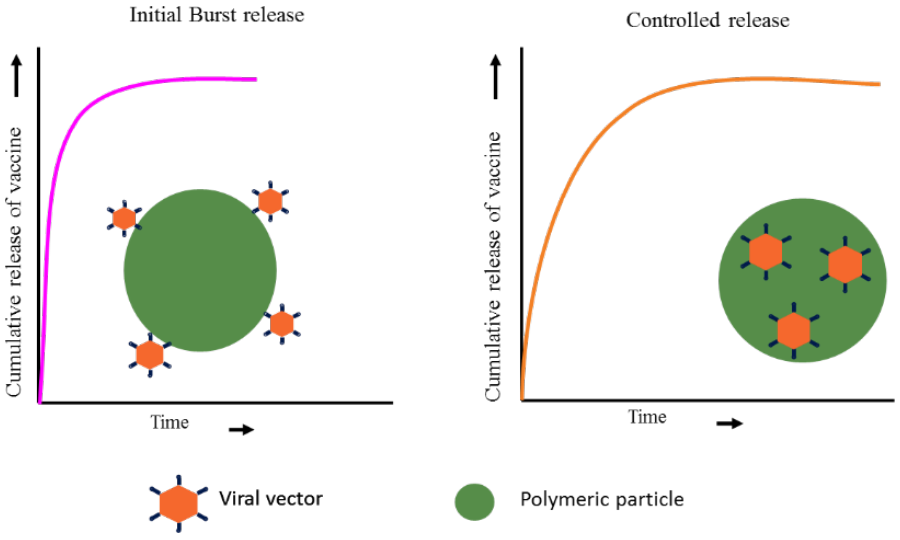


**Figure 2-4:** Schematics of probable drug release from polymeric particles

Composites of biodegradable polymers are gaining importance in biomedical implants, primarily due to the relatively small range of available polymers and copolymers for in vivo use. This field has experienced enormous growth in size and sophistication over the past three decades in terms of both the scientific base and application, which is summarized in several publications[97–101]. Composite particles can be conferred with unique structural and mechanical properties on the basis of the specific properties of the respective polymer used. The concept of biomimicry of several materials can be developed and can lead to a new generation of scaffolds by using composite particles. Such composites may be of two biodegradable polyesters, or of a polyester with a different type of polymer, such as poly (ethylene glycol) or PEG, chitosan or alginate. Combination of polymers helps us to control drug release rates and biodegradation rates. In general, synthetic polymers are more expensive than the natural polymers. Also, natural polymers are abundant, and some may be obtained at a relatively low cost. The combination of a natural polymer and a man-made polymer can produce one versatile material with novel properties and also gives us more parameter to modulate to tune the release kinetics for our application.

Pulsatile vaccine release kinetics are observed when a core-shell structure is used[16,102]. Oil-based PLGA microcapsules (OPM), a reservoir system composed of true core-wall capsule structures with an oily core reservoir of antigen, in which the vaccine is dispersed, enclosed by an outer polymer shell is developed presenting a pulsatile release[102]. We used a combination of polymers which are incorporated into each other as well as to produce a core-shell structure to synthesize biodegradable polymer composites which can give pulsatile release kinetics to mimic the prime-boost regimen. We hypothesize that by utilizing polymers with different degradation rates and properties can be used to demonstrate a pulsatile release profile as shown in **Figure 2-5**. In this composite particle, polymer 1 will serve as the core and encapsulate the required vaccine titer for the booster dose; it will also serve a compact/smooth platform for polymer 2 to form an outer layer. The outer layer will minimize the slow, sustained release of the vaccine (as seen in **Figure 2-4**), and we

will get a burst release as the outer layer degrades completely. Therefore we chose polymers with different degradation kinetics to validate this concept.

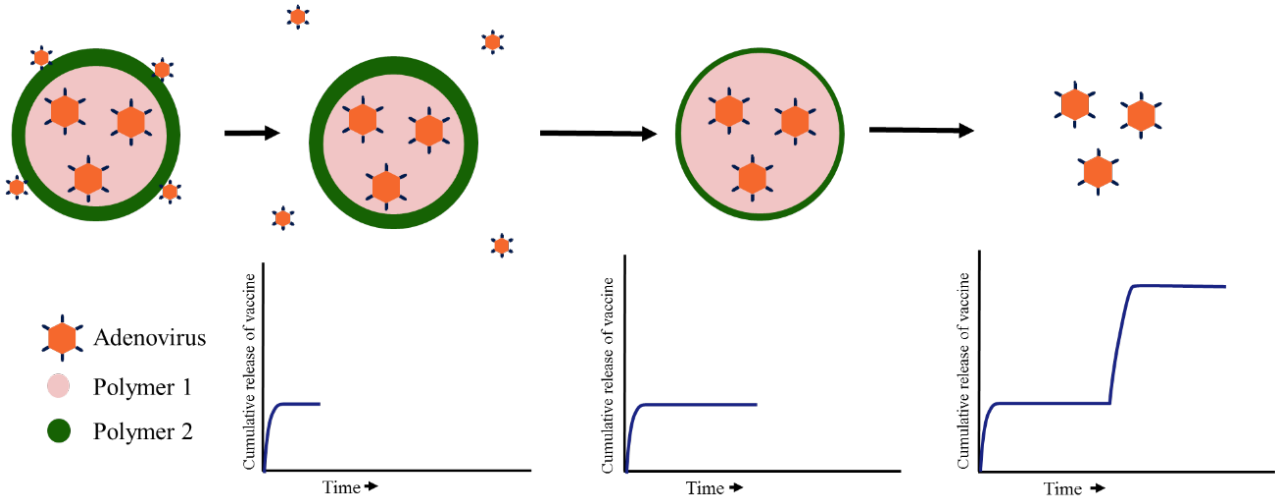


**Figure 2-5:** Proposed release of viral vector from a polymeric composite particle

## 2.5 Poly-D, L-lactic-co-glycolic acid (PLGA)

PLGA is the most widely studied and well characterized biocompatible and biodegradable polymer as it has shown immense potential as a drug/gene delivery carrier and as scaffolds for tissue engineering[57,58,72,84,103]. It is also FDA approved for use as degradable sutures in the body[48]. PLGA polymers can potentially transport antigens or adjuvants to the anticipated location at determined rates and durations, effectually regulating the immune response over a period of time. PLGA polymer has been reported to effectively aid in directing antigens to APCs by efficiently trafficking through local lymphoid tissue for uptake by dendritic cells (DCs)[48]. Encapsulation of proteins in PLGA particles enhances and prolongs antigen presentation by DCs[48]. PLGA particles can deliver exogenous antigens that can be cross-presented through MHC I complexes to $CD8^{+}$cells and have the special capability to reach the MHC I pathway after their internalization by dendritic cells (DCs)[48,57].

The understanding of the physical, chemical and biological properties of the polymer is helpful, before formulating a controlled drug delivery device. PLGA is co-polymer of lactic acid and glycolic acid where polylactic acid (PLA) contains asymmetric carbon which is present in D or L enantiomeric forms, and

glycolic acid is void of any methyl side groups. PLGA usually contains D and L lactic acid forms in equal ratio. PLGA is produced from ring-opening polymerization (ROP) of cyclic lactide and glycolide monomers and depending on the ratio of lactic acid to glycolic acid, properties of the co-polymer like hydrophobicity, crystallinity, molecular weight, glass transition temperature, and the rate of release of drug/macromolecule can be varied. Due to a wide range of factors that can be altered to get the desired results makes PLGA a very versatile polymer.

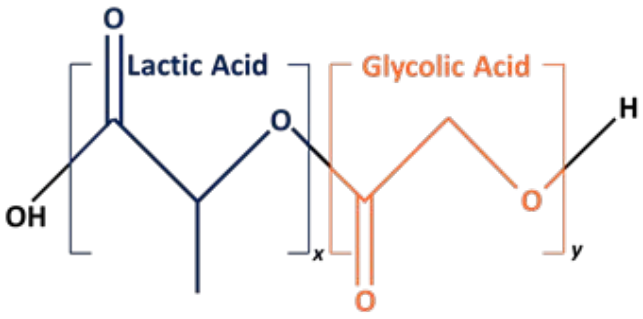


**Figure 2-6:** Structure of PLGA

The physical properties like the molecular weight and the polydispersity index affect the mechanical strength of polymer, therefore, its ability to be formulated as a drug delivery device. Also, these properties control the polymer biodegradation rate and hydrolysis[104]. PLGA degrades via hydrolysis of its ester bonds in water or can be enzymatically degraded *in vivo* to produce biocompatible, safe by-products which are eliminated by normal metabolic pathways via the Krebs cycle[84]. Unlike pure poly-lactic and poly-glycolic acid show poor solubility, PLGA can be dissolved in a wide range of solvents, including chlorinated solvents, tetrahydrofuran, acetone or ethyl acetate and it can be processed into any shape and size. Lactic acid is more hydrophobic than glycolic acid, and hence lactide-rich PLGA copolymers are less hydrophilic, absorb less water, and therefore degrade more slowly. Another property that affects the degradation is the crystallinity; glycolic acid is crystalline in nature and hence it co-polymer PLGA has lower crystallinity than polyglycolic acid. The (glass transition temperature) of the PLGA copolymers are above the physiological temperature of $37^0$C and hence they are glassy in nature.

### 2.5.1 Production of PLGA

Macromolecule therapeutics are the leading candidates for which controlled release devices are being researched on to increase site-specific targeting action and reduce systemic toxicity. Using controlled release devices also helps in avoiding degradation of therapeutics before it reaches the target site, also helps in maintaining the activity of these therapeutics. Drug release from these devices usually occurs through erosion and diffusion of drugs from these devices or a combination of both. There are many techniques available for the production of PLGA particles such as single/double emulsion, phase separation, spray drying, coacervation, and extrusion. Single or double emulsion processes are the most widely used method to synthesize there particles and are also used to encapsulate a variety of vaccines in the particles[45,46,84,89,105–107] owing to ease of productions and high encapsulation efficiencies. Single emulsion process involves oil-in-water (o/w) emulsification while double emulsion technique involves water-in-oil-in-water (w/o/w) emulsion.

Single emulsion technique is best suited for hydrophobic or water-insoluble drugs whereas double emulsion technique (**Figure 2-7**) is used for water-soluble molecules like proteins, peptides, vaccines[48]. Briefly, molecule to be encapsulated is dispersed in the water phase ($w_1$) which is further mixed with PLGA dissolved in organic solvent (o phase). This mixture is emulsified using a homogenizer or sonicator creating microemulsion droplets with therapeutic encapsulated inside these emulsion droplets. Further, a continuous phase consisting of an emulsifier ($w_2$ phase) is added to this mixture. This helps in creating a stable emulsion and can form droplets with smaller size having a uniform size distribution. This entire mixture is then stirred together and the organic solvent (o phase) is allowed to evaporate which hardens the emulsion droplets. These hardened particles are then washed further multiple times to remove the excess reactants and usually freeze-dried before storage.

There are many factors like $w_1/o/w_2$ ratio, the molecular weight of polymers, emulsifier concentration and polymer concentration, the energy input to the system that can affect the physical properties of the particles like size, surface charge and surface morphology. This polymer preparation technique can produce

spherical, porous or hollow microparticles, by varying the solvent evaporation rate. It is therefore important to control the solvent evaporation rate in all microparticle preparation techniques to have reproducible particle morphology.

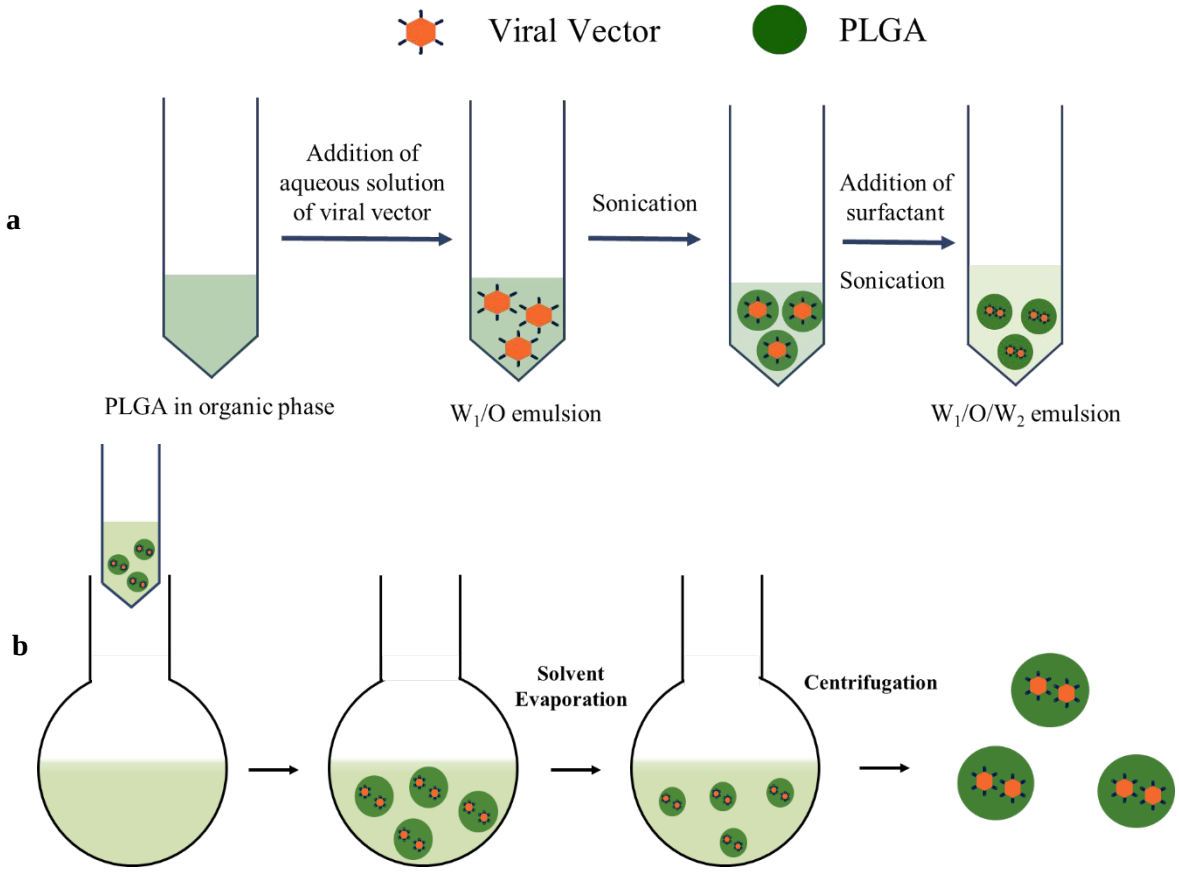


**Figure 2-7:** Production of PLGA particles. a) Development of $w_1/o/w_2$ emulsion b) Solvent evaporation process

## 2.6 Chitosan

Chitosan is currently being studied in numerous applications in fields such as waste and water treatment, agriculture, fabric and textiles, cosmetics, nutritional enhancement, and food processing[108–110]. Chitosan is enzymatically or chemically produced from chitin by deacetylation. Chitin, a heteropolymer and water-insoluble homopolymer of β-1, 4-linked N-acetylglucosamine (GlcNAc) units, is a structural component of insects, crustacean, parasites, and fungi, comprising also human pathogens such as *Candida albicans*. It is the most abundant natural polysaccharide after cellulose and occurs in a wide variety of manners. Three hydrogen-bonded crystalline forms have been characterized: α-chitin with antiparallel chains, β- chitin with parallel chains and γ-chitin with a three-chain unit cell, two "up" - one "down"[111]. α - Chitin is by far the most common form found in fungi and most protistan and invertebrate exoskeletons[112].

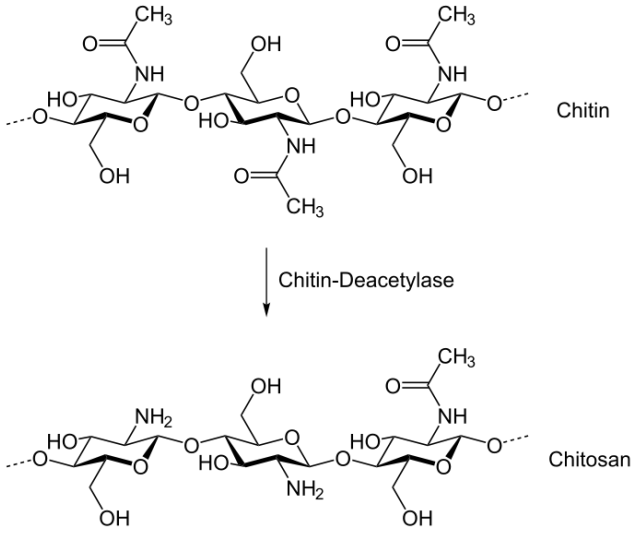


**Figure 2-8:** Chemical Conversion of chitin to chitosan

Chitosan is an attractive material due to its fibrous nature, hydrophilicity, biocompatibility, biodegradation, and potential adjuvant properties[108]. Chitosan can be metabolized by enzyme like lysozyme which naturally presents in the body. Chitosan exhibits antibacterial[113], non-toxic[109], immunomodulating[34] and mucoadhesive properties[75,95]. Chitosan polymer is also responsive to structural and surface manipulation according to the intended application[114]. Depending on the degree of deacetylation the solubility of chitosan is various solvents changes which affect its use in the synthesis of polymeric particles.

Chitosan is a semi-crystalline polymer, and the degree of crystallinity is a function of the degree of deacetylation. Crystallinity is maximal for both chitin (i.e., 0% deacetylated) and fully deacetylated (i.e., 100%) chitosan with intermediate degrees of deacetylation giving a minimal crystallinity[115].

Although antigens may be taken up by the immune cells, the insufficient adjuvant activity may result in limited immunogenicity. It has been shown that chitosan with 70% degree of deacetylation shows the best adjuvancy properties[112,116]. Analogous to other polysaccharides, chitosan has unique structural and physicochemical characteristics that differ considerably from typical synthetic polymers. Chitosan's structure is like to that of cellulose, but it has better processability due to the presence of amino groups (pKa 6.2) in its chains[108]. In fact, its chemistry is largely determined by its amino and hydroxyl groups that act as potential sites for chemical enzyme immobilization or simply for altering the polymer's functionality[108–110]. The primary amino groups on the molecule are highly reactive and provide a mechanism for side group attachment using a variety of mild reaction conditions opening various routes of attaching ligands, adjuvants, targeting moieties on the surface of the particles[109,113,115]. It has been seen that chitosan administered in the form of an emulsion enhanced both T and B cell responses[117] and subcutaneous implantation increased the number of white blood cells, particularly neutrophils and activated both polymorphonuclear cells and macrophages[115].

## 2.7 Release of Drugs/Macromolecules from PLGA and Chitosan Delivery Devices (Mechanisms)

The success of drug delivery device is based on various parameters like pharmacodynamic activity of the drug, bioavailability of the drug at the site of action, specific targeting, low toxicity and high therapeutic efficacy. Parameters like bioavailability and therapeutic efficacy can be modulated using controlled delivery devices. Research in the controlled drug delivery has increased exponentially in the past few years which has increased the efforts towards an understanding of the molecular mechanisms of the drug transport through these devices. Various theories are available on how these biodegradable polymers degrade which are explained here for the two polymers we have chosen, namely, PLGA and chitosan. PLGA and chitosan polymers degrade either through hydrolytic cleavages or enzymatic degradation or a combination of both

*in vitro* and *in vivo*. Degradation of the polymeric delivery device is affected by chemical composition, molecular weight, hydrophobicity, glass transition temperature, crystallinity, size, and porosity[16]. While this certainly complicates the optimization process, it also provides multiple opportunities to modulate the release of the vector from the composite. The release kinetics of the vector are influenced mainly, by the degradation rates of the polymers and the rate of diffusion of the vector as well as the degradation products from the polymer matrix. Various parameters like drug-drug interaction, polymer-drug interactions, initial porosity, the size of the particles, the molecular weight of the polymers and the type of polymers used, will affect degradation and diffusion determining the rate of drug release of the vector[104,118–121].

Usually, degradation of the biodegradable polymers can be divided into two processes: surface erosion and bulk erosion **(Figure 2-9)**. In surface erosion, the polymer degrades from the exterior surface whereas in bulk erosion degradation occurs throughout the whole material equally. Surface erosion causes the material to shed off its surface, but in bulk erosion, the material loses volume throughout equally. Bulk-degrading materials will exhibit far different kinetics than surface-degrading materials[118,121,122]. Surface degrading materials will generally produce an inherently smooth and continuous release profile unless a more complex, layered approach is adopted[123,124].

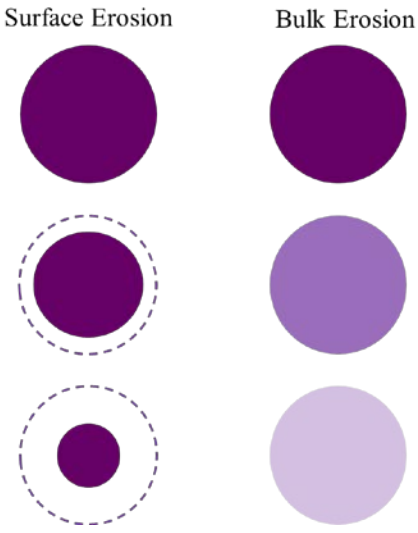


**Figure 2-9**: Illustration of bulk and surface erosion

The release from spherical biodegradable particles can usually be divided into three phases:

1. Phase 1

This phase is usually characterized by burst release which can be attributed to drug molecules associated with the surface or drug molecules encapsulated close to the surface which is easily accessible by hydration[118,125,126] and penetration of water molecules through pores on the particles formed during synthesis or formed due to release of the initial burst. Other reasons for burst release may be the formation of cracks and the disintegration of particles during synthesis, lyophilization or storage[118,127]. Initial burst from the particles also depends on the size of the particles with smaller particles giving a higher burst compared to larger particles[16]. This might be due to the higher surface area to volume ratio of smaller particles[16] as compared to larger particles. Moreover, this burst could further depend on surface properties like the charge of the particles.

Burst release leads to unoccupied sites on the surface of the particles increasing the rate of diffusion of water through the polymer matrix. Additionally, the initial surface morphology will have a consequence on the diffusion of water molecules through the polymer matrix. This diffusion of water through the polymer matrix leads to random chain scission of the polymer due to hydrolytic cleavages. The rate of chain scission process will be highly dependent on the internal porosity of the particles, and therefore the resistance offered to the water molecules for diffusion[84]. During this phase, the molecular weight of the polymer declines significantly, but no appreciable weight loss and no soluble monomer products formed[84].

2. Phase 2

Subsequently, the initial burst is followed by a slow release phase of the viral vector encapsulated inside the particles. As the polymer starts to degrade during phase I, the pores formed on the surface of the particles as well as in the internal of the polymer matrix increase in diameter and in quantity. As the chain scission process continues, degradation products and the vector inside the polymer matrix, start diffusing from the polymer matrix. However, macromolecules like proteins, vaccines, and viral vectors face increased

resistance for diffusion owing to their large size as compared to small molecule drugs. In order to increase the rate of diffusion of degradation products and drug molecule from the polymer matrix, the internal porosity of the particles should be increased by varying the synthesis parameters, but this will also lead to an increase in the rate of diffusion of water molecules in the polymer matrix leading to increase in the rate of degradation. As this pore formation process continues, some of the pores collapse together forming larger pores or continuous pores, and some of the pores undergo pore closure[118].

These pore forming processes are highly dependent on the properties of the polymer like polymer molecular weight, crystallinity, glass transition temperature and the flexibility of polymer chains. In this phase, a decrease in molecular weight accompanied by rapid loss of mass and soluble oligomeric and monomer products are formed[84]. The increasing accumulation of degradation products, as well as the drug molecule in the interior, increases the pressure inside the particles; if this pressure exceeds the particle might burst to release the encapsulated molecule.

3. Phase 3

In this phase, rapid diffusion of degradation products, as well as drug molecules, occurs through the polymer matrix. This leads to the collapse of the polymer structure leading to the formation of soluble monomer products from the soluble oligomeric fragments[119]. This phase represents a state of complete polymer solubilization and is usually a period of faster release.

However, all particles do not follow this traditional triphasic release and depending on physical characteristics of the particles as well as the polymers used, the release profile may vary and one or more than one of these phases might control the release kinetics. Many researchers have used mathematical models to study these mechanisms for biodegradable particles which are utilized to understand release kinetics of the release of the molecules[118,120,125,129–132], but there is still much to understand about the release kinetics in this ever-growing drug delivery field.

PLGA mainly degrades by hydrolytic ester bond cleavage. When polymer chains are cleaved down to a critical size (approximately 15 monomer units in length), they become soluble and can diffuse out of the bulk material resulting in the release of encapsulated molecules and loss of structural integrity. PLGA polymer biodegrades finally into lactic and glycolic acid. It is very important to consider that as PLGA degrades, the oligomers and monomers that are formed are acidic in nature which decreases the pH in the interior of the particle considerably[132] which autocatalyzes degradation rate of the particles. Eventually, lactic acid enters the tricarboxylic acid cycle and is metabolized and subsequently eliminated from the body as carbon dioxide and water[78]. In a study conducted using $^{14}C$-labeled PLA implant, it is concluded that lactic acid is eliminated through respiration as carbon dioxide. Glycolic acid is either excreted unchanged in the kidney or it enters the tricarboxylic acid cycle and ultimately eliminated as carbon dioxide and water.

Chitosan can be degraded by enzymes which hydrolyze glucosamine–glucosamine, glucosamine–N-acetyl-glucosamine and N- acetyl-glucosamine–N-acetyl-glucosamine linkages[133]. Chitosan is thought to be degraded mainly by lysozyme and by bacterial enzymes in the colon[108]. The rate of degradation of chitosan will depend on the degree of deacetylation (DD) with increasing DD the degradation rate is reduced.

# Chapter 3: Controlling the *in vitro* Release Behavior of Macromolecules by Using a PLGA-Chitosan Composite Polymeric Delivery Device

## 3.1 Introduction

Drug delivery devices have a substantial impact on the development of medical technologies, greatly enhancing the performance of traditional pharmaceuticals. Drug delivery has advanced tremendously in the past few decades that we no longer depend only on the conventional pharmaceutical formulation to treat diseases like diabetes, cancer, infectious diseases[7–16]. Drug delivery devices are widely nanoscale molecules or structures that can improve the pharmacokinetics and bioavailability of therapeutics, which is usually termed as nanomedicine[1]. These drug delivery applications occupy about three-quarters of research activities in the nanomedicine market[1]. To address the new drug development needs the pharmaceutical industry is turning towards innovative delivery strategies which hold the key to success.

Macromolecule therapeutics constitute a multibillion-dollar market, yet their formulation and controlled delivery still pose a considerable challenge[134]. Due to their structural complexity which is required for specificity, these therapeutics have entered the mainstream of modern medicine and are indispensable however these complex structures are difficult to formulate and deliver[135]. Alongside novel delivery devices, a lot of novel drugs are also being introduced in the market. The recent focus has shifted towards macromolecular therapeutics like peptides[17,18], proteins[19,20], enzymes, monoclonal antibodies[21–23], viral vectors[10,22,24–26]. Modulating release of the drugs, increasing their bioavailability, decreasing toxicity, overcoming the barriers encountered in the body, improving pharmacokinetics and pharmacodynamics of these drugs are just some of the ways nanomedicine can offer solutions to using these drugs.

Viral vectors signify high potential as gene delivery carriers for treating various infectious diseases and cancer due to their high transduction efficiencies[136]. Viral vectors consist of a non-replicating virus that encompasses an antigen against whom immunity is desired. Some of the advantages of these viral vectors are ease of production, a good safety profile, ability to potentiate strong immune responses[40]. Adenovirus

has provided vector platform for various vaccines like influenza[56], tetanus[55], HIV based vaccines[25,40]. Human adenoviral vectors of serotypes 2 (Ad2) and 5 (Ad5) efficiently transfer genes to a wide variety of dividing and non-dividing cells *in vivo* and have been therefore used in a number of gene therapy approaches[51,52,137]. Advances in the Ad5 production of these viral vectors, altering gene expression and the advent of nanomedicine will give us remarkable opportunities to develop delivery systems that can help us gain full potential of these viral vectors. New advances in the delivery of these vectors will significantly improve the efficacy of adenoviral delivery.

Smart delivery technologies containing polymeric or solid particulate delivery[84,103,138–142], liposomal delivery systems[68,143,144], hydrogels[145,146] are being developed for effective delivery to overcome barriers presented by our body. Polymeric delivery holds a lot of potential due to ease of manufacturing, controllable size distribution, high drug carrying capacity, tunable properties, ease of surface functionalization[147]. Various triggered release particles can be synthesized which respond to change in pH[9], enzymes present in the body[148,149], redox potential, magnetic field[138,150], ultrasound[151], light[149] which consequently will help to address various problems like cellular uptake, drug release or clearance[27]. These polymers can be divided into natural polymers like chitosan, alginate, carboxymethyl cellulose, dextran and synthetic polymers like polyesters, polyanhydrides, polyamides, polyurethanes. Natural polymers are cheap and biocompatible[147], but it is difficult to control the properties for these polymers; whereas properties for synthetic polymers can be controlled, but most of the synthetic polymers are expensive.

If we use a combination of natural and synthetic polymers, we could overcome the disadvantages of each system and combine them together as one versatile material. Poly-lactic-glycolic acid (PLGA) has attracted a very high interest and is the most widely studied polymer in the field of nanomedicine due to its properties like biodegradable, biocompatible, tunable properties, ease of manufacturing particles, and degradation by bulk erosion whereas some of the shortcomings are hydrophobicity of PLGA particles, acidic degradation products generated during hydrolysis[84] whereas chitosan is a particularly attractive material due to its hydrophilicity, biocompatibility, biodegradation, and potential adjuvancy properties.

Chitosan is enzymatically or chemically produced from chitin by deacetylation. Chitosan can be metabolized by enzyme like lysozyme which naturally presents in the body. Chitosan exhibits antibacterial[113], non-toxicity[109], immunomodulating[34] and mucoadhesive properties. Chitosan polymer is also amenable to structural and surface manipulation according to the intended application[114].

Herein, we provide a controlled release formulation with PLGA-chitosan composite polymeric particle. Ad-eGFP is used as a model macromolecule which is encapsulated inside these composite particles. A modified double emulsion technique was used to synthesize these particles and various different parameters like polymer concentrations, time addition of polymers, and the concentration of emulsifier is varied to control the release of Ad-eGFP from these composites. Synthesizing a PLGA-chitosan composite will help us tune the release kinetics of particles by modulating the degradation rates of the polymers and utilizing these composites as one versatile particle.

## 3.2 Materials and methods

### 3.2.1 Materials

All materials were purchased from commercial suppliers and used without further modification unless noted otherwise. Poly-lactic glycolic acid (PLGA) with lactide: glycolide ratio of 50:50 (MW 30 – 60 kDa) (inherent viscosity 0.55-0.75 dL/g), low molecular weight chitosan (MW 50 – 190 kDa) (viscosity in 1 w/v % acetic acid is 20-300 cps), polyvinyl alcohol (PVA) (MW 30 – 70 kDa) (viscosity in water 4 - 6 cps), D-(+)-trehalose dehydrate were purchased from Sigma Aldrich Chemical Co. (St. Louis, MO). Enhanced green fluorescent expressing adenovirus type 5 (Ad-eGFP) with CMV promoter at a titer of 1 $x10^{11}$ Viral pt/ml was purchased from Vector BioLabs (Malvern, PA). Dulbecco Modified Eagle Medium (DMEM) was purchased from HyClone, GE Healthcare Life Sciences (Logan, Utah), Irradiated and heat inactivated Fetal Bovine Serum (FBS) was purchased from VWR Life Sciences Seradigm (Radnor, PA) and penicillin/streptomycin (antibiotic) was purchased from Corning Cellgro (Manassas, VA). PerfeCTa SYBR Green FastMix was purchased from Quantabio (Beverly, MA) for real-time PCR analysis. PCR primers for

quantification of Ad-eGFP were purchased from ThermoFisher (Carlsbad, CA). Fluorescein isothiocyanate, isomer 1 (95%) (MW 389.39) was purchased from VWR Life Sciences (Alfa Aesar, Ward Hill, MA). Dichloromethane (DCM), acetic acid (AA), acetonitrile (ACN), ammonium hydroxide ($NH_4OH$) were of analytical grade. Deionized water used throughout the study was obtained from a Milli-Q Purelab Flex 2 water purification system (Elga LLC, Woodridge, IL).

### 3.2.2 Synthesis of PLGA particles

PLGA particles were prepared by double emulsion method at room temperature reported by Nagai et al.[89] with minor modifications. In brief, 400 µl of Ad-eGFP was added to 10 w/v % solution of PLGA (200 mg PLGA dissolved in 2 ml DCM). This mixture was sonicated at 5 % amplitude for 30 seconds to create a water-in-oil ($w_1/o$) emulsion. 10ml of 3 w/v % PVA was added, and this mixture was sonicated at 5% amplitude for 30 seconds to create a water-in-oil-in-water ($w_1/o/w_2$) emulsion. This mixture was added to 30 ml PVA in round bottom flask in order to keep water to oil ratio constant at 1:20. This mixture was stirred for 4 hours to let the DCM evaporate and harden the nanoparticles. After the stirring was completed, the particles were centrifuged at 10,000 rpm for 20 min and given 4 washes with DI water. The particles were suspended in 1 ml 2 w/v % trehalose in DI water and frozen at -80$^0$C overnight; then lyophilized overnight at a temperature of -105$^0$C and pressure of 0.01 mbar using a Labconco FreeZone-4.5 lyophilizer (purchased from Labconco Corporation, Kansas City, MO). These lyophilized particles were stored at -80$^0$C until further use. **Table 3-1** summarizes further results.

### 3.2.3 Synthesis of PLGA-Chitosan composite particles

400 µl of Ad-eGFP was added to 2 ml solution of PLGA (w/v % described in **Table 3-1**). This mixture was sonicated at 5 % amplitude for 30 seconds to create a water-in-oil ($w_1/o$) emulsion. 2 ml solution of chitosan (w/v % described in **Table 3-1**) dissolved in 0.1M AA was added and this mixture was sonicated again at 5 % amplitude for 30 seconds to create a water-in-oil-in-water ($w_1/o/w_2$) emulsion. 10 ml PVA solution was added to this mixture followed by sonication at 5 % amplitude for 30 seconds. This mixture was added to 28 ml PVA in round bottom flask in order to keep water to oil ratio constant at 1:20. This

mixture was stirred for 4 hours to let the DCM evaporate and harden the nanoparticles. A slight modification was used to study the effect of the distribution of chitosan in the composite on the release profile. Briefly, after the preparation of $w_1/o$ emulsion, 10 ml of PVA was added, and a $w_1/o/w_2$ emulsion was created by sonication at 5% amplitude for 30 seconds. This emulsion was further added to 28 ml of PVA in round bottom flask. Chitosan solution was added after 2 hours to this mixture, i.e., after partial hardening of PLGA; this solution was stirred further for 2 hours.

After the stirring was completed, the particles were centrifuged at 10,000 rpm for 20 min and given 4 washes with DI water. The particles were suspended in 1 ml 2 w/v % trehalose in DI water and frozen at -$80^0$C overnight and then were lyophilized overnight at a temperature of -$105^0$C and pressure of 0.01 mbar using a Labconco FreeZone-4.5 lyophilizer. These lyophilized particles were stored at -$80^0$C until further use. Controls were synthesized using the same method without addition of Ad-eGFP. **Table 3-1** summarizes further results.

### 3.2.4 Qualitative determination of the distribution of chitosan in the composite

Chitosan consists of primary amines in the polymer backbone. Fluorescamine isothiocyanate (FITC) dissolved in ethanol was covalently attached to chitosan. Briefly, 2 mg/ml of FITC was dissolved in ethanol, and it was added to 1 w/v % of chitosan dissolved in 0.1M AA. The ratio of FITC to chitosan solution was kept 1:3 and this solution was reacted at $4^0$C overnight. Chitosan was precipitated out by addition of 5 ml of 0.1 M $NH_4OH$. Excess FITC was washed with 20% ethanol until the fluorescence of the supernatant measured at 495 nm/519nm was equal to that of DI water. This fluorescently tagged chitosan was further used during composite synthesis to verify the distribution of chitosan and study the effects of different time addition of polymers on the release profile. These images were captured with an EVOS cell imaging system (ThermoFisher Scientific, Waltham, MA, USA).

### 3.2.5 Particle sizing and surface morphology

#### *3.2.5.1 Dynamic Light Scattering (DLS)*

The hydrodynamic diameter, polydispersity index (PDI) and surface charge (zeta potential) of composite particles were analyzed by dynamic light scattering and laser Doppler electrophoresis using Zetasizer Nano ZS (Malvern Instruments Inc., UK). The size of PLGA and composites were characterized by backscatter detection (173°), and the zeta potential was calculated using Smoluchowski model[152]. Measurements were performed with particles collected after the 4$^{th}$ wash in DI water.

**Table 3-1:** Process parameters for the synthesis of PLGA and composite particles

| Sr no | Process of addition of polymers | PVA (w/v %) | PLGA (w/v %) | Chitosan (w/v %) |
|---|---|---|---|---|
| 1 | Polymers were added together | 3 | 10 | 1 |
| 2 | | 3 | 10 | 3 |
| 3 | | 3 | 10 | 3 |
| 4 | | 1 | 10 | 3 |
| 5 | Polymers added separately (Chitosan was added after 2 hours of partial hardening of PLGA) | 3 | 1 | 3 |
| 6 | | 3 | 10 | 1 |
| 7 | | 3 | 10 | 3 |
| 8 | | 3 | 10 | 3 |
| 9 | | 3 | 10 | 3 |
| 10 | Pure PLGA | 3 | 10 | 0 |
| 11 | | 3 | 10 | 0 |

$o/w_2$ ratio was kept constant at 1:20; Particles 1 to 4 were synthesized by addition of both the polymers (PLGA and Chitosan) together whereas particles 5 to 9 were synthesized by addition of chitosan after partial hardening of PLGA particles. Particle 7 and 8 were synthesized with the same initial conditions; particle 8 was freeze dried before utilizing them for release studies whereas particle 9 was not freeze dried.

#### *3.2.5.2 Scanning Electron Microscopy*

Surface Morphology of PLGA and composite particles were characterized using Zeiss EVO 50, Carl Zeiss Meditec (Oberkochen, Germany) operating at a voltage of 20K. Freeze dried particles were laden on a double-sided carbon tape which was mounted on Al-stub and this stub was gold-coated using EMS 550×, Carl Zeiss Meditec (Oberkochen, Germany) to avoid melting of particles due to high energy electron beam.

#### *3.2.5.3 Fourier Transform Infrared Spectroscopy (FTIR)*

The existence of both PLGA and chitosan was determined with FTIR analysis of the particles. Samples were prepared by adding the analyte suspended in water to potassium bromide which was dried overnight to remove excess water. The mixture was then formed into a pellet, and this pellet was further used for analysis. A Nicolet 6700 was used for analysis with 64 scans of each sample.

### 3.2.6 *In vitro* release studies

In 1.5 ml Eppendorf tube, approximately 6 mg of each type of freeze-dried composite was weighed in triplicates and suspended in 1.2 ml DMEM media (DMEM culture media supplemented with 10% FBS and 1% antibiotics) through sonication at 5 % amplitude and vortexing. These tubes were incubated at $37^0$C on a RotoFlex tube mixer for a total of 210 days with intermediate sample collection described below. The tubes were taken out of the incubator at different times and centrifuged at 7000 rpm for 10 minutes in a microfuge. 1ml of the supernatant was removed from these tubes and fresh 1 ml of DMEM media was added to maintain the sink conditions. These particles were suspended again using vortexer and incubated at $37^0$C on the RotoFlex tube mixer until next time. The collected supernatant was stored at -$80^0$C until further analysis.

### 3.2.7 Real-time polymerase chain reaction (qPCR)

Loading capacity and analysis of the released Ad-eGFP at every time point was characterized using qPCR. Briefly, to quantify loading capacity of the particles, 1mg of each of the composites and pure PLGA particles were dissolved using 600 µl of ACN at 175 rpm and $23^0$C in a shaking incubator to extract the

Ad-eGFP encapsulated in the particles. After 4 hours of incubation, 1 ml of DI water was added to these vials and further incubation was carried out at $40^0$C and 275 rpm overnight to evaporate the ACN in water. Ad-eGFP in the ACN phase is now suspended in the water phase which can be further used for analysis.

The collected supernatant (from *in vitro* studies) for each sample was thawed at room temperature and 400 µl of each sample was pipetted in a vial to which 600 µl of ACN was added followed by further incubation at 175 rpm and $23^0$C. After 2 hours of incubation, 1 ml of DI water was added to these vials followed by further incubation at $40^0$C and 275 rpm overnight to evaporate the ACN in water. Ad-eGFP released from each particle type at different times was then analyzed using qPCR. The primer sequences used for the PCR analysis are as follows: Forward primer: 5' - AGC TGA AGG GCA TCG ACT TC - 3' and Reverse primer: 5' - AGC AGG ACC ATG TGA TCG C - 3'. TaqMan real-time quantitative PCR was carried out using the Bio-Rad CFX96 Touch™ real-time PCR detection system (Hercules, CA). The final reaction volume of 20 µl consisted of 10 µl SYBR Green FastMix, 0.04 µl of each primer (10 µM), 4.92 µl DNase free water, and 5 µl template solution. All samples were amplified under the following conditions: $95^0$C for a 3-min, then 39 cycles of $95^0$C for a 10-second hold, $55^0$C for 30-second hold. The results were analyzed with Bio-Rad CFX Manager (Bio-Rad Laboratories, Hercules, CA). The amplification and standard curves are reported in **Appendix 2**. Loading Capacity was calculated using the following equation:

$$Loading\ Capacity = \frac{(Total\ number\ of\ viral\ particles\ \ encapsulated)}{Total\ weight\ of\ particles}$$

### 3.2.8 Statistical Analysis

All experiments were completed in triplicate (n =3). Results are shown as the average of all replicates ± standard deviation. Results were compared using Student's T-test or one-way ANOVA, where applicable, and considered significant with p values less than 0.05.

## 3.3 Results and Discussion

### 3.3.1 Physical properties of composites

#### *3.3.1.1 Qualitative distribution of chitosan in the composites*

Chitosan, a natural polymer, has been used widely for gene/viral delivery owing to its properties like it is mucoadhesive, biocompatible, cationic[109]. It is a linear polysaccharide composed of D-glucosamine and N-acetyl-D-glucosamine; the proportion of D-glucosamine and N-acetyl-D-glucosamine depends on the degree of deacetylation[108]. FITC is a derivative of fluorescein molecule functionalized with an isothiocyanate reactive group (-N=C=S). This derivative is reactive towards nucleophiles including amine and sulfhydryl groups; therefore primary amines in the polymer backbone of chitosan are chemically conjugated to FITC[153]. FITC has excitation and emission spectrum peak wavelengths of approximately 495 nm/519 nm, giving it a green color which can be observed under the GFP filter in the EVOS microscope. The qualitative distribution of chitosan can be observed in **Figure 3-1**. It can be seen that when both PLGA and chitosan are added together during the synthesis (**Figure 3-1(a)**), chitosan is distributed all over the particle which suggests that chitosan and PLGA get incorporated into each other. Alternatively, when chitosan and PLGA are added separately (i.e., chitosan is added after partial hardening of the PLGA particles) a layer of chitosan is formed around PLGA as observed in **Figure 3-1(b)**. This could be because chitosan gets adsorbed on the surface of PLGA particles leading to the core-shell structure of the composite particles with PLGA as the core and chitosan as the outer shell. Therefore, by varying addition time of the polymers, we can alter the distribution of chitosan in the composite particle which might lead to different release characteristics.

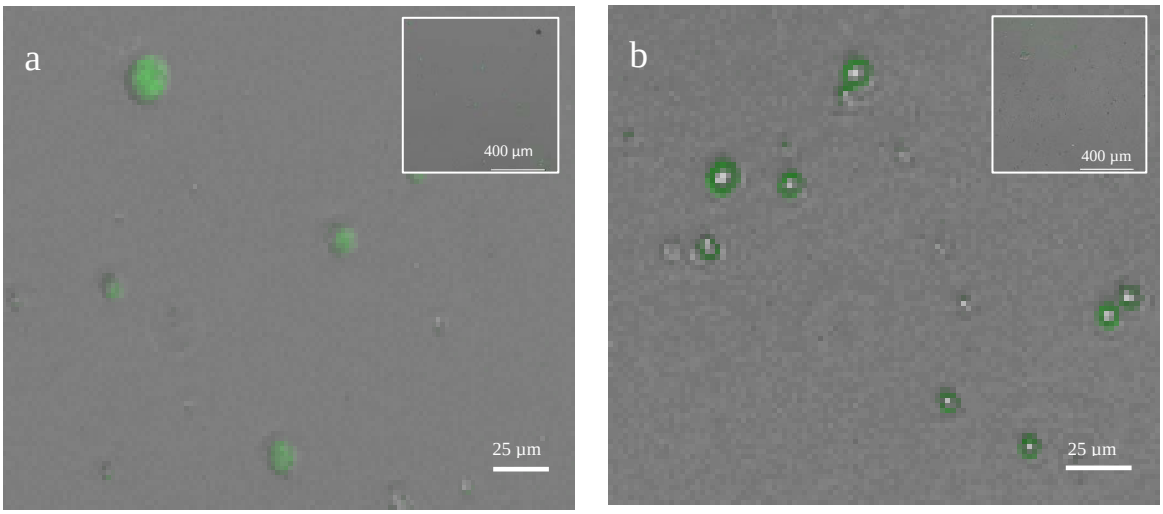


**Figure 3-1:** FITC tagged chitosan was used for synthesis of the composites. (a) Composite particles when both the polymers were added together; (b) Composite particles when PLGA and chitosan were added separately (i.e. chitosan was added after partial hardening of PLGA particles)

### *3.3.1.2 Surface Charge and Size distribution*

Double emulsion process is a widely studied procedure for the synthesis of PLGA particles and is easily scalable. Factors like PLGA concentration, chitosan concentration, emulsifier concentration, polymer molecular weight, and time addition of polymers have an effect on size, surface charge, the release of macromolecule encapsulated, and degradation of the particles[16,154,155]. The surface charge for all particle types is given in **Table 3-2**. Particles 1 to 4 were synthesized by addition of both the polymers (PLGA and chitosan) together whereas particles 5 to 9 were synthesized by addition of polymers (PLGA and chitosan) separately, i.e., chitosan was added after partial hardening of PLGA particles. Zeta potential is the potential at the slipping/shear plane of a particle moving under the influence of electric field. It is also termed as the potential difference between the electric double layer of electrophoretically mobile particles and a layer of dispersant around at the slipping plane[152]. PLGA polymer is an anionic polymer due to the presence of hydroxyl groups[78] whereas chitosan is a cationic polymer due to the presence of primary amines[113]. The zeta potential presents a positive zeta potential in case of all the composites indicating the presence of chitosan on the surface of particles.

**Table 3-2:** Effect of process parameters on surface charge

| Sr no | PVA (w/v %) | PLGA (w/v %) | Chitosan (w/v %) | Zeta Potential (mV) |
|---|---|---|---|---|
| 1 | 3 | 10 | 1 | 47.9 ± 0.68 |
| 2 | 3 | 10 | 3 | 41.1 ± 2.17 |
| 3 | 3 | 10 | 3 | 44.9 ± 1.22 |
| 4 | 1 | 10 | 3 | 46.7 ± 0.70 |
| 5 | 3 | 1 | 3 | - |
| 6 | 3 | 10 | 1 | 5.7 ± 0.19 |
| 7 | 3 | 10 | 3 | 10.1 ± 1.02 |
| 8 | 3 | 10 | 3 | 10.1 ± 1.02 |
| 9 | 3 | 10 | 3 | 22.3 ± 0.34 |
| 10 | 3 | 10 | 0 | 0.85 |
| 11 | 3 | 10 | 0 | 0.47 |

$o/w_2$ ratio was kept constant at 1:20; Particle 7 and 8 were synthesized with the same initial conditions; particle 8 was freeze dried before utilizing them for release studies whereas particle 9 was not freeze dried. All measurements were performed in triplicates.

Size of particles plays a vital role in the degradation of PLGA and subsequently, the release of the macromolecules encapsulated in the particle. Size has a large effect on the encapsulation efficiency, release profile, toxicity, uptake of the particles by the cells, and determining the degradation rate of the particles[78,84,156]. The effect of varying process parameters on the hydrodynamic diameter of the particles can be seen in **Figure 3-2.** These process parameters affect size as well as the inherent structure of the particles and hence affecting the release of macromolecule encapsulated.

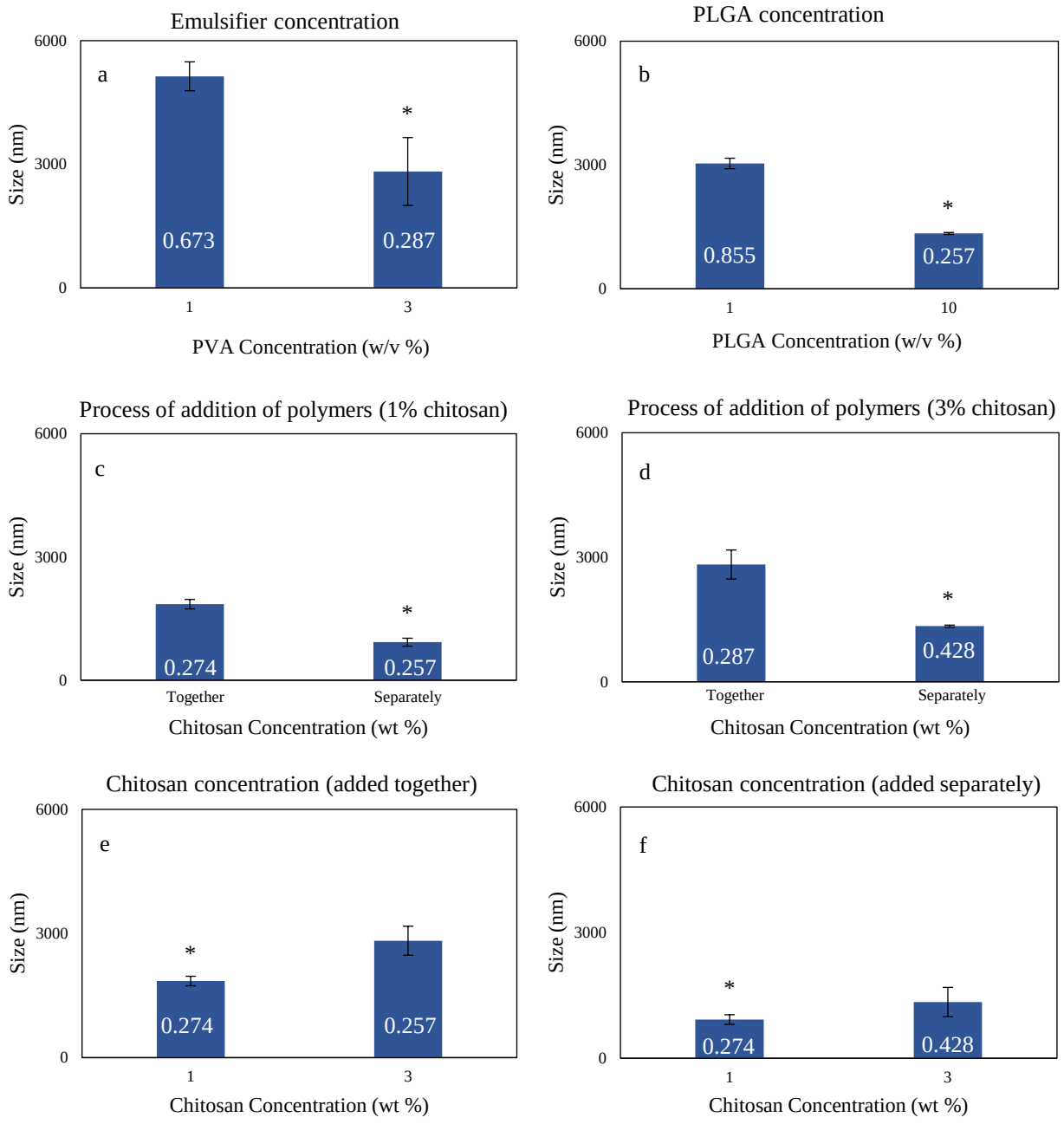


**Figure 3-2:** Effect on size of the particles by varying one of the input process parameters out of emulsifier(PVA) concentration, PLGA concentration, chitosan concentration and process of addition of both the polymers (together or separately). Other parameters for the synthesis are as follows (a) 10% PLGA and 3% chitosan, added together (b) 3% PVA and 3% chitosan; added separately (c) 3 % PVA, 10% PLGA, 1% Chitosan; (d) 3% PVA, 10% PLGA, 3 % Chitosan (e) 3% PVA and 10 % PLGA; added together (f) 3% PVA and 10% PLGA; added separately. All measurements were performed in triplicates (*$p < 0.05$) and they represent average diameter of the particles measured in DLS. The values in the bar charts represent polydispersity index (PdI).

Formation of emulsion droplets depends on the inertial forces between droplets which are dependent on the energy input in the system (sonication amplitude, sonication time, stirring speed)[78,157]. It is observed that in the absence of an emulsifier, emulsions formed during the production are stable for only a finite period of time, as the emulsion droplets tend to coalesce and separate out into component phases. Emulsifiers are compounds that typically have a polar or hydrophilic (i.e., water-soluble) part and a non-polar (i.e., hydrophobic or lipophilic) part, which stabilizes an emulsion by increasing its kinetic stability. Therefore, surfactant/emulsifier is usually added to these emulsions to create a stable emulsion. Emulsifier reduces the surface tension at the interface of continuous ($w_2$) phase and an oil phase, thus avoiding coalescence of emulsion droplets and stabilizes the emulsion[158]. It has been observed that increasing concentration of emulsifier reduces the interfacial tension between the oil and water phase which prevents the coalescence of emulsion droplets[107,159]. Additionally, the increase in emulsifier concentration leads to an increase in viscosity of the $w_2$ phase, reducing emulsion droplet collision and coalescence, therefore creating a more stable emulsion[78,107]. As we increase the emulsifier (PVA) concentration, we see that the size of the composite particles decreases (**Figure 3-2(a)**), additionally the PdI of the particles follows the same trend ($PdI_{1\%}$ = 0.673and $PdI_{3\%}$ = 0.287). The size and size distribution of the particles depends on the stability of the initial emulsion droplets, and therefore this stable emulsion further leads to small sized particles with narrow size distribution. If a higher concentration of PVA is used during synthesis, it leads to uniform distribution of particles[107] as is evident from this study. This difference in size distribution is likely a result of the higher viscosity of $w_2$ phase, preventing the particles from coalescing. Alternatively, some scientists report that increase in PVA concentration leads to increase in viscosity of the $w_2$ phase, which necessitates an increase in energy input to get smaller droplets which might have an effect on the activity of the macromolecules to be encapsulated[34,64,82,84]; but it should be noted we did not increase energy input in this study.

Furthermore, increasing the PLGA concentration increases the viscosity of o-phase, and therefore at the same energy input, it leads an increase in the size of the emulsion droplets and hence increases the size

of the particles[64,157,159]. With the same energy input in the system, it leads to an increase in the size of the particles with increasing polymer concentration. But as can be seen in **Figure 3-2(b)**, the size of the composite particles decreased with increase in PLGA concentration. Note that the size of the particles represented here is the Z-average hydrodynamic diameter of the particles but if we look at the intensity weighted peak of hydrodynamic diameter, it is observed that the size of the particles with 1% PLGA is 772.9 nm (data not shown). This huge difference in the average diameter and intensity weighted average might be attributed to high polydispersity of the particles observed when PLGA 1 w/v % is used (PdI = 0.855).

Additionally, it is seen **(Figure 3-2 (c) and (d))** that addition of both polymers (PLGA and chitosan) separately, i.e., addition of chitosan after partial hardening of PLGA results in significantly smaller particles as compared to when chitosan and PLGA are added together ($p_{1\%\ chitosan} = 0.0004$, $p_{3\%\ chitosan} = 0.013$). This is because when polymers are added together, chitosan might be incorporated in the matrix of PLGA leading to the increase in diameter; as opposed to when added separately, the partial hardening of PLGA particles reduces the size of emulsion droplets in the system to which chitosan is added leading to the formation of small particles. It was further observed that when both polymers were added separately, the size of the particles is significantly bigger than the size of pure PLGA particles (Diameter of PLGA particles = 977.87 nm) ($p = 0.0007$). This increase in size is likely due to the shell of chitosan adsorbed on partially hardened PLGA particles. Additionally, when chitosan concentration was altered, we see that the hydrodynamic diameter of the composite particles with 3 w/v % chitosan was significantly greater than 1 w/v % chitosan (when added together, $p = 0.032$; when added separately, $p = 0.013$) (**Figure 3-2 (e) and (f))**. Increasing chitosan concentration leads to an increase in viscosity of $w_2$ phase, thereby reducing collision of emulsion droplets and hence resulting in smaller particles. Moreover, the amount of chitosan added to the synthesis increases with increasing chitosan concentration thereby increasing the association of chitosan and PLGA due to opposite charges of both the polymers. Therefore, for the same amount of PLGA, we will have more chitosan incorporated in PLGA matrix (when both polymers are added together) or higher adsorption of

chitosan on the surface of PLGA particles (when both polymers are added separately). Therefore, it is possible to control the size of the particles for intended application by varying process parameters in the double emulsion technique for the synthesis of composite particles.

*3.3.1.3 Surface Morphology*

**Figure 3-3** shows the scanning electron micrographs for composites as well as pure PLGA particles. We can see that the PLGA particles and composites synthesized by double emulsion method here are generally spherical in shape with a smooth/compact surface. Smooth surface morphology is essential to prevent leakage of any Ad-eGFP encapsulated in the particles. This type of structure is usually seen when particles are manufactured using double-emulsion method[89]. Note, (a) and (b) have a small number of cracks on the particles which is likely the result of the high energy electron beam incident on the particles. It is observed that when the high energy beam was incident on the particles, it led to swelling of the particles and then crumple as shown by the arrow.

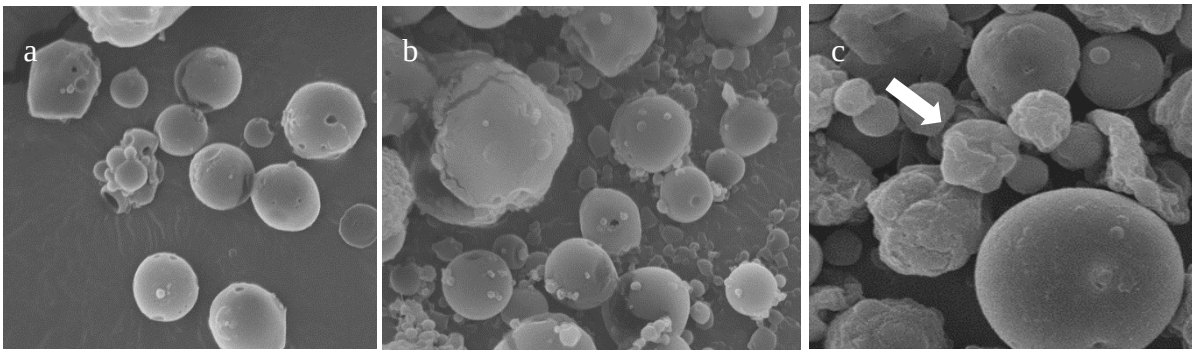


**Figure 3-3:** Scanning electron micrographs of PLGA-chitosan composite and pure PLGA particles. a) 10% PLGA and 3% chitosan when both PLGA and chitosan are added together b) 10 % PLGA and 3% chitosan when both polymers are added separately (i.e. chitosan is added after partial hardening of PLGA particles) c) 10 % PLGA particles (pure)

### *3.3.1.4 FTIR*

The vibrational spectrum of chemical bonds in the molecule is considered to be a unique property and characterizes that molecule[160]. The qualitative aspects of FTIR are one of the most dominant aspects of this versatile analytical method. Infrared spectra of each of the sample (PLGA, chitosan, and composite) can be used to qualitatively detect the presence of each of the polymers in the composite particles as shown in **Figure 3-4**. PLGA has carboxylic acid groups (-C=O) which gives a symmetric stretching at 1760 $cm^{-1}$ [160], and chitosan molecules have primary amine groups in their backbone owing to the bending vibrations at

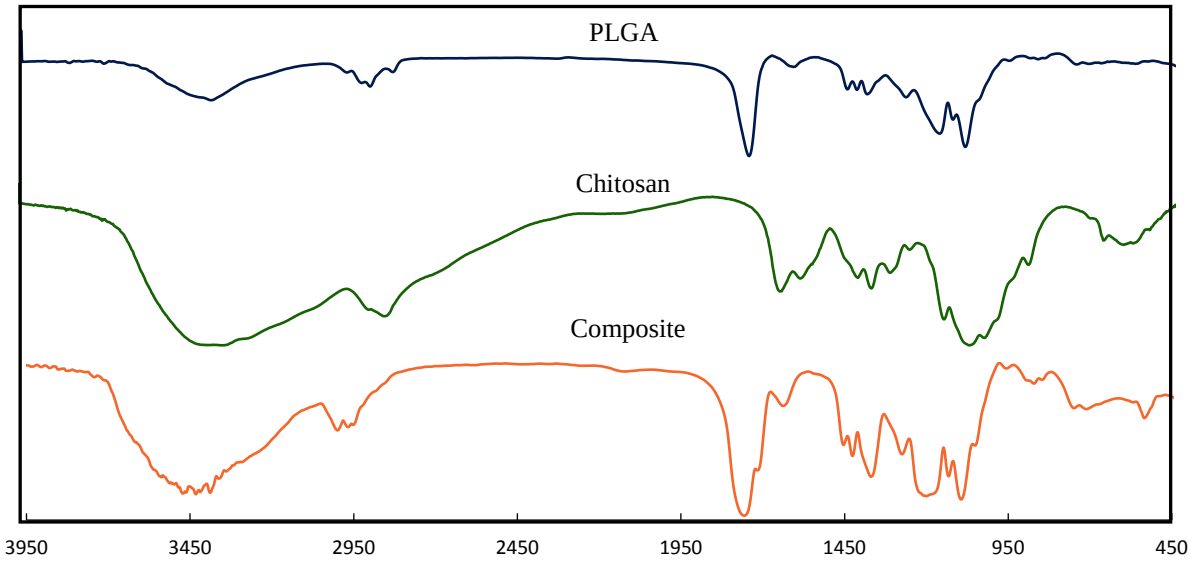


**Figure 3-4:** FTIR spectra of PLGA, Chitosan and Composite particles.

1650 $cm^{-1}$ [161]. The broad peak at 3450 $cm^{-1}$ is either due to hydrogen bonding, vibrational stretching of hydroxyl groups (-OH) or bending vibrations of the primary amines ($-NH_2$)[160]. These results indicate the presence of both PLGA and chitosan in the composite. All the compounds also exhibited a peak at 2950 $cm^{-1}$ representing the symmetric and asymmetric stretching vibrations of $–CH_3$ present in both the polymers. The peaks between 1450 - 1090 $cm^{-1}$ correspond to vibrational stretching of methylene -C-H bends and skeletal C-C vibrations[160].

### 3.3.2 Loading Capacity of Ad-eGFP in the particles

Loading capacity with extraction ($LC_{ext}$) denotes the total encapsulation quantified by dissolving the freeze-dried particles in acetonitrile whereas the loading capacity after 215 days is the cumulative release ($LC_{cumu}$) of Ad-eGFP as the particles degrade and release the adenoviral vector. We used real-time PCR to quantify the Ad-eGFP released in the aqueous media due to its high sensitivity, specificity and reproducibility[162] as compared to other methods to detect DNA like optical measurement at 280 nm, protein assays. The total loading capacity for composite and PLGA particles is shown in **Figure 3-5**. We can see that there are no significant differences in $LC_{ext}$ when any of the parameters are varied which might be due to very high variation in their measurements resulting from lack of solubility of both the polymers (PLGA and chitosan) in a common solvent. PLGA polymer is completely soluble in acetonitrile which is used to dissolve the particles whereas as composite particles are not soluble in this solvent. Chitosan is only soluble in acetic acid, but this solvent cannot be used in PCR machine. Therefore, there is no common solvent that can dissolve both the polymers leading to incomplete dissolution and extraction in the aqueous phase.

The emulsifier concentration does not have a significant effect on the loading capacity of particles. Particles with higher PLGA concentration leads to higher loading capacity ($p = 0.0044$) which might be attributed to the increase in viscosity of the o-phase, which leads to increase in resistance for diffusion of Ad-eGFP from $w_1$ to $w_2$ phase leading to higher encapsulation. Note that, for a composite particle with 1% PLGA concentration we could only quantify $LC_{cumu}$, as with 1 w/v % PLGA the yield was very low and the entire sample was used to study the *in vitro* Ad-eGFP release. Additionally, when the energy input is kept constant, the increase in PLGA concentration leads to the formation of bigger emulsion droplets which might lead to higher encapsulation.

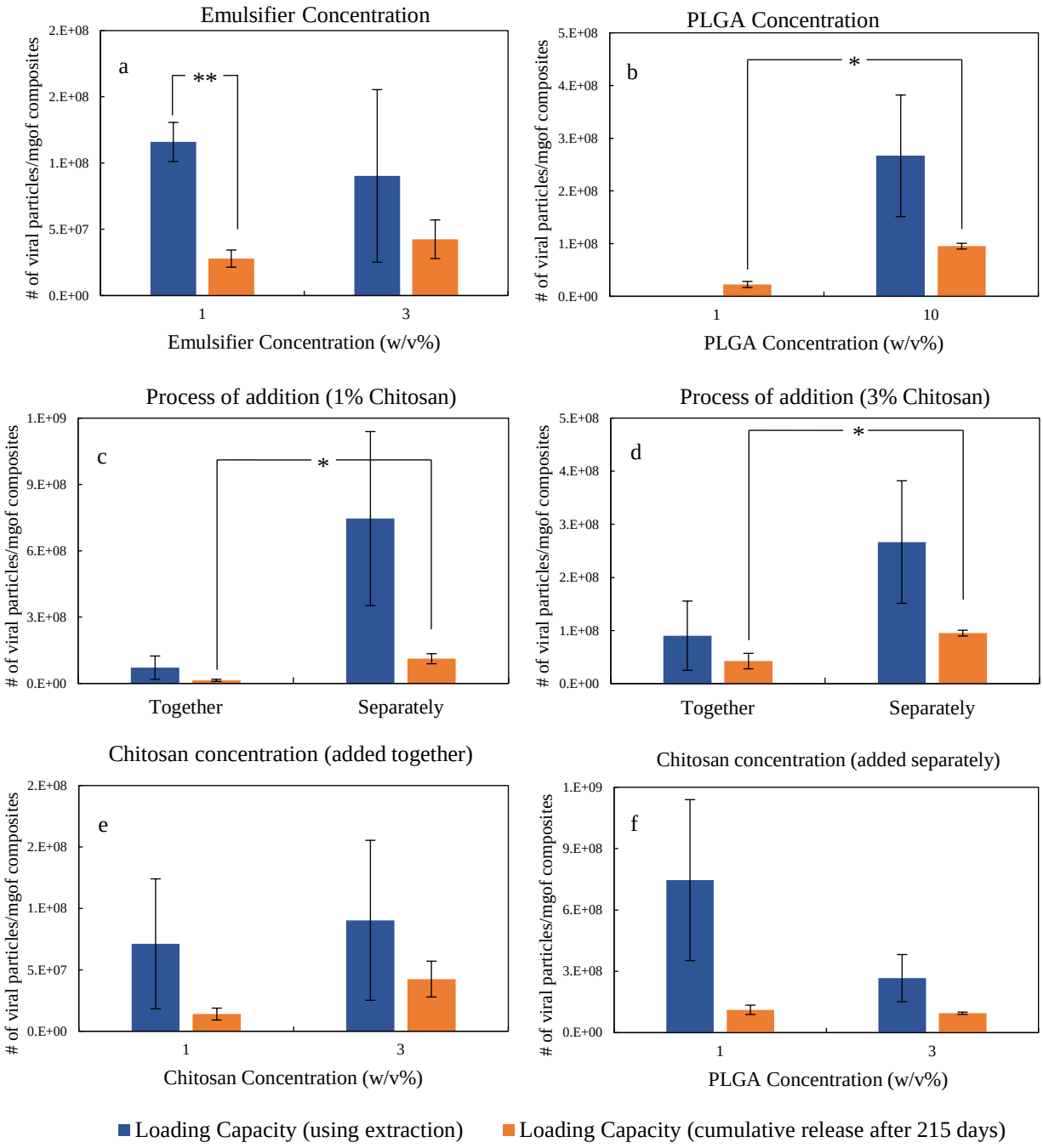


**Figure 3-5:** Effect on $LC_{ext}$ and $LC_{cumu}$ of the particles by varying one of the input process parameters out of emulsifier(PVA) concentration, PLGA concentration, chitosan concentration and process of addition of both the polymers (together or separately). Other parameters for the synthesis are as follows (a) 10% PLGA and 3% chitosan, added together (b) 3% PVA and 3% chitosan; added separately (c) 3 % PVA, 10% PLGA, 1% Chitosan; (d) 3% PVA, 10% PLGA, 3 % Chitosan (e) 3% PVA and 10 % PLGA; added together (f) 3% PVA and 10% PLGA; added separately. All measurements were performed in triplicates (*$p < 0.05$) (**$p < 0.05$)

$LC_{cumu}$ for composite particles when both polymers are added separately led to significantly higher encapsulation ($p_{1\%\ chitosan} = 0.013$ and $p_{3\%chitosan} = 0.008$) as compared to when polymers are added together. When both are added together, the AD-eGFP suspended in the aqueous phase has a tendency to leach out to the outer continuous phase ($w_2$). This leads to their diffusion out of the $w_1$/o emulsion droplets. This tendency to diffuse out could also be attributed to the electrostatic association of Ad-eGFP and chitosan. On the other hand, when both polymers are added separately, PLGA emulsion droplets are partially hardened, and the resistance for their diffusion out of the partially hardened emulsion droplet increases, therefore, leading to higher encapsulation. Moreover, it is also observed that we were able to obtain higher loading capacities with the smaller size of the particles with composite particles. The change in concentration of chitosan did not show any significant change in the loading capacities.

$LC_{ext}$ values of PLGA particles is significantly greater ($p < 0.05$) than all the composite particles indicating higher loading capacity with PLGA particles. This is likely due to leaching of adenovirus from the $w_1$/o emulsion during the production of composite particles, owing to the strong electrostatic attraction between chitosan and adenovirus. Extraction method might not be the most effective method to quantify the loading capacity[89,163] for these type of particles, and a different method similar to digestion method[164] should be used to quantify the encapsulated quantities. We did try to degrade the particles faster using lysozyme, but we observed that the particles did not degrade completely and there were still lumps of polymer left behind leading difficulty to quantify using qPCR (results not shown). Recently it was observed that even for pure PLGA particles extraction method might lead to lower values of loading capacity due to low extraction efficiencies when the organic solvent (acetonitrile) is evaporated from the system[155,163]. Successful encapsulation of adenoviral vectors in pure PLGA and composite particles was demonstrated with loading capacities of more than $10^6$ viral particles/mg of composites.

### 3.3.3 *In vitro* release profiles

Herein, we chose DMEM supplemented with 10% FBS and 1% antibiotics as the release medium as to mimic the *in vivo* conditions. Release of the encapsulated adenoviral vector can be varied by changing

various synthesis parameters like emulsifier concentration, polymer concentrations, the energy input to the system, time of addition of polymers, and the molecular weight of polymers. Some of these parameters are studied herein and their effect on the release profiles is illustrated in this section. It should be noted that the release profiles reported in this section have been shown as scatter plots with connected data points in order to illustrate the trend in the release. These lines are not continuous and do not represent any model fit.

#### *3.3.3.1 Effect of emulsifier concentration:*

PVA is a non-ionic, nontoxic polymer which degrades slowly. It is the most widely used emulsifier for the production of PLGA particles[78]. Usually, a change in PVA concentration has a large effect on the size of the particles as well as the surface morphology[64,107,157] leading to small particles with increasing PVA concentration. The release of Ad-eGFP from the composite particles is illustrated in **Figure 3-6**. It can be seen that the release of Ad-eGFP does not show significant differences in the release profile.

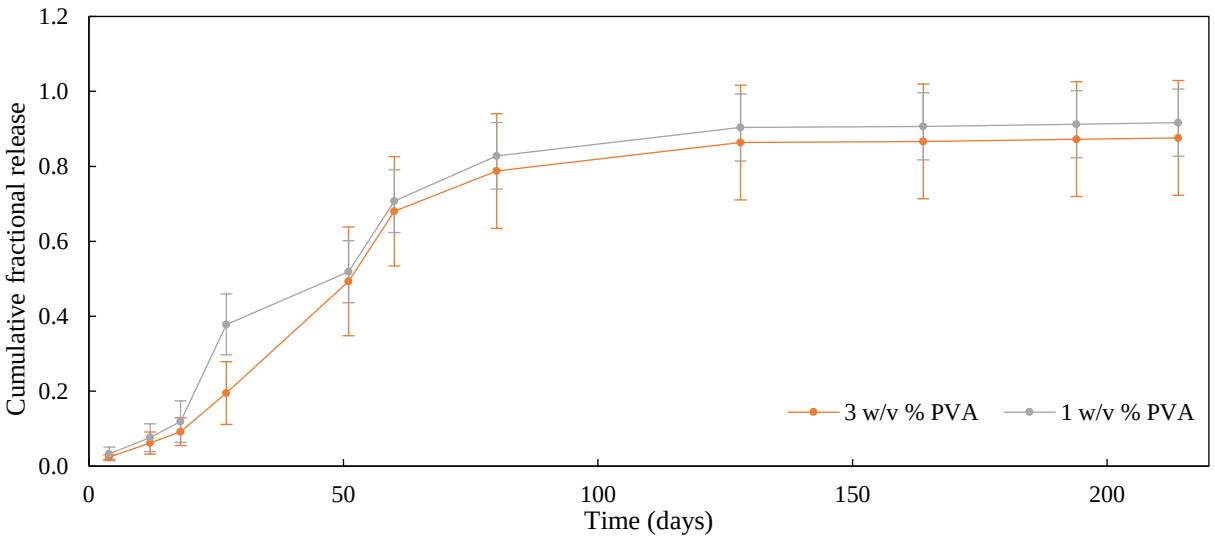


**Figure 3-6:** Release of Ad-eGFP from composite particles with changing emulsifier (PVA) concentration (n = 3)

*3.3.3.2 Effect of PLGA concentration:*

PLGA concentration has an effect on the physical characteristics of the composite particles, and hence this affects the release profile. It is usually seen that higher concentration of PLGA leads to a denser internal structure, therefore low internal porosity[64,78,157] leading to encapsulation at the core of the particle rather than distributed all over the PLGA matrix. The porosity of the particles affects the release profile of the encapsulated molecule, with higher internal porosity leading to faster release[64,159]. Another reason for the higher porosity of the particles is that lower viscosities of the polymer concentration tend to increase the tendency of coalescing the droplets in the inner water phase ($w_1$) leading to bigger pores and less tortuous network[159]. The release profile of Ad-eGFP from the composites is illustrated in **Figure 3-7**. It can be seen that 1 w/v % PLGA concentration gave a faster release of Ad-eGFP as opposed to the Ad-eGFP release from 10 w/v % PLGA. The high porosity of PLGA with low concentration can also be found in case of composites as PLGA emulsion droplets were partially hardened here before chitosan was added. This high porosity might be resulting in lower resistance for diffusion of Ad-eGFP encapsulated and therefore a faster release. Moreover, it has been observed that the degradation products diffuse out of the PLGA matrix slower for the larger particles as the path length for diffusion is bigger than for the smaller particles[157]. This leads in further reduction of the pH in the polymer matrix which can go to as low as 1.5 [165–167] affecting the activity and structure of Ad-eGFP. As increasing the polymer concentration leads to larger particles this might have adverse effects on the integrity of the adenovirus encapsulated.

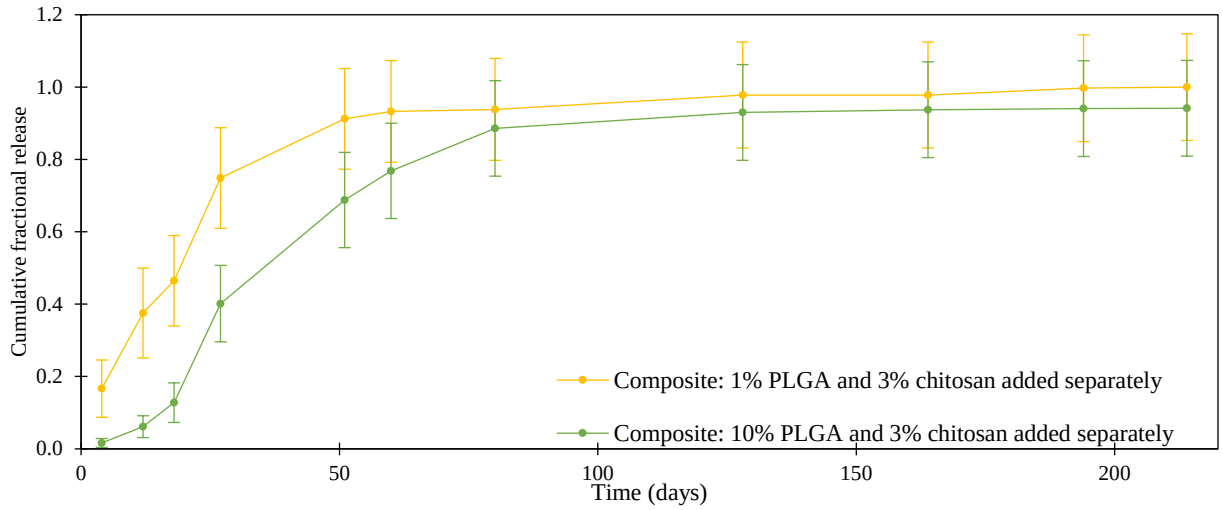


**Figure 3-7:** Release of Ad-eGFP from composite particles with changing PLGA concentration (n = 3)

### *3.3.3.3 Effect of distribution of chitosan in the composite:*

As stated in section 3.1.1, when the process of addition of the polymers was varied it produces composite particles with different distributions of chitosan in the composites. When the polymers were added together, the composite particles had Ad-eGFP encapsulated with PLGA and chitosan incorporated in each other's matrix and when chitosan was added after partial hardening of PLGA particles, i.e., both polymers were added separately it produces Ad-eGFP encapsulated in PLGA particles with chitosan layer on the surface of the particles resembling a core-shell structure. We examined the effect of this process of addition on the release of Ad-eGFP *in vitro* with two different chitosan concentrations. The release profile with the varying process of addition is given in **Figure 3-8**.

It is observed that composites produced with both polymers added together give a faster release as compared to when both polymers added separately. The composites when both polymers are added separately gives a very slow initial release and then shows an increase in the rate of release. When both the polymers are added together, it is likely that as PLGA and chitosan both degrade simultaneously by hydrolysis, leading to the formation of pores on the surface of the particle. As the pores formed increase with time on the surface, it leads to a continuous increase in the release rate of Ad-eGFP.

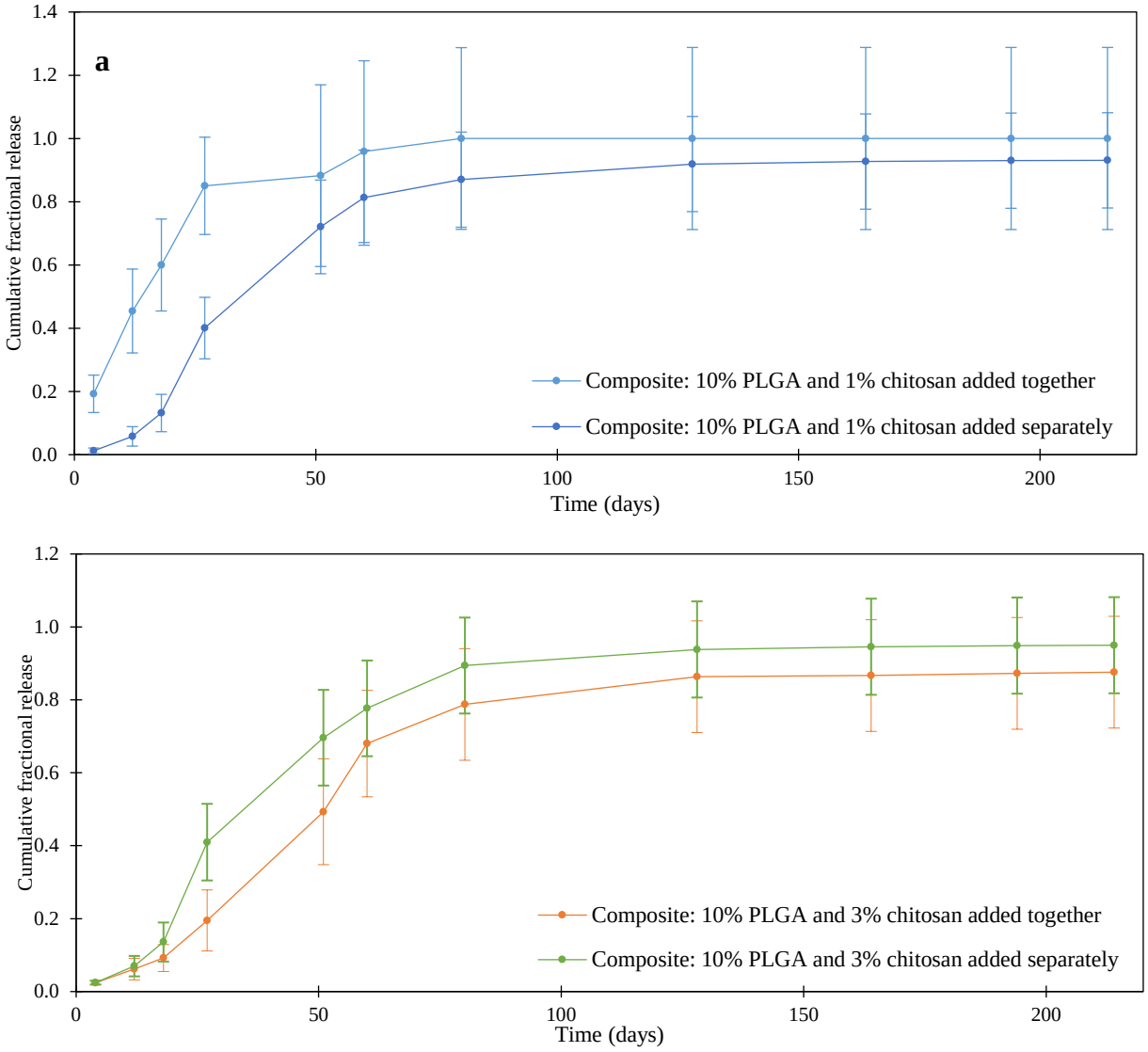


**Figure 3-8:** Release of Ad-eGFP from composites with varying process of addition of polymers. (a) 10% PLGA and 1 % chitosan; (b) 10% PLGA and 3% chitosan. (n = 3)

On the other hand, when polymers were added separately, as PLGA polymer degrades due to hydrolysis the presence of shell of chitosan on the exterior increases the resistance for Ad-eGFP to diffuse in the aqueous phase which might lead to the slow release of Ad-eGFP initially. This lead to simultaneous increase in the osmotic pressure in the interior of the particle as well as increasing the rate of degradation from the interior due to the accumulation of the degradation products which is likely the cause for faster release after 18 days.

*3.3.3.4 Effect of chitosan concentration:*

Chitosan has been used as an excipient in different formulations, such as tablets, matrix, micro- and nanoparticles[121,168,169]. Usually, neutral or anionic particles are used for drug delivery, but cationic polymers like chitosan have been shown to be excellent carriers for DNA, proteins, peptides[169]. Chitosan undergoes degradation by hydrolytic cleavages or can be degraded enzymatically. Chitosan concentration was varied to see an effect on the release profile of Ad-eGFP; we did not use any value above 3% as it was observed that the viscosity of chitosan dissolved in acetic acid increases drastically making it very difficult to handle the viscous solution. When we increased the concentration of chitosan, it is observed that the size of the particles increased significantly with an increase in concentration ($p < 0.05$). The total loading capacity of the composites, however, did not show any significant difference with changing chitosan concentration ($p > 0.05$).

The release profile of Ad-eGFP with changing chitosan concentration is illustrated in **Figure 3-9**. When both polymers were added together (**Figure 3-9(a)**), it can be observed that an increase in the concentration of chitosan leads to slower release. The increase in chitosan concentration might lead to an increase in resistance for the diffusion of Ad-eGFP resulting in a slower release. Alternatively, the presence of higher amount of chitosan in the composite leads to an increase in electrostatic association of Ad-eGFP and chitosan giving a slower release. Furthermore, when both polymers were added separately (**Figure 3-9(b)**), it can be observed that there are no significant differences in the release of Ad-eGFP though their hydrodynamic diameters are significantly different. Therefore, the core-shell structure did give us a slow release followed by an increase in the rate of release but the increase in chitosan concentration is not significant enough to slow the release of Ad-eGFP further. Furthermore, the polydispersity of the composite particles might lead to an increase in variation of the release leading to large error bars in the release profiles.

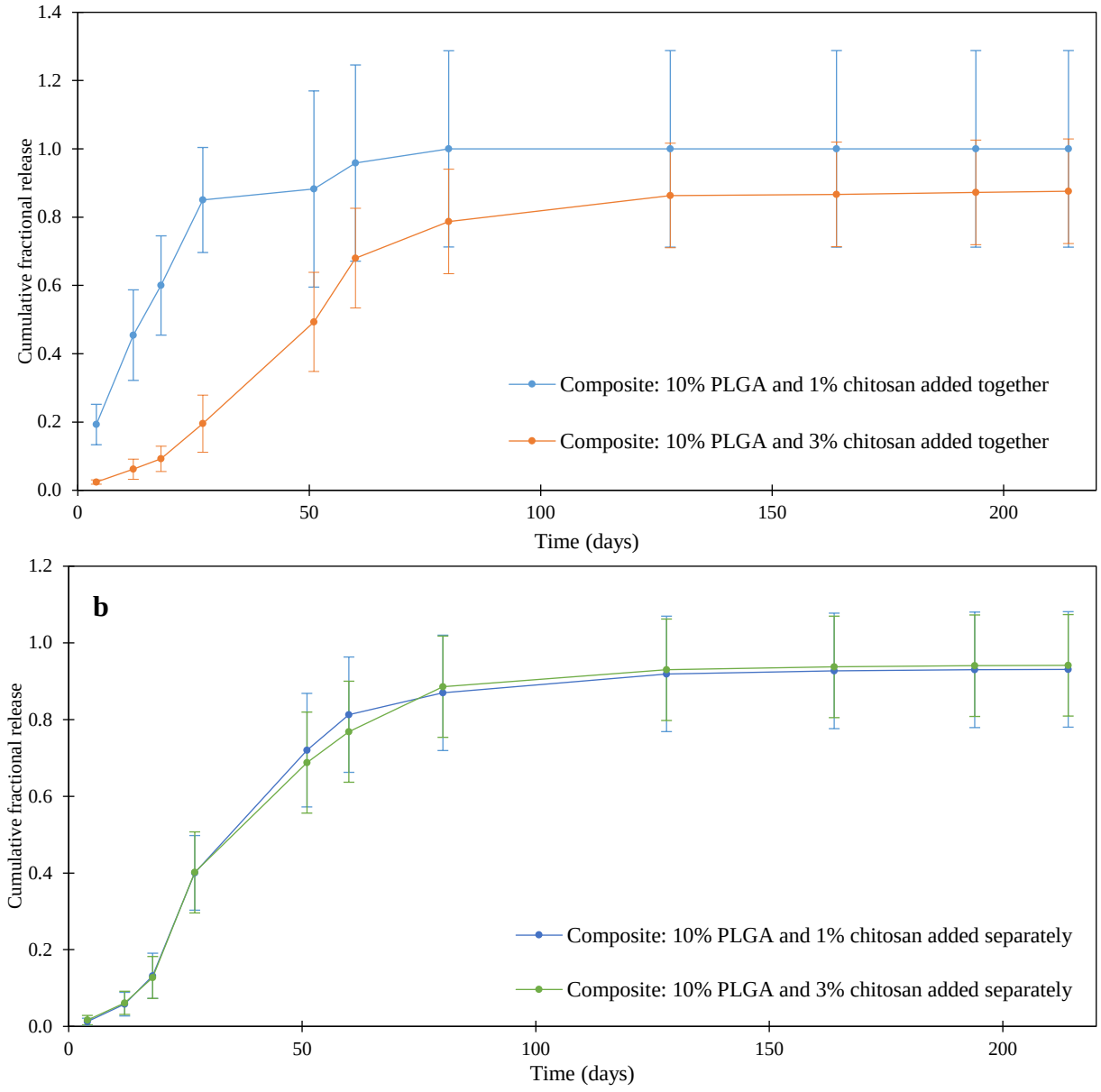


**Figure 3-9:** Release of Ad-eGFP from composites with changing chitosan concentration. (a) Changing chitosan concentration when both polymers added together (b) Changing chitosan concentration when both polymers added at separately (n = 3)

*3.3.3.5 Effect of freeze-drying:*

Lyophilization/freeze-drying is a very well-established and widely used method for preservation of biodegradable particles for long-term storage as well as storage method under sterile conditions[79,169,170]. Particles encapsulated with bioactive macromolecules need to be stored at low temperature for long-term preservation of activity and structure. If the particles are stored in aqueous solutions, these particles start hydrolyzing affecting the integrity of the particles as well as if particles are directly frozen when suspended in aqueous solutions, it leads to developing cracks on the particles and might lead to early leakage of encapsulated molecules[170]. Direct freezing in aqueous solutions will lead to crystallization of ice inducing high mechanical stress on the particles for a long period of time, leading to their destabilization, particle aggregation, the formation of undesired degradation products[127,168,170,171]. Lyophilization is a dehydration process to improve the handling and storage of nanoparticles and to increase their shelf-life. Dehydration occurs through sublimation of aqueous solution under vacuum; even when particle undergoes this process they are put under a lot of stress and therefore many different cryoprotectants like trehalose, mannitol, glucose are used to reduce these stresses[127]. When cryoprotectants are added before freeze drying, they form a glassy matrix around the particles avoiding particle aggregation and reducing the concentration of water and therefore ice crystals around the particles leading to a reduction in mechanical stresses on the particles[127,172]. Among the various cryoprotectants available trehalose is widely used owing to the absence of internal hydrogen bonds, allowing the more flexible formation of hydrogen bonds with nanoparticles during lyophilization, less hygroscopicity and low chemical reactivity[127]. If we increase the concentration of trehalose for freeze drying, it further reduces the concentration of water, reducing freezing stress on the particles. Also, it is found that particles suspended in aqueous media after lyophilization have a similar size distribution as before freezing of the particles[127,170,173].

It was found here that the loading capacity of the particles that were freeze-dried was significantly higher than the ones that were not freeze-dried ($p = 0.008$). This is likely due to the undesired release of Ad-eGFP, changes in the stability of particles and Ad-eGFP, or possible disintegration of Ad-eGFP due to

long exposure to aqueous media. The release of Ad-eGFP from the particle with and without freeze-drying can be seen in **Figure 3-10.** The release profile of both sets of particles is not significantly different. It shows that freeze-drying of the particles will not affect the release profile of Ad-eGFP and also helps in preserving the size distribution and stability during storage.

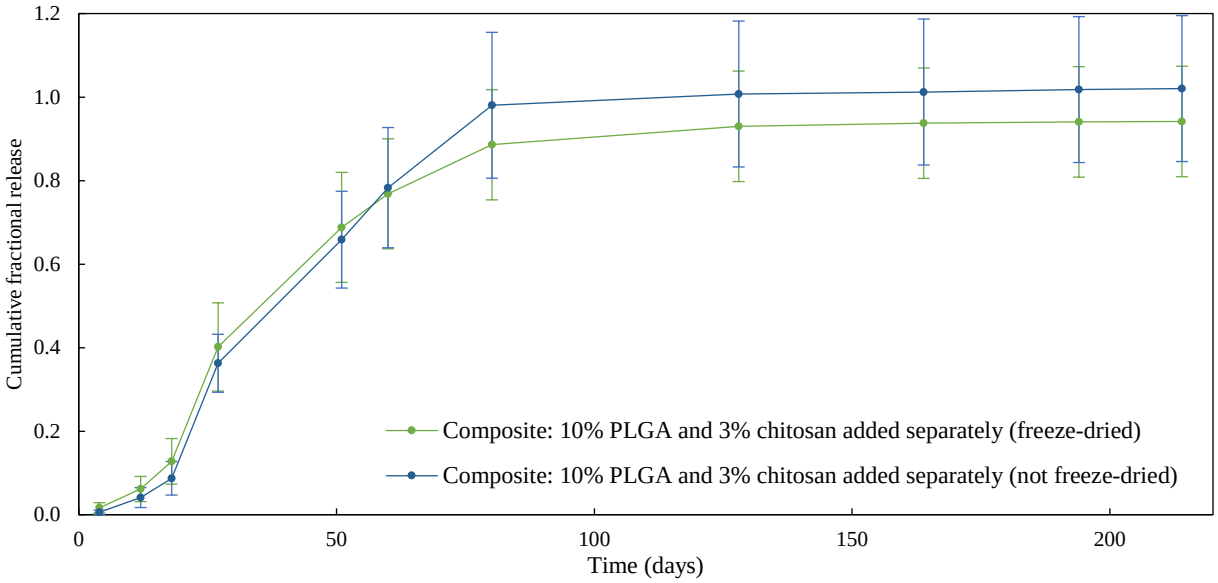


**Figure 3-10:** Release of Ad-eGFP from composites with and without freeze-drying (n = 3).

## 3.4 Conclusion

The properties of materials and the process parameters strongly influence the properties of composite particles and the resultant controlled release rate. In this study, successful encapsulation of adenoviral vector was observed in the composite particles as well as pure PLGA particles using a double emulsion technique which lead to smooth surface morphology. It was possible to modulate the size of the particles by varying the process parameters like emulsifier concentration, PLGA concentration, and distribution of chitosan and chitosan concentration which will play an important role for manipulating the release of the adenoviral vector *in vitro* and *in vivo*. Increase in emulsifier concentration lead to smaller particles with a more narrow size distribution; this change did not affect the loading capacity and the rate of release. Increase in PLGA concentration led to higher loading capacities with slower release of Ad-eGFP, but it should be noted that increase in PLGA concentration also leads to the denser internal structure as well as bigger

particles which might affect the activity of adenovirus encapsulated. On the contrary, the chitosan concentration did not have significant effects on the loading capacities as well as the release profile of the particle. We successfully modified the distribution of chitosan in the composites creating two distinct composites which had a significant effect on the size, loading capacity as well as the release of Ad-eGFP. It is observed that we could get higher loading capacities with the small size of the particles when both polymers were added separately which might lead to higher stability of macromolecules in the particles. The variation of process parameters had a significant effect on the size of the particles whereas the release of Ad-eGFP is related to polymer concentrations and distribution of chitosan in the composite particle. Further optimization with a change in polymer molecular weight could be performed to modulate the release of adenovirus.

## Chapter 4: Conservation of Adenoviral Activity

Recombinant human adenoviral vectors have the ability to transfer genes efficaciously to a range of cell types in vivo. These non-replicating adenoviral vectors have been engineered to incorporate and express a variety of antigens and are safe for the host and environment. Adenoviral vector system has been shown to induce potent humoral and cell-mediated immune responses, exhibits intrinsic adjuvant properties, induces innate immunity, has effective immunological memory, provides a natural presentation of immunogens and has a broad host tropism. Ad5-vectored vaccines have demonstrated to be adaptable for induction of protective immunity in humans and a large variety of experimental animal species. Moreover, they do not vary significantly as a function of either the antigen being expressed or the species being immunized. Therefore, the range of pathogens that can be addressed and the host species that can be protected are virtually limitless as long as the molecular antigen is characterized and can be synthesized by recombinant methods. In spite of these important characteristics and their extensive successful use in humans and experimental animals, this technological opportunity has been underutilized. Determination of adenoviral vector activity is crucial to its use *in vivo*. It is possible that encapsulated Ad-flu did undergo physical and chemical changes like hydrolysis, deamidation, and aggregation[16]. Higher temperatures impart energy that increases the chances of Ad-flu attaining a non-native conformation; aqueous media further increases Ad-flu degradation by increasing mobility and rate of hydrolysis and deamidation[16].We quantified the activity of Ad-eGFP using Fluorescent Focus Unit Assay (FFU) after encapsulation. The biological activity of encapsulated and released vector are determined using a focus-forming assay in which the concentration of biologically active vector particles is assayed by enumerating the number of infected cells 48 hours after a series of sample dilutions are inoculated onto 293-HEK cells.

## 4.1 Material and methods

### 4.1.1 Materials

All materials were purchased from commercial suppliers and used without further modification unless noted otherwise. Enhanced green fluorescent expressing adenovirus type 5 (Ad-eGFP) with CMV promoter at a titer of $1 \times 10^{11}$ PFU/ml was purchased from Vector BioLabs (Malvern, PA). Dulbecco Modified Eagle Medium (DMEM) was purchased from HyClone, GE Healthcare Life Sciences (Logan, Utah), Irradiated and heat inactivated Fetal Bovine Serum (FBS) was purchased from VWR Life Sciences Seradigm (Radnor, PA) and penicillin/streptomycin (antibiotic) was purchased from Corning Cellgro (Manassas, VA). Deionized water used throughout the study was obtained from a Milli-Q Purelab Flex 2 water purification system (Elga LLC, Woodridge, IL). 293 - Human Embryonic Kidney (HEK) cells were purchased from ATCC (Manassas, VA) and maintained with DMEM media supplemented with 10% FBS and 1% antibiotics.

### 4.1.2 Fluorescent Focus Unit Assay

293 - HEK cells were plated in a 24-well plate at a concentration of $1 \times 10^5$ cells/well. While plating the cells, viral concentrations ($5 \times 10^7$ to $2 \times 10^8$ viral pt/ml) were added to the wells along with the media to create a standard curve. Additionally, Ad-eGFP encapsulated in the particles (0.5 mg/ml) was incubated with the cells. These cells were incubated with Ad-eGFP for 24 hours followed by measuring the fluorescent foci on the microscope. Fluorescent images were captured with an EVOS cell imaging system (ThermoFisher Scientific, Waltham, MA, USA). These foci were counted using the ImageJ software developed at the National Institutes of Health, USA.

## 4.2 Results

### 4.2.1 FFU Assay

FFU assay shows information on the activity of viral particles present as compared to qPCR which will give us a viral concentration comprising of both active and inactive virus. Various dilutions of Ad-eGFP ($5 \times 10^7$ to $2 \times 10^8$ viral pt/ml) were incubated with the plated cells for 24 hours. Incubation of Ad-eGFP with the cells leads to an increase in foci formed with time as shown in **Figure 4-1.**

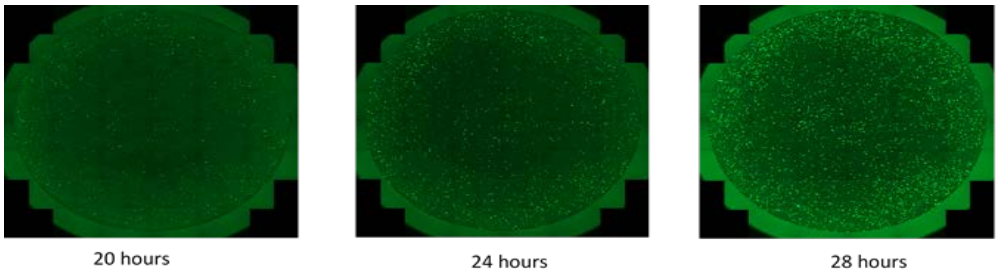


**Figure 4-1:** Images taken using optical microscope at various time intervals. These foci formed were counted using ImageJ to get a standard curve.

### 4.2.2 Conservation of Adenoviral Activity

The activity of Ad-vectors might be hampered during the production of particles using the double emulsion technique[16,60,76,174]. Therefore, our synthesis procedure could affect the adenoviral activity. In order to verify the encapsulated Ad-eGFP was active, particles at the concentration of 0.5 mg/ml were incubated with 293 HEK cells. It was observed that even after encapsulation, adenovirus still retained its activity (**Figure 4-2**).

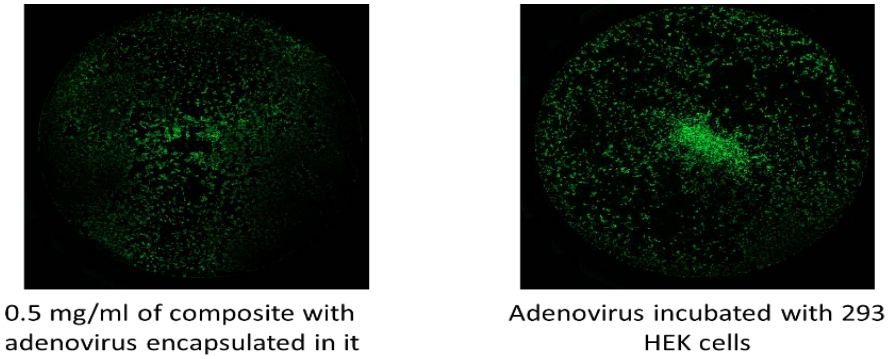


**Figure 4-2:** Adenoviral activity was conserved even after the synthesis procedure which involved using organic solvents which may have dissociated the virus.

# Chapter 5: An *in vitro* and *in vivo* study to control the release of adenoviral vectors from polymeric composite particle

## 5.1 Introduction

Vaccines are medicines one of medicine's most significant accomplishments. They have saved more lives and prevented more human and animal suffering than any other single medical intervention. Vaccines are noteworthy as they not only help treat the diseases but effective administration helps us eradicate the disease as well. Smallpox has been eradicated[29,32], and polio is on the brink of elimination[33], due to aggressive vaccination campaigns. Diseases such as measles, mumps, rubella, diphtheria, tetanus, pertussis, *Haemophilus influenzae* type b (Hib) disease, polio, and yellow fever are now under control due to vaccination[29]. Other diseases, including hepatitis B virus (HBV), foot and mouth disease in cattle and pneumococcal infection are better contained due to vaccines, but there is still much that needs to be done to eradicate many such diseases, even in the developed world[29].

Small molecule drug delivery has advanced tremendously in the past few decades that we no longer depend only on the conventional pharmaceutical formulation to treat diseases like diabetes, cancer, infectious diseases[7–16]. Delivery of vaccines has lagged behind these important new technological advances since we still depend on traditional dosage systems since the 1900s in humans as well as animals[16,30,35]. Spectacular advances in immunology and the advent of molecular medicine has given us remarkable opportunities to develop delivery systems that can help us gain full potential of these vaccines.

Vaccines work by mimicking disease agents and stimulating the immune system to build up defenses against them[30,35]. A vaccine typically consists of a disease-causative microorganism which is often prepared from killed or inactivated forms of the microbe, its toxins (referred to as toxoids) or one of its surface proteins[40]. It stimulates the body's immune system to recognize it as a risk, destroy it, and retain a record of it, and any such consecutive related infection can be more easily recognized by the immune system and destroyed. Recent approaches have focused on utilizing technologies such as recombinant DNA methods

to develop DNA and subunit vaccines, as well as conjugate vaccines in which a weak antigen is linked to a stronger immunogen such as a protein or membrane complex[22]. With the advent of this new technology, new delivery devices and new efforts for efficient vaccine dosages are required. Some examples of recent developments in the different types of vaccines as well as delivery systems are viral vectored vaccines, virosomes, virus-like particles (VLPs), polymeric delivery devices, liposomes, immunostimulating complexes[16,28,34,36,40,49].

While older vaccines require complex, costly and time-consuming industrial manufacture of antigens, vectored vaccines can be designed, synthesized and expanded rapidly and economically. Modern vaccine development is increasingly seeking novel adjuvants and delivery systems to boost immunogenicity. Immune responses by viral vectored vaccine have found to increase when a prime-boost regimen is employed. These vectors are themselves immunostimulatory and they are safe for the patient, operators and the environment. This type of delivery system has many advantages like ease of production, a good safety profile, and potential for nasal and mucosal immunization[25,55,56]. Adenovirus has provided vector platform for various vaccines like influenza[56], tetanus[55], HIV based vaccines[25,40]. The prime-boost regimen has been found to induce strong T cell responses leading to its current status as a promising technology. This vector system has been shown to induce potent humoral and cell-mediated immune responses, has intrinsic adjuvant properties, induces innate immunity, has effective immunological memory, provides a natural presentation of immunogens and has a broad host tropism[10,24,41].

The multi-bolus regimens of vaccine administration are unfeasible in case of animals as well as human beings. A single dose composition to eliminate the need for reimmunization will help transform traditional vaccines to achieve full and sustained protection. Nanotechnology offers incredible potential in the biomedical field with abilities like control size, shape, composition and surface properties. Use of nanotechnology in vaccinology has grown so rapidly that it has led to the coining of the term “nanovaccinology.” The idea of using controlled release technologies to simplify vaccination schedules was first proposed by Preis and Langer[38]. PLGA has attracted a very high interest due to its potential as a

drug carrier in the controlled release of encapsulated drugs and is the most frequently used biodegradable polymer to be used as a single dose vaccine[16,47,48,84,90,155,175,176]. Using polymeric particles, we do get a continuous release of the vaccine[86–90,92,93], but in order to resolve the shortcoming of the prime-boost regimen in vaccine delivery, we need a better delivery system. Chitosan is enzymatically or chemically produced from chitin by deacetylation. Chitosan is an attractive material due to its fibrous nature, hydrophilicity, biocompatibility, biodegradation, and potential adjuvancy properties. Chitosan can be metabolized by enzyme like lysozyme which naturally presents in the body. Chitosan exhibits antibacterial[113], non-toxicity[109], immunomodulating[34] and mucoadhesive properties. Chitosan polymer is also responsive to structural and surface manipulation according to the intended application[114]. Different degradation kinetics of both the polymers used may be promising to achieve a pulsed delivery system for vectored vaccines.

Herein, we used an adenoviral vectored vaccine encapsulated in the biodegradable and biocompatible polymeric composite particles. Double emulsion process is a widely studied procedure for the synthesis of PLGA particles and is easily scalable. This process is utilized here with minor modifications to synthesize PLGA as well as PLGA-chitosan composite particles.

## 5.2 Materials and methods

### 5.2.1 Materials

All materials were purchased from commercial suppliers and used without further modification unless noted otherwise. Poly-lactic glycolic acid (PLGA) with lactide: glycolide ratio of 50:50 (MW 30 – 60 kDa) (inherent viscosity 0.55-0.75 dL/g), low molecular weight chitosan (MW 50 – 190 kDa) (viscosity in 1 w/v % acetic acid is 20-300 cps), polyvinyl alcohol (PVA) (MW 30 – 70 kDa) (viscosity in water 4 - 6 cps), D-(+)-trehalose dehydrate were purchased from Sigma Aldrich Chemical Co. (St. Louis, MO). Dichloromethane (DCM), acetic acid (AA), acetonitrile (ACN) were of analytical grade. Ad-flu was supplied by Altimmune Inc. (Gaithersburg, MD). Deionized water used throughout the study was obtained

from a Milli-Q Purelab Flex 2 water purification system (Elga LLC, Woodridge, IL). Dulbecco Modified Eagle Medium (DMEM) was purchased from HyClone, GE Healthcare Life Sciences (Logan, Utah), Irradiated and heat inactivated Fetal Bovine Serum (FBS) was purchased from VWR Life Sciences Seradigm (Radnor, PA) and penicillin/streptomycin (antibiotic) was purchased from Corning Cellgro (Manassas, VA). PerfeCTa SYBR Green FastMix was purchased from Quantabio (Beverly, MA) for real-time PCR analysis. PCR primers for quantification of Ad-flu were purchased from ThermoFisher (Carlsbad, CA)

### 5.2.2 Synthesis of PLGA particles

PLGA particles were prepared by double emulsion method at room temperature reported by Nagai et al.[89] with minor modifications. In brief, 700 µl of Ad-flu ($4.6 \times 10^{10}$ ifu/ml) was added to 10 w/v % solution of PLGA (100 mg PLGA dissolved in 1 ml DCM). This mixture was sonicated at 5 % amplitude for 30 seconds to create a water-in-oil ($w_1/o$) emulsion. 5ml of 3 w/v % PVA was added, and this mixture was sonicated at 5% amplitude for 30 seconds to create a water-in-oil-in-water ($w_1/o/w_2$) emulsion. This mixture was added to 15 ml PVA in round bottom flask in order to keep water to oil ratio constant at 1:20. This mixture was stirred for 4 hours to let the DCM evaporate and harden the nanoparticles. After the stirring was completed, the particles were centrifuged at 10,000 rpm for 20 min and given 4 washes with DI water. The particles were suspended in 1 ml 2 w/v % trehalose in DI water and frozen at $-80^0$C overnight; then lyophilized overnight at a temperature of $-105^0$C and pressure of 0.01 mbar using a Labconco FreeZone-4.5 lyophilizer (purchased from Labconco Corporation, Kansas City, MO). These lyophilized particles were stored at $-80^0$C until further use. **Table 5-1** summarizes further results.

### 5.2.3 Synthesis of PLGA-Chitosan composite particles

700 µl of Ad-flu ($4.6 \times 10^{10}$ ifu/ml) was added to 10 w/v % solution of PLGA (100 mg PLGA dissolved in 1 ml DCM). This mixture was sonicated at 5 % amplitude for 30 seconds to create a water-in-oil ($w_1/o$) emulsion. 1 ml solution of 3 w/v % chitosan dissolved in 0.1M AA was added, and this mixture was sonicated again at 5 % amplitude for 30 seconds to create a water-in-oil-in-water ($w_1/o/w_2$) emulsion. 5 ml

3 w/v % PVA was added to this mixture followed by sonication at 5 % amplitude for 30 seconds. This mixture was added to 14 ml PVA in round bottom flask in order to keep water to oil ratio constant at 1:20. This mixture was stirred for 4 hours to let the DCM evaporate and harden the nanoparticles. A slight modification was used to synthesize core-shell structure of particles. Briefly, after the preparation of $w_1/o$ emulsion, 5 ml of 3 w/v % PVA was added and a $w_1/o/w_2$ emulsion was created by sonication at 5% amplitude for 30 seconds. This emulsion was further added to 14 ml of PVA in round bottom flask. Chitosan solution was added after 2 hours after partial hardening of PLGA, and this solution was stirred further for 2 hours.

After the stirring was completed, the particles were centrifuged at 10,000 rpm for 20 min and given 4 washes with DI water. The particles were suspended in 1 ml 2 w/v % trehalose in DI water and frozen at -$80^0$C overnight and were lyophilized overnight at a temperature of -$105^0$C and pressure of 0.01 mbar using a Labconco FreeZone-4.5 lyophilizer. These lyophilized particles were stored at -$80^0$C until further use. Controls were synthesized using the same method without addition of Ad-flu. **Table 5-1** summarizes further results.

### 5.2.4 Particle sizing and surface morphology

#### *5.2.4.1 Dynamic Light Scattering (DLS)*

The hydrodynamic diameter, polydispersity index (PDI) and surface charge (zeta potential) of composite particles were analyzed by dynamic light scattering and laser Doppler electrophoresis using Zetasizer Nano ZS (Malvern Instruments Inc., UK). The size of PLGA and composites were characterized by backscatter detection (173°), and the zeta potential was calculated using Smoluchowski model[152]. Measurements were performed with particles collected after $4^{th}$ wash in DI water.

#### *5.2.4.2 Scanning Electron Microscopy*

Surface Morphology of PLGA and composite particles were characterized using Zeiss EVO50 SEM operating at a voltage of 20K. Freeze dried particles were laden on a double-sided carbon tape which was

mounted on Al-stub, and this stub was gold-coated using (write model) to avoid melting of particles due to high energy electron beam.

#### *5.2.4.3 Fourier Transform Infrared Spectroscopy (FTIR)*

The existence of both PLGA and chitosan was determined with FTIR analysis of the particles. Freeze dried particles were placed directly on the diamond crystal which was used for analysis. A Nicolet 6700 was used for analysis with 32 scans of each sample. Data is converted to percentage absorbance for analysis.

### 5.2.5 *In vitro* release studies

In 1.5 ml Eppendorf tube, approximately 1 mg of each type of freeze-dried composite was weighed in triplicates and suspended in 1.2 ml DMEM culture media through sonication at 5 % amplitude and vortexing. These tubes were incubated at $37^0$C on a RotoFlex tube mixer for a total of 120 days with intermediate sample collection described below. After every time point, the tubes were taken out of the incubator and centrifuged at 7000 rpm for 10 minutes in a microfuge. 1ml of the supernatant was removed from these tubes, and fresh 1 ml of DMEM media was added to maintain the sink conditions. These particles were suspended again using vortexer and incubated at $37^0$C on a RotoFlex tube mixer until next collection point. The collected supernatant was stored at $-80^0$C until further analysis.

### 5.2.6 Real-time polymerase chain reaction (qPCR)

Loading capacity and analysis of the released Ad-flu at every time point was characterized using qPCR. Briefly, to quantify loading capacity of the particles, 1mg of each of the composites and pure PLGA particles were dissolved using 600 µl of ACN at 175 rpm and $23^0$C in a shaking incubator to extract the Ad-flu encapsulated in the particles. After 4 hours of incubation, 1 ml of DI water was added to these vials, and further incubation was carried out at $40^0$C and 275 rpm overnight to evaporate the ACN in water. Ad-flu encapsulated in the ACN phase is now suspended in the water phase which can be further used for analysis.

The collected supernatant (from *in vitro* studies) for each sample was thawed at room temperature. 400 µl of each sample was pipetted in a vial to which 600 µl of ACN was added followed by further incubation at 175 rpm and $23^0$C. After 2 hours of incubation, 1 ml of DI water was added to these vials, and further incubation was carried out at $40^0$C and 275 rpm overnight to evaporate the ACN in water. Ad-flu now suspended in the aqueous phase was then analyzed using qPCR. The primer sequence used for the PCR analysis are as follows: Forward primer: 5' - ATT TCT GTC CAG TTT ATT CAG CAG - 3' and Reverse primer: 5' - AAG ATA GTG GGT GCG GAT GG - 3'. TaqMan real-time quantitative PCR was carried out using the Bio-Rad CFX96 Touch™ real-time PCR detection system (Hercules, CA). The final reaction volume of 20 µl consisted of 10 µl SYBR Green FastMix, 0.04 µl of each primer (10 µM), 4.92 µl DNase free water, and 5 µl template solution. All samples were amplified under the following conditions: $95^0$C for a 3-min, then 39 cycles of $95^0$C for a 10-second hold, $55^0$C for 30-second hold. The results were analyzed with Bio-Rad CFX Manager (Bio-Rad Laboratories, Hercules, CA). The amplification and standard curves are reported in **Appendix 2**. Loading capacity and encapsulation efficiency were calculated using the following equations:

$$\%\ Encapsulation\ Efficiency = \frac{\left(\frac{viral\ particles}{mg\ of\ PLGA}\right) \times 100}{\frac{(Total\ number\ of\ viral\ particles)}{mg\ of\ PLGA}}$$

$$Loading\ Capacity = \frac{(Total\ number\ of\ viral\ particles\ )}{(Total\ weight\ of\ the\ particles\ )}$$

5.2.7 *In vivo* studies to determine an antibody response

The female CD-1 outbred stock of mice was purchased Charles River Laboratories (Wilmington, MA). These mice were about 9-weeks old when purchased with an average weight of about 31 gm. All mice handling procedures were approved in accordance with the NIH and Auburn Institutional Animal Care and Use Committee (IACUC) guidelines. The mice were maintained on a normal diet throughout the study. To

determine an optimum antibody response, following dosages were given subcutaneously to all the mice at time zero: a.) 5 mice with 1 x $10^6$ ifu/mouse; b.) 5 mice with 1 x $10^7$ ifu/mouse; c.) 5 mice with 1 x $10^8$ ifu/mouse; and d.) 3 mice with buffer. Mice were sacrificed at 30 and 60 days and their sera were collected using the following procedure. Mice were anesthetized with a mixture of ketamine and dexmedetomidine diluted in saline, injected intraperitoneally. After mice reached general anesthesia (as determined by lack of response to toe pinch), the left axilla was incised so as to form a tissue pocket from which blood from great vessels of the axilla was aspirated into a 1ml syringe and transferred to a microcentrifuge tube. The injection site and visceral organs were examined for lesions and any suspected abnormalities visually. This serum collected from the mice was further analyzed with Hemagglutination (HAI) assay.

### 5.2.8 *In vivo* studies to determine the antibody response from the Ad-flu released from the particles

The female CD-1 outbred stock of mice was purchased Charles River Laboratories (Wilmington, MA). These mice were about 9-weeks old when purchased with an average weight of about 31 gm. All mice handling procedures were approved in accordance with the NIH and Auburn Institutional Animal Care and Use Committee (IACUC) guidelines. The mice were maintained on a normal diet throughout the study. To evaluate the release of Ad-flu from the particles, CD1 female mice were injected with Ad-flu encapsulated in pure PLGA and composite (10% PLGA and 3% chitosan added at different times) particles. Mice were sacrificed at 28, 63, 107 days and mice sera were collected for further analysis using the procedure mentioned in **Section 5.2.7**. HAI assay was performed with these sera. Following groups were used: 18 (6+6+6) mice were injected intramuscularly with non-encapsulated Ad-flu, 23 (8+8+7) mice were given intramuscular injection with non-encapsulated Ad-flu, and subcutaneous injection of Ad-flu encapsulated in PLGA, and 25 (8+8+9) mice were given intramuscular injection with non-encapsulated Ad-flu, and subcutaneous injection of Ad-flu encapsulated in composite particle. Negative controls included 14 (5+5+4) mice with no treatment.

### 5.2.9 HAI Assay

In order to detect the anti-influenza antibodies, hemagglutination inhibition assay (HAI) was performed. Briefly, 150 µl of serum was mixed with 450 µl receptor destroying enzyme II (RDE) in Eppendorf tubes and incubated at $37^0$C. After 18 hours of incubation, this reaction was inhibited by incubating these tubes at $56^0$C in a water bath for 30 min. These tubes were then centrifuged, and the supernatant was removed; 900 µl of PBS was added to these tubes with storage of tubes at 2 – $8^0$C until further use. 25 µl of RDE treated sera was mixed with 25 µl of PBS solution in 96 well plates followed by addition of 25 µl of influenza virus to test sera. This plate was incubated for 45-60 min at room temperature. 50 µl of 0.5 % red blood cell solution was added to each well followed by incubation at room temperature for 45-60 min. Then the plate was read with the HI titer recorded as the highest dilution of the sera with a well-formed button. Positive controls and negative controls were also utilized to test the reliability of the assay.

### 5.2.10 Statistical Analysis

All experiments were completed in triplicate (n =3). Results are shown as the average of all replicates ± standard deviation. Results were compared using Student's T-test or one-way ANOVA, where applicable, and considered significant with p values less than 0.05.

## 5.3 Results and Discussion

### 5.3.1 Physical properties of PLGA and composite particles

Factors like PLGA concentration, chitosan concentration, emulsifier concentration, polymer molecular weight, time addition of polymers have an effect on size, surface charge, the release of macromolecule encapsulated, and degradation of the particles[16,154,155]. Particles 1 and 2 were synthesized by addition of both the polymers (PLGA and Chitosan) at the same time to produce a composite particle with PLGA and chitosan polymers incorporated in each other's matrix. Particles 3 and 4 were synthesized by addition of chitosan after partial hardening of PLGA particles to produce a core-shell structure with Ad-flu

encapsulated inside PLGA with chitosan on the outside constituting as the outer layer. These two structures were synthesized to investigate the effect of particle's inherent structure on the release profile of Ad-flu. **Table 5-1** summarizes on initial process conditions, size and surface charge.

**Table 5-1:** Initial process parameters with size and surface charge

| Sr no | PLGA (w/v %) | Chitosan (w/v %) | Ad-flu (ifu/ml) | Size (nm) | PDI | Zeta Potential (mV) |
|---|---|---|---|---|---|---|
| 1 | 10 | 3 | $4.6 \times 10^{10}$ | 4130 ± 312.4 | 0.363 | 38.2 ± 0.83 |
| 2 | 10 | 3 | 0 | 2196 ± 177.8 | 0.51 | 40.7 ± 0.17 |
| 3 | 10 | 3 | $4.6 \times 10^{10}$ | 1878 ± 139.4 | 0.085 | 40.0 ± 0.63 |
| 4 | 10 | 3 | 0 | 1634 ± 288.1 | 0.265 | 2.4 ± 0.35 |
| 5 | 10 | 0 | $4.6 \times 10^{10}$ | 1569 ± 137.8 | 0.243 | -9.9 ± 0.13 |

$o/w_2$ ratio was kept constant at 1:20; Particles 1 and 2 were synthesized by addition of both the polymers (PLGA and Chitosan) together whereas particles 3 and 4 were synthesized by addition of chitosan after partial hardening of PLGA particles. Particles 2 and 4 are respective controls with no Ad-flu encapsulated. All measurements were performed in triplicates.

Zeta potential is the potential at the slipping/shear plane of a particle moving under the influence of electric field. It is also termed as the potential difference between the electric double layer of electrophoretically mobile particles and a layer of dispersant around at the slipping plane[152]. This data obtained from the dynamic light scattering can be used to examine the surface charge of the particle. PLGA polymer is an anionic polymer due to the presence of hydroxyl groups[78] whereas chitosan is a cationic polymer due to the presence of primary amines[113]. The zeta potential of pure PLGA particles shows a negative zeta potential however we see a shift towards positive zeta potential in case of both types of composites indicating the presence of chitosan on the surface of particles.

Size of particles plays a very important role in the degradation of PLGA, and consequently, the release of the molecules encapsulated in the particle. Size has a large impact on the encapsulation efficiency, release

profile, toxicity, uptake of the particles by the cells, determining the rate of surface or bulk erosion of the particles[47,78,107,154,156,177,36–39]. It has been discovered that bulk erosion dominates in larger particles as the path length of the diffusion of low molecular weight oligomers and monomers is shorter than that for the larger particles[178,179,181]. Addition time of the polymers plays a very important role in the release profile, as the inherent structure produced after the synthesis is completely different. When both the polymers were added together, PLGA and chitosan get embedded in each other's matrix through a phenomenon called complex coacervation[182,183] whereas when both the polymers were added separately, it creates a core-shell structure with PLGA particles and chitosan layer on the outside. The difference in hydrodynamic diameters of these two composites (composite # 1 and 3) are statistically significant ($p = 0.006$). The time of addition of polymers also has an effect on the polydispersity index of the particles displaying composite particles with the core-shell structure as highly monodispersed (PdI = 0.085). Pure PLGA particles are smaller than composite particle 1 ($p = 0.007$), but the pure PLGA and composite particle 3 are similar in size ($p = 0.2$).

**Figure 5-1** shows the scanning electron micrographs for composites as well as pure PLGA particles. We can see that the PLGA particles and composites synthesized by double emulsion method here were basically spherical in shape and have a smooth surface. Smooth surface is essential to prevent leaching of any Ad-flu encapsulated in the particles. Micrograph (a) shows a hollow particle resembling a core-shell structure. This type of structure is usually seen when particles are manufactured using double-emulsion method[89]. In general, it was observed that the pure PLGA particles were mechanically "weak" as compared to the composite particles as it was observed that when the electron beam was incident on PLGA particles (**Figure 5-1e**), these particles started collapsing; but it was not observed in the composite particles which might be mechanically reinforced by the presence of chitosan did now show this phenomena.

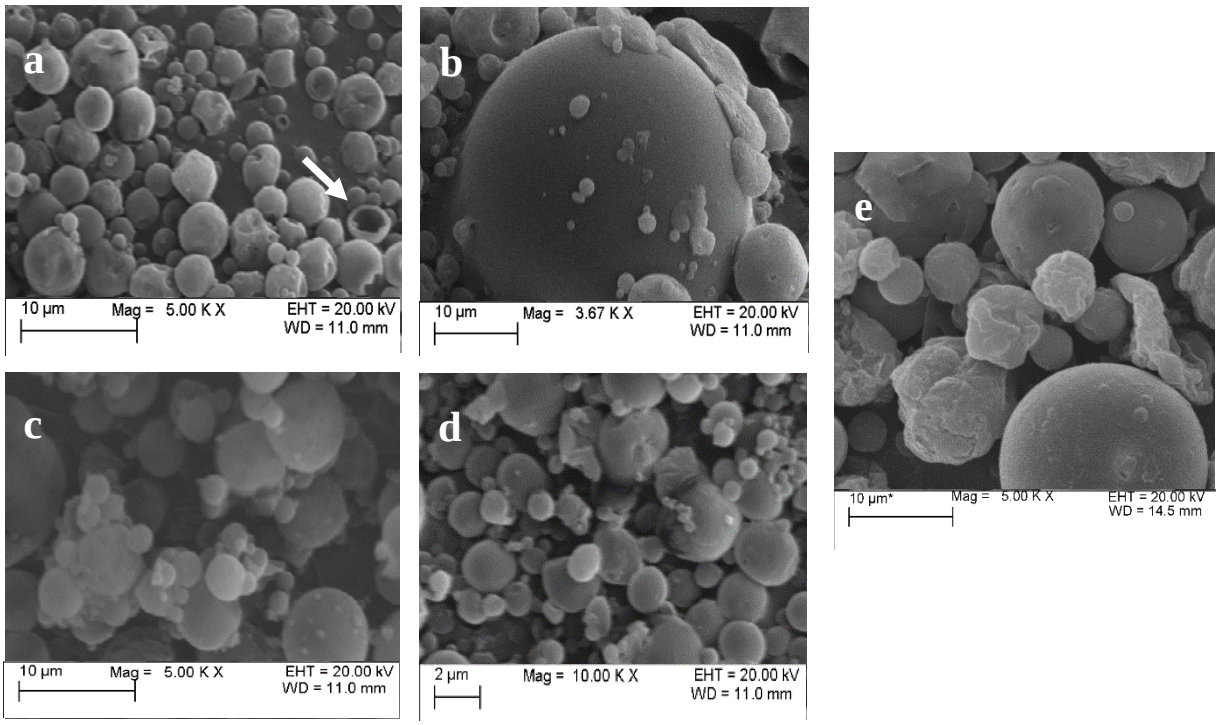


**Figure 5-1:** Scanning electron micrographs of composite particles and PLGA. (a) and (b) represent the composite particles with 10 wt% PLGA and 3 w/v % chitosan added together; whereas (c) and (d) represent composite particles with 10 wt% PLGA and 3 w/v % chitosan added at different times; and (e) represents pure PLGA particle

The vibrational spectrum of chemical bonds in the molecule is considered to be a unique property and characterizes that molecule[160]. The qualitative aspects of FTIR are one of the most powerful attributes of this versatile analytical technique. Both the polymers PLGA and chitosan have a distinct chemical structure which was used to distinguish them in the infrared spectra. Infrared spectra of each of the sample (PLGA, chitosan, and composite) can be used to qualitatively detect the presence of each of the polymers in the composite particles as shown in **Figure 5-2**. Chitosan molecules have a primary amine group which stretches at 1650 $cm^{-1}$ [161] and the broad peak at 3450 $cm^{-1}$ is either due to the hydroxyl groups (-OH) or primary aromatic amines ($-NH_2$)[160]. PLGA has a carboxylic acid group (-C=O) which demonstrated a symmetric stretching at 1760 $cm^{-1}$ [160]. The peak at 1090 $cm^{-1}$ corresponded to vibrational stretching of methylene -C-H bends and skeletal C-C vibrations[160] whereas C-O-C stretching vibrations were represented at 1190 $cm^{-1}$. The spectrum of composite particles exhibited peaks at 1760 $cm^{-1}$, 1190 $cm^{-1}$ and 1090 $cm^{-1}$

which correlate to asymmetric stretching of –C=O, C-O-C stretching vibrations, vibrational stretching of C-H bends and skeletal C-C vibrations. The presence of reduced peaks corresponding to amines in the composite particle spectrum might be the result of low concentrations of amines on the particles. Note, following the synthesis the particles were washed multiple times with DI water before measuring and hence pure polymers components should not be present in the samples.

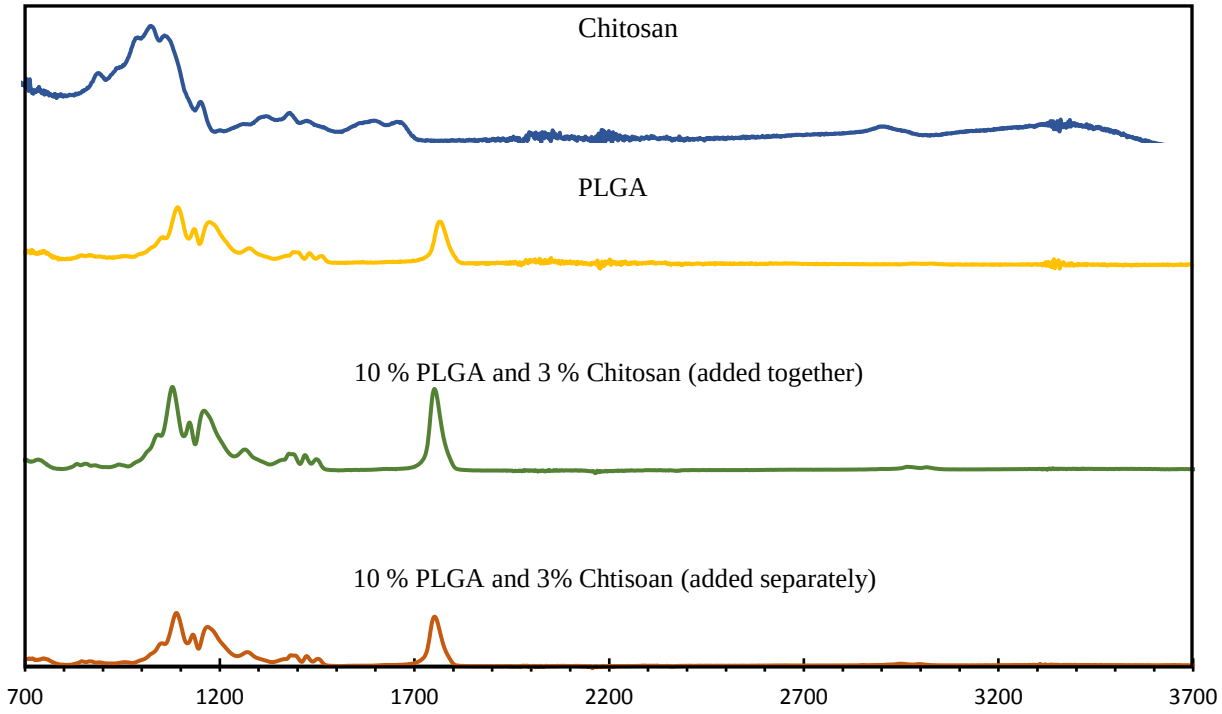


**Figure 5-2:** ATR-FTIR spectra of pure PLGA polymer, pure chitosan polymer, and composite particle # 2 (10% PLGA and 3% chitosan added together) and composite particle # 4 (10% PLGA and 3% chitosan; chitosan added after partial hardening of PLGA particles)

### 5.3.2 Loading Capacity and Encapsulation efficiency of Ad-flu in the particles

There are many methods used to calculate the adenoviral loading in the particles like using qPCR[184,185] or optical measurement at 280 nm[136,186] by extraction of adenovirus in the aqueous phase by dissolving particles in the organic solvents like acetonitrile, dichloromethane[89] or by digestion of particles using enzymes[187] and NaOH/SDS[89]. We used real-time PCR with the extraction method to quantify the total

encapsulation of the particles due to its high specificity and reproducibility[162]. Loading capacity with extraction denotes the total encapsulation quantified by dissolving the freeze-dried particles whereas the loading capacity after 120 days is the cumulative release of Ad-flu as the particles degrade and release the vector. The total loading capacity with extraction and cumulative release is shown in **Figure 5-3**. All the particles had a total loading of more than $10^7$ ifu/mg of particles which was more than the effective dose required for the antibody response (explained in *in vivo* section).

We see that after 120 days (**Figure 5-3**), the total amount of Ad-flu released *in vitro* from the composites were higher or similar to the total encapsulated values calculated using extraction method indicating that the loading capacity calculated with extraction method might be an underestimation of the total loading capacity. It is likely an underestimation of the total encapsulated Ad-flu[163] because acetonitrile was used to dissolve the particles while quantifying the loading capacity using extraction method and chitosan is not soluble in acetonitrile leading the particles in incomplete solubilization. Therefore, all the Ad-flu encapsulated was not extracted in the aqueous phase which might have led to lower quantities than actual encapsulated. Chitosan is only soluble in acetic acid and this solvent cannot be used in qPCR equipment posing a challenge to find any common solvent to dissolve the composites. Recently it has been seen that extraction method might not be the most effective method to quantify the loading capacity[89,163] and a different method similar to digestion method[164] or enzymatic degradation[109] should be used to quantify the encapsulated amount. We did try to degrade the particles faster using lysozyme, but we observed that the particles did not degrade completely and there were still lumps of polymer left behind leading difficulty to quantify using qPCR (results not shown). Another reason for the underestimation might be due to the fact that chitosan is a cationic polymer and Ad-flu is negatively charged[174], hence the electrostatic attraction between chitosan and Ad-flu might be the reason for lower extraction of Ad-flu into the aqueous phase. Consequently, we used the cumulative release of Ad-flu over the release period to quantify the total Ad-flu encapsulated.

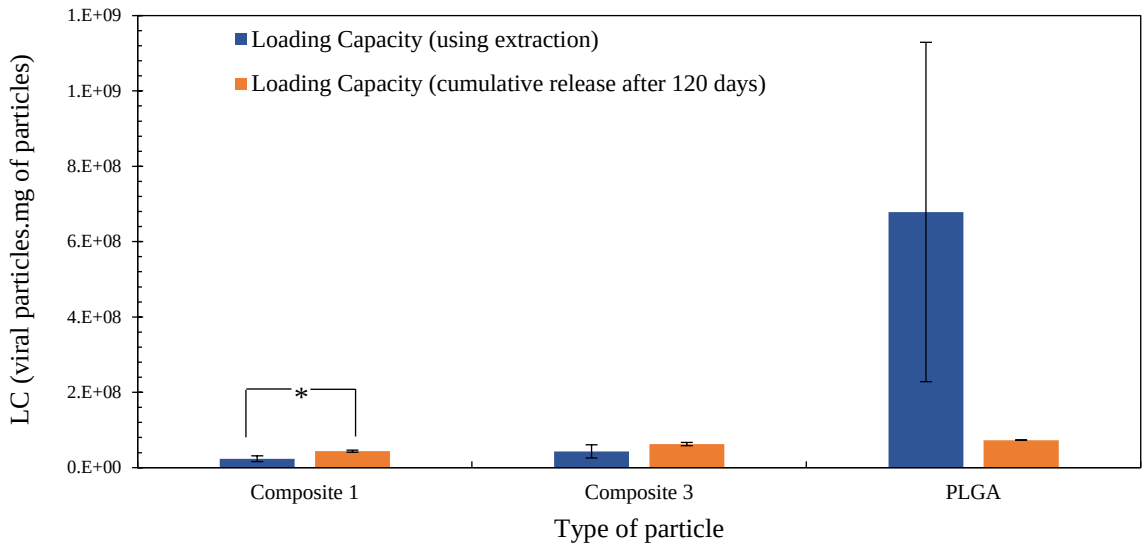


**Figure 5-3:** Quantification of total Ad-flu encapsulated with extraction method as compared to Ad-flu released in 120 days. (n = 3) (* $p < 0.05$ when extraction and cumulative release compared). Note, for cumulative release with 120 days in pure PLGA particles, there was not enough sample left to perform the experiment in triplicates. Additionally, the controls did not give any desired PCR product.

In case of pure PLGA particles, the total release over 120 days is less than the total encapsulated values calculated by extraction method. Note that only 11 % of the Ad-flu encapsulated was detected at the end of 120 days. As PLGA degrades, the local pH at the degradation site is very low. Therefore it is possible that the acidic products formed might disintegrate the Ad-flu DNA, which was eventually not detected using qPCR. It is very unlikely for PLGA and Ad-flu to associate with each other owing to the static repulsion between them. However, the composites contain degradation products of both PLGA and chitosan together, which likely stabilizes the released Ad-flu, leading to detection using qPCR. Alternatively, absorbance at 280nm might be used in the future to quantify the Ad-flu in these particles.

The encapsulation efficiencies (**Table 5-2**) were calculated using the total amount of Ad-flu released over 120 days. We saw that addition of chitosan might have led to lower encapsulation efficiencies in for composite particles as compared to PLGA particles. This might be, due to the association of chitosan and Ad-flu, causing the Ad-flu to leach out of the $w_1/o$ emulsion. We observed that when both polymers are added together, it has lower efficiency as compared to when both polymers were added separately, this is

likely because when the chitosan is added after partial hardening of PLGA particles in particle # 3, very little Ad-flu leached out of this double emulsion giving higher encapsulation.

**Table 5-2:** Encapsulation efficiency of Ad-flu encapsulated in composite particles

| Particle # | Time of Addition | PLGA | Chitosan | Encapsulation Efficiency (%) |
|---|---|---|---|---|
| 1 | Both polymers added together | 10 | 3 | 13.5 ± 0.68 |
| 3 | Chitosan added after partial hardening of PLGA particles | 10 | 3 | 19.3 ± 0.46 |
| 5 | Pure PLGA | 10 | 0 | 22.5 |

### 5.3.3 *In vitro* release profiles and degradation of particles

Herein, we chose DMEM supplemented with 10% FBS and 1% antibiotics as the release medium as to mimic the *in vivo* conditions. The *in vitro* release profile for the particles is shown in **Figure 5-4.** We saw a burst release for the initial five days where 62%, 68% and 82% of the total load released in 120 days for composite particles # 1, 3 and pure PLGA particle # 5 respectively. This initial burst can be explained by surface desorption of Ad-flu on the surface of the particles or Ad-flu encapsulated close to the surface of the particles which is usually seen with these type of particles[16,76,102]. Smaller particles have a higher surface area to volume ratio; therefore, a higher amount of Ad-flu might be present at particle surface than at the interior of the particles[16] which is why we see the burst following a trend with the size of particles (Burst release$_{particle\#1}$ < Burst release$_{particle\#3}$ < Burst$_{particle\#5}$). Another reason for a lower burst from the composites might be the strong electrostatic attraction between chitosan and Ad-flu might have restricted the burst from the composite particles; therefore, we got lower burst release from composite particles as compared to PLGA.

Subsequent release after the initial burst depends on the degradation kinetics of the polymers PLGA and chitosan. Both these polymers are biocompatible and biodegradable which degrade by hydrolytic cleavages in aqueous media, but chitosan backbone consists of highly reactive primary amine groups indicating that chitosan undergoes surface erosion[16,109,125,187] and PLGA is known to undergo bulk erosion[16,79,188] and hence both will display different degradation kinetics. Chitosan (produced by deacetylation of chitin) degradation depends on the degree of deacetylation[109]. It is found that half-life of chitosan is as low as 15 days (52% deacetylated) to more than 90 days (for anything higher than 71% deacetylated)[161]. Bulk eroding PLGA (50:50) degrades faster than surface eroding 75% deacetylated chitosan; hence as aqueous media penetrates through the surface of the particles, PLGA polymer chains undergo hydrolytic cleavages forming oligomers[16,81]. Pores are formed due to PLGA degradation, and these small pores consequently grow and eventually coalesce with neighboring pores to form fewer, larger pores. Pores may also be shut due to the mobility of the polymer chains and their ability to rearrange[118]. Once the pores are large enough for the Ad-flu to escape the polymer matrix, owing to the concentration gradient, Ad-flu diffuses into the aqueous media. But chitosan on the surface acts as a diffusion barrier for Ad-flu leading to the build-up of osmotic pressure. And therefore, after the initial burst effect, we see a slow release in the case of the composites as compared to PLGA particles.

The release profiles for the composites and PLGA showed a similar trend. This can be due to the high concentration of PLGA (10 w/v %) we used. It is observed that at high polymer concentrations (above 5 w/v %), the viscosity of the oil phase increases leading to a denser internal structure, therefore low internal porosity[64,78,157] and hence it is possible that Ad-flu might be encapsulated at the core of the particle rather than distributed all over the PLGA matrix. Hence the diffusive path length for Ad-flu in this dense internal structure of PLGA is more tortuous. Therefore, all the particles might behave as a core-shell particle with Ad-flu encapsulated in the core of the particle with polymer shell on the outside.

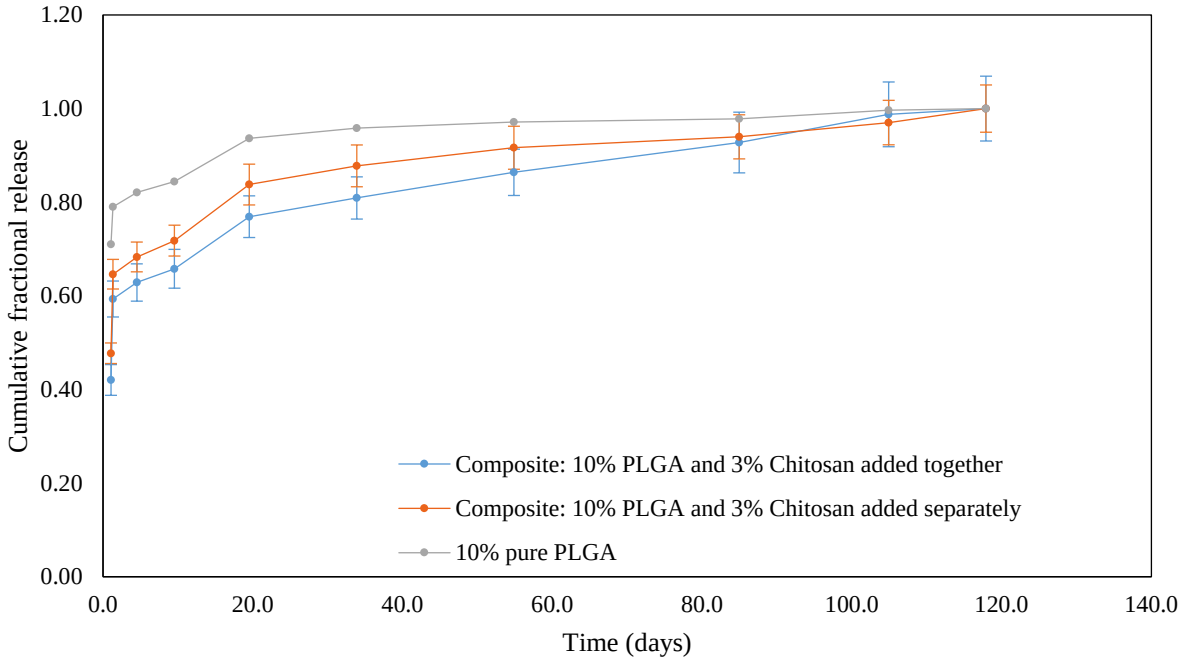


**Figure 5-4** *In vitro* release profile of Ad-flu from the composites (n = 3). Note, for pure PLGA particles there was not enough sample left to perform the experiment in triplicates. Additionally, the controls did not give any desired PCR product. It should be noted that the release profiles reported in this section have been shown as scatter plots with connected data points in order to illustrate the trend in the release. These lines are not continuous and do not represent any model fit.

Pulsatile vaccine release kinetics were observed when a core-shell approach was used[16,102]. Oil-based PLGA microcapsules (OPM), a reservoir system composed of true core-wall capsule structures with an oily core reservoir of antigen, in which the vaccine is dispersed, surrounded by an outer polymer shell was developed which presented a pulsatile release[102]. But, it is also observed that loading capacity, as well as the encapsulation efficiency of particles increases with increasing concentration of PLGA and the release rate of the encapsulated molecule is slower when higher concentrations of the polymer are used[64,78,169,189].

As PLGA degrades, it starts developing more hydrophilic regions leading to greater water penetration and faster degradation rate of PLGA; this also leads to a reduction in glass transition temperature of PLGA making the polymer more rubbery[16,78] affecting the structural integrity of the particles. Consequently, as the Ad-flu concentration in the polymer matrix reduces, the void created is occupied by water and other degradation products which are oligomers of PLGA or lactic and glycolic acid. This accumulation of

degradation products inside the polymer matrix auto-catalyzes the degradation of PLGA[78,132]. For larger particles these degradation products diffuse out of the matrix slower than the smaller particles as the path length to diffuse out is greater in case of larger particles further reducing the pH in the polymer matrix which can go to as low as 1.5 [165–167] affecting the activity and structure of Ad-flu.

### 5.3.4 *In vivo* release profiles

CD1 mice were injected subcutaneously with Ad-flu dose of 1 x $10^6$ ifu/mice, 1 x $10^7$ ifu/mice and 1 x $10^8$ ifu/mice and injected with non-encapsulated Ad-flu. No evidence of inflammation or foreign body reaction was observed in either experimental or control groups. The antibody response at 30 and 60 days was measured using HAI assay and can be seen in **Figure 5-5.** The basis of the HAI assay is that antibodies of influenza virus will prevent attachment of the virus to red blood cells and therefore hemagglutination is inhibited when antibodies are present. The highest dilution of serum that inhibits hemagglutination is called the HAI titer of the serum. If the serum comprises no antibodies reacting with the H1N1 strain, then

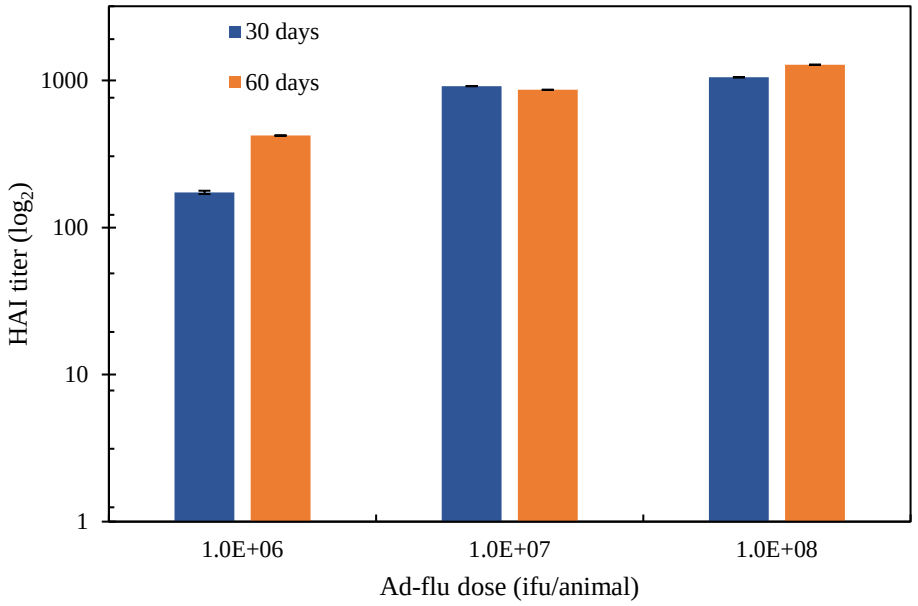


**Figure 5-5** Evaluating optimum dosage for particle encapsulation. Following dosages of NE (non-encapsulated) Ad-flu were injected subcutaneously to the mice: 1 x $10^6$ ifu/anime (n = 5), 1 x $10^7$ ifu/mic (n = 5), 1 x $10^8$ ifu/mice (n = 5). Data represented as geometric mean of the obtained values. This assay was performed by Jianfeng Zhang at Altimmune Inc. (Gaithersburg, MD)

hemagglutination will be detected in all wells. Similarly, if antibodies to the virus are present, hemagglutination will not be observed until they are adequately diluted. Ad-flu dosage of $10^6$ ifu/mice was found to be optimum, and we proceeded with this dosage to be encapsulated in the particles and for injections later in the *in vivo* studies.

CD1 mice were given a prime Ad-flu dose with 1 x $10^6$ ifu/mice and injected with Ad-flu encapsulated in pure PLGA particles and Ad-flu encapsulated composite particle # 3 (PLGA 10 w/v % and chitosan 3 w/v %, added at different times) of the same dosage (1 x $10^6$ ifu/mice) to mimic the boost injection. No evidence of inflammation or foreign body reaction was observed in either experimental or control groups, indicating biocompatibility in vivo. The antibody response at 28, 63 and 107 days can be seen in **Figure 5-6.**

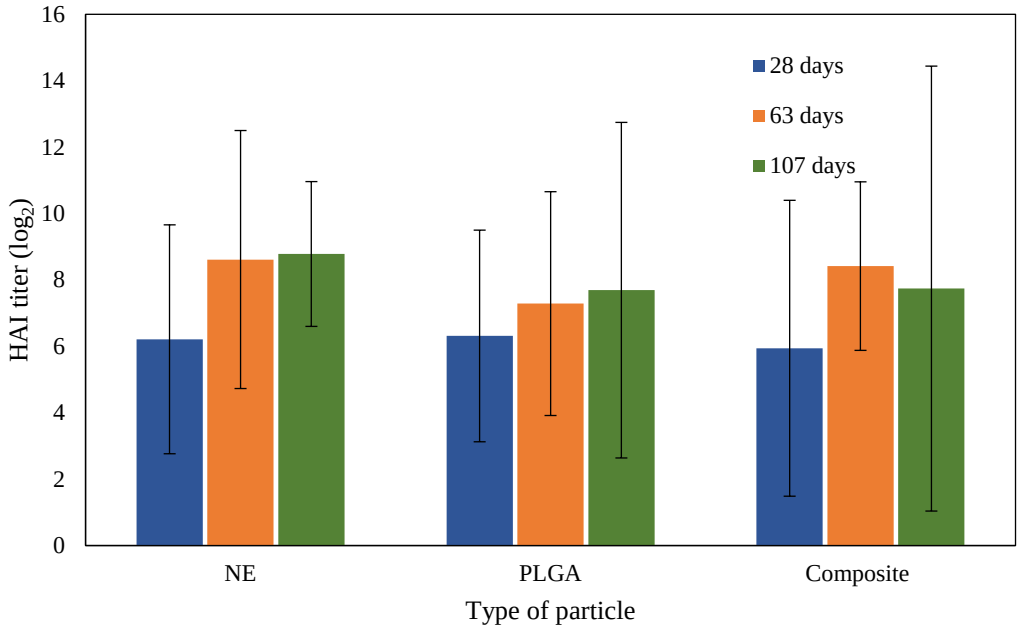


**Figure 5-6** *In vivo* antibody response with NE (non-encapsulated Ad-flu) (n = 6), pure PLGA (10 w/v %) particles (n = 8), composite particles (10 w/v % PLGA and 3 w/v % chitosan added at different times) (n = 8). Data represented as geometric mean of the obtained values. This assay was performed by Jianfeng Zhang at Altimmune Inc. (Gaithersburg, MD)

It is observed that the mice which received one injection of non-encapsulated Ad-flu did not show any significant change in the antibody response. Also, we can see from the release profile *in vivo* that there are

no significant differences in the antibody response from the mice which received a prime injection and boost injections with the particles. Owing to the inherent immunogenicity of adenoviral vaccines, it generates strong dose-dependent innate and adaptive immune responses[51,52]. These responses are characterized by the secretion of pro-inflammatory cytokines and chemokines like tumor necrosis factor-alpha (TNF-α), interleukin (IL)-1β (IL-1β), IL-6, IL-12, interferon-γ (IFN-γ)[51]. At a high vector dose, it is generally found that the efficacy of gene-transfer is reduced strikingly owing to primary inflammatory responses; these inflammatory responses are the cause for Ad-specific cellular and humoral responses[51]. We see that in the initial 6 days there was a burst of approximately 2 x $10^7$ ifu/ml of Ad-flu from both types of particles. In addition, we also injected the mice with a primary dose of $10^6$ ifu/ml which increased the quantity of Ad-flu at prime injection, which might have been resulted in generating Ad-flu-specific T-cells mediated through $CD8^+$ cytotoxic T-cells limiting the duration of transgene expression[190,191]. Also, single, large doses of Ad provoke neutralizing antibody responses directed to proteins of the viral particle, which prevent binding to target cells[74]. Alternatively, the reason for lack of antibody response from the mice injected with particles might be that repeat dosing is ineffective with adenoviral vaccines owing to initial strong immune responses[74]. Furthermore, it is generally found that nanoparticulate carriers (especially chitosan[192]) provide adjuvant activity by enhancing antigen delivery or by activating innate immune responses[68]. Following delivery of adenoviral vector , transgene expression is at a high level but is transient, being low or undetectable in most tissues after two weeks[74].

Another important factor to be looked into is the activity of Ad-flu which might be affected due to the encapsulation of the particles as well as incubation of the particles at $37^0$C. It is possible that encapsulated Ad-flu did undergo physical and chemical changes like hydrolysis, deamidation, aggregation[16]. Higher temperatures impart energy that increases the chances of Ad-flu attaining a non-native conformation; aqueous media further increases Ad-flu degradation by increasing mobility and rate of hydrolysis and deamidation[16]. Though the external aqueous media is buffered, the internal core of the particle matrix has a very low local pH (explained in *in vitro* studies), which may cause the Ad-flu to aggregate and lose its

activity. A denser polymer matrix as in the case of all the particles here increases the resistance for the Ad-flu to diffuse in the external aqueous phase increasing its residence time in the core of the particle. Due to the low local pH, it is possible that Ad-flu lost its activity and hence we did not see an antibody response.

A solution to minimize the deleterious effects of the low local pH would be using small particles, which reduces the path length for Ad-flu as well as oligomers and monomers to diffuse in the aqueous media in the exterior. Considering the activity of the Ad-flu, the lower path length of diffusion in the smaller particles and core-shell structure of the composite, we chose composite #3 and pure PLGA particle (positive control) for *in vivo* studies. Also, if we use a high-capacity helper-dependent adenoviral vector which has shown to greatly attenuate Ad-specific cellular immune responses and mediate high levels of transgene expression for a substantial period of time will give us an efficient delivery device for Ad-flu[51].

### 5.4 Conclusion

We have shown the successful synthesis of PLGA and composite particles with double emulsion method with a wide range of sizes. Controlling various synthesis parameters like sonication amplitude, PLGA concentration, chitosan concentration, and emulsifier concentration helped control the size of the particles. Optimizing each of these components to modulate the release of molecules from the particles is a very important as each component has an independent effect on the release kinetics. This also makes the process of optimization very challenging taking into account various components that need to be considered. We showed successful encapsulation of Ad-flu in PLGA and composite particles with efficient loading capacity, but further studies need to be performed to quantify the activity of Ad-flu. The release of the vaccine from the composites depends on the concentrations, viscosities, molecular weight of the polymers used along with the degree of deacetylation of chitosan. The most important factors in single dose vaccine design are macromolecule stability and release kinetics, which together influence efficacy. Kinetics of vaccine release and degradation of the polymer could be controlled by changing the synthesis parameters and can be utilized to modulate an optimal immune response.

Incorporation of polysaccharides[16] or PEGylation of vaccine[50] needs to considered to maintain the activity of the encapsulated molecule. Along, with that acid-induced degradation of Ad-flu might be avoided using excipients like $Mg(OH)_2$, $MgCO_3$, $NaHCO_3$ to counteract the acidity[16]. We do get a pulse at 20 days, but further studies need to be performed with lower concentrations of PLGA to see an effect on the release kinetics. Using lower concentrations of PLGA will also help in decreasing the size of the particles as well as will reduce the internal density of the polymer chains in the particles which will help in increasing the diffusion rate of the molecule encapsulated. Surface eroding chitosan will help from preventing continuous diffusion of the encapsulated molecules in case of lower concentrations of PLGA and help in getting the pulsed release that we expect. Formulation techniques that reduce macromolecule interaction with organic solvents, as well as that, can maintain its activity at body temperature should be chosen to improve commercialization potential and vaccine recovery.

# Chapter 6: Understanding the mechanism of vaccine release from the composites

## 6.1 Introduction

Drug delivery has advanced significantly in the past few decades that we have advanced from using simple pills to controlled delivery devices to personalized medicine[18,135,193,194]. Moreover, scientists are developing novel solutions to solve delivery problems by controlling the release rate of drugs, efficient targeting of drugs. The major challenges that we face today are how to convert these lab-scale devices to actual use so that it reached the patients. Most of the delivery devices, either don't reach the clinical trials due to the large amounts of money encountered or many of them fail during these clinical trials. Molecular understanding of the release of drugs from these devices could give us a better understanding of the mechanisms of the release. One way to do this is by conducting more experiments to get a proper understanding, but that can turn out to be expensive. Mathematical modeling can help us to analyze how various parameters affect the release of drugs quantitatively.

Mathematical models can lessen the number of experiments needed to probe different conditions and designs. It also helps to expand the understanding of the physical and chemical mechanisms of release, particularly when the effects of different phenomena or multicomponent systems are together. They can help us understand the effect of shape, size, composition, surface charge on the kinetics of the release profile. Eventually, it is projected that the systemic use of mathematical models to forecast drug release rates and behavior can lower costs and experimental times, leading to more effective mathematical models to predict macromolecule release rates and behavior can lower costs and experimental times, leading to more effective formulations and more precise dosing regimens[7,118,178,179,195].

## 6.2 Mathematical modeling

Mathematical models in polymeric drug delivery can be classified into diffusion controlled, erosion controlled and swelling and dissolution controlled systems[195,196]. Most of the times release rate is a function of all the types. The purpose of mathematical modeling is to simplify the complex release process and to

gain insight into the release mechanisms of a specific material system. Thus, a mathematical model mainly focuses on one or two dominant driving forces. Empirical models usually assume a zero-order process is controlling overall drug release whereas mechanistic models consider specific physicochemical phenomena like diffusional mass transfer to model the release. Empirical models are easier to use, but mechanistic theories are generally more accurate and much more powerful when stimulating the effect of device design variables on the resulting drug release patterns[7,122,179]. If matrix erosion is much slower than drug diffusion through the polymer, the drug release kinetics is diffusion-controlled, alternatively, in erosion-controlled systems, the drug diffusion rate from the matrix is low, and it remains within the matrix. Herein, we have used empirical/semi-empirical models and mechanistic models to characterize the release of the composite and PLGA particles.

## 6.3 Empirical/Semi-empirical models

### 6.3.1 Korsmeyer-Peppas model

This is a semi-empirical equation most widely used the equation for modeling of drug release from the delivery device. This equation is used to characterize the release of molecules from delivery devices when the release mechanism is unknown or when more than one type of release mechanism can exist. Korsmeyer-Peppas equation sometimes called, Peppas equation, Ritger-Peppas equation or power law relates the drug release exponentially to elapsed time[118,197]. The equation is as follows[197,198]:

$$\frac{M_t}{M_\infty} = k_k t^n$$

where, $M_t$ cumulative amount of molecule release at time $t$, $M_\infty$ is cumulative amount of drug released at infinite time, $k_k$ is the rate constant incorporating the characteristics of the system and the drug with units of $t^{-n}$, and $n$ is the release exponent in order to characterize the type of release mechanism. Depending on the value of $n$, the mechanism of release of molecule from the device can be characterized as in **Table 6-1**. Some of the limitations for the use of this model are that it can be used only up to a cumulative release of

60% of the encapsulated molecule. This equation can also be used for geometries other than sphere like cylinders or thin-films; the values of release exponent for these geometries are different[198].

**Table 6-1:** Diffusional release mechanisms for sphere[197]

| **Release Exponent ($n$)** | **Transport mechanism** | **Release mechanism** |
|---|---|---|
| 0.43 | Fickian Diffusion | Diffusion controlled |
| $0.43 < n < 0.85$ | Anomalous transport | Polymer-swelling controlled |
| 0.85 | Case II transport | Zero-order release |
| Higher than 0.85 | Super Case II transport | Polymer-swelling controlled |

### 6.3.2 Peppas-Sahlin Model

Another semi-empirical equation which is a modified version of the above mentioned Peppas equation which takes into account the Fickian as well as non-Fickian transport into account is given below. Fickian diffusional release occurs by molecular diffusion of the encapsulated drug owing to chemical potential gradient whereas non-Fickian diffusion is associated with swelling of the polymer in drug delivery devices. The equation is as follows[130]:

$$\frac{M_t}{M_\infty} = k_{1s}t^m + k_{2s}t^{2m}$$

where, $M_t$ cumulative amount of molecule release at time $t$, $M_\infty$ is cumulative amount of drug released at infinite time, $k_{1s}t^m$ is the contribution due to Fickian diffusion (F) and $k_{2s}t^{2m}$is the relaxational contribution (R), and $m$ is the Fickian diffusion exponent for any shape of the device. This model can be used only for initial 60% of the release. The ratio of relaxational to Fickian diffusion can be used to calculate the contribution of each type of mechanism, and this ratio is calculated as:

$$\frac{R}{F} = \frac{k_{2s}}{k_{1s}}\, t^m$$

### 6.3.3 Hopfenberg Model

This model is the most widely for surface eroding devices with different geometries like cylinders, slabs and spheres. This model assumes that the rate of drug release from the surface erodible system is proportional to the surface area of the device. The equation is as follows[197]:

$$\frac{M_t}{M_\infty} = 1 - \left[1 - \frac{k_h t}{C_0 a_0}\right]^n$$

where, $M_t$ cumulative amount of molecule release at time $t$, $M_\infty$ is cumulative amount of drug released at infinite time, $k_h$ = erosion rate constant, $C_0$ is the initial concentration of the molecule inside the device, $a_0$ = initial radius of the sphere or cylinder or half-thickness of slab, $n$ = 1, 2 and 3 for slab, cylinder and sphere respectively. This model assumes that drug release from the delivery device is controlled by the erosion of the matrix and time dependent diffusional resistances do not affect the rate of release.

## 6.4 Mechanistic models

### 6.4.1 Autocatalytic model

As described in **section 2-7**, degradation of PLGA results in the formation of oligomers and/or monomers of lactic acid and glycolic acid which are acidic in nature. These acidic products autocatalyzes the degradation of PLGA and therefore has a major impact on the release of the encapsulated molecule. Siepmann et al.[125,132] developed a model to demonstrate the importance of these autocatalysis effects for spherical particles. It was assumed that the release of the molecule encapsulated is diffusion controlled and the diffusivity of the molecule is a function of the radius of the delivery device. The equations used to model the drug release are as follows:

$$\frac{M_t}{M_\infty} = 1 - \left[\frac{6}{\pi^2}\sum_{n=1}^{\infty}\frac{1}{n^2} exp\left(-\frac{n^2\pi^2}{R^2} D_e t\right)\right]$$

$$D_e[cm^2/s] = 1.1 \times 10^{-15} R[\mu m]^{1.887}$$

where, $M_t$ cumulative amount of molecule release at time $t$, $M_\infty$ is cumulative amount of drug released at infinite time, $R$ is the initial radius of the delivery device, $D_{eff}$ is the effective diffusivity that depends on the radius of the particle, $t$ is the time.

## 6.5 Results and Discussion

### 6.5.1 Pure PLGA particles

#### *6.5.1.1 Comparison of experimental release to Peppas models (60% release)*

Peppas and Peppas-Sahlin equations can be used to characterize the mechanism for the initial 60% of the release. The values of diffusion rate constants and release exponents for pure PLGA particles are given in **Table 6-2.** Note that, the initial burst is ignored while characterizing the release behavior of Ad-flu encapsulated because the initial burst results from surface adsorbed molecules. For Ad-flu encapsulated in PLGA particles, after ignoring the burst we get a 60% release in initial 10 days which constitutes for only two data points and therefore these models could not be used to characterize the release of Ad-flu. Adjusted $R^2$ values are reported to take into account the number of parameters used to fit the model.

**Table 6-2:** Values of rate constant and release exponent for Ad-eGFP encapsulated in pure PLGA particles

**Particle synthesized with 10 w/v % PLGA (Control particles)**

| **Peppas** | | | **Peppas-Sahlin** | | | |
|---|---|---|---|---|---|---|
| **n** | **k** | **Adjusted $R^2$** | **$k_1$s** | **$k_2$s** | **m** | **Adjusted $R^2$** |
| 1.351 | 0.0047 | 0.9908 | 0.01 | 0.001 | 0.907 | 0.989 |

As n > 0.85, it can be concluded (as mentioned in **Table 6-1**) that Ad-eGFP release from the PLGA particles follows a super Case II Non-Fickian transport and therefore the release in this period might be controlled by the swelling of the polymer. Therefore, we also used the Peppas-Sahlin model which takes into account the diffusional as well as the relaxational stresses in order to characterize the release from the

particles. The release profile in this initial period along with the fractional release of Ad-eGFP due to Fickian diffusion is given in **Figure 6-1**.

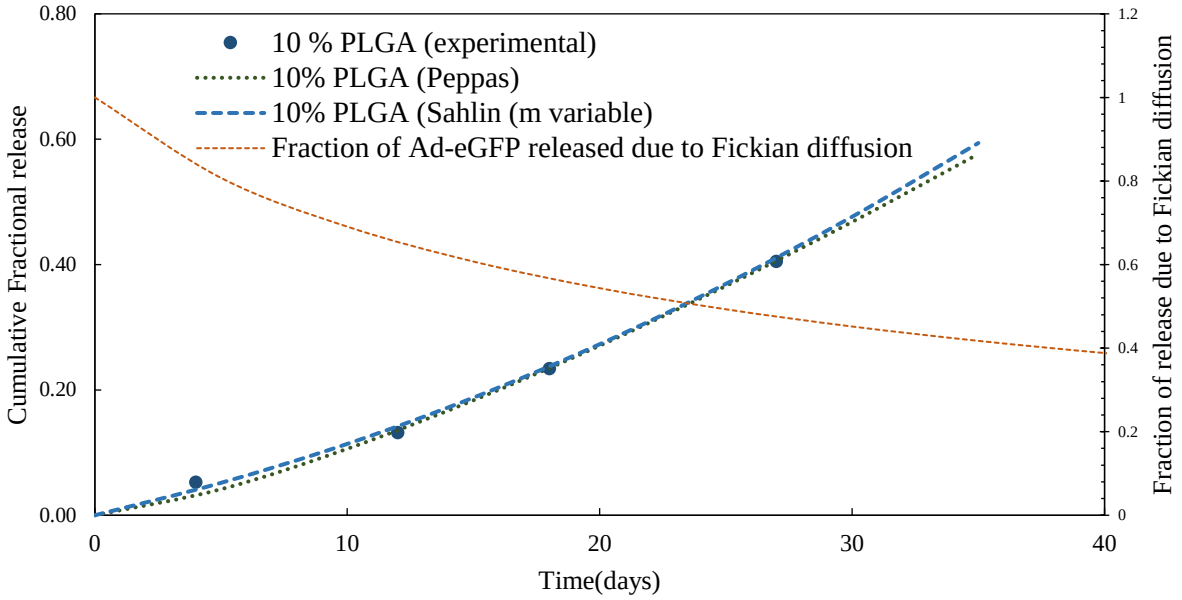


**Figure 6-1:** Release of Ad-eGFP from PLGA particles compared to theoretical release as calculated using Korsmeyer-Peppas and Peppas Sahlin semi-empirical models. The secondary axis represents the fractional release of Ad-eGFP due to Fickian diffusion calculated using Peppas-Sahlin equation. This model can be utilized to calculate fraction of Ad-eGFP released due to Fickian diffusion from the composites at a certain time.

### *6.5.1.2 Comparison of experimental release to Autocatalytic and Hopfenberg models*

We used the Hopfenberg model (used for surface eroding devices) and Autocatalytic model (developed by Siepmann et. al[132]) to characterize the release of Ad-eGFP over the entire duration of release. The release profiles of Ad-eGFP and Ad-flu compared to these models is shown in **Figure 6-2.** It can be observed that the release profile of Ad-eGFP and Ad-flu from pure PLGA particles follows the Hopfenberg model partly but are not in agreement with the autocatalytic model. Autocatalysis effects might not be the rate controlling degradation mechanism here because of the small size of PLGA particles as compared to the size of PLGA particles (7.6 to 53 µm) used by Siepmann et al[132]. This lead to smaller diffusive path lengths for the degradation products to diffuse through the matrix leading to the low residence time of the acidic products

in the polymer matrix for smaller particles. Therefore, the effect of autocatalysis is minor and hence the release profile is not in accordance with the autocatalytic model. Alternatively, the non-agreement of the autocatalytic effect might be due to the different molecular interactions of adenoviral vectors with PLGA polymer. Moreover, it is assumed during the development of the autocatalytic model that the effective diffusivity depends on the size of the particle and stays constant during the whole duration of degradation[132]. But the effective diffusivity of the particles may not stay constant with time as the pores formed on the surface might lead to increased or decreased diffusivity of the molecules. Therefore, change in diffusivity over the period of time needs to be considered.

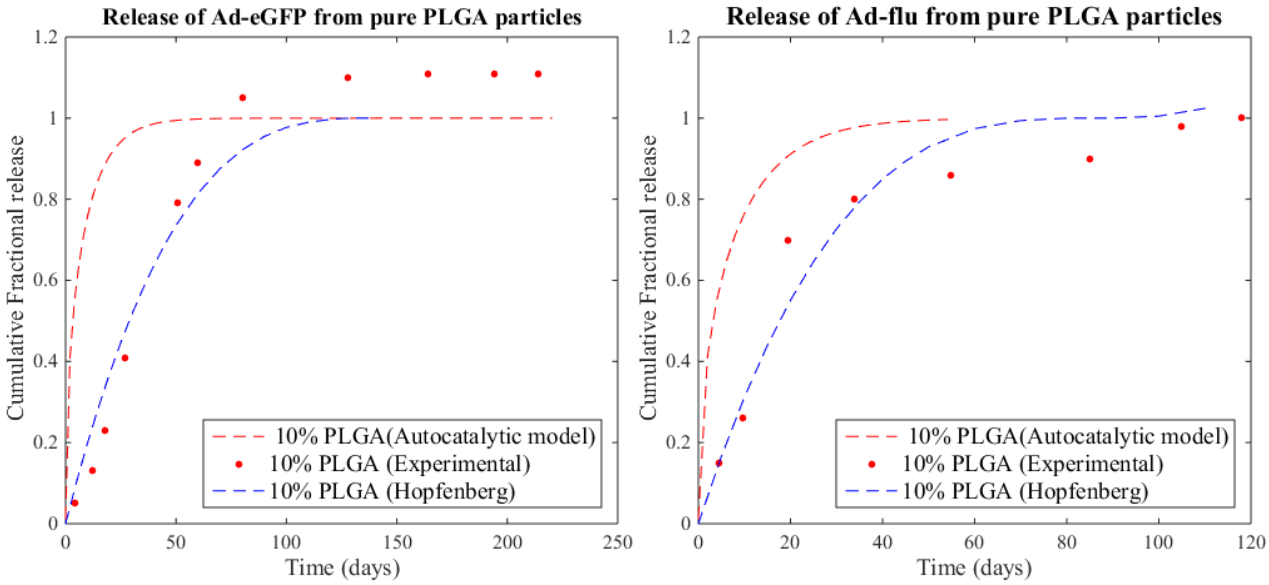


**Figure 6-2:** Release of Ad-eGFP and Ad-flu compared with surface eroding and autocatalytic model.

### 6.5.2 Composite Particles

#### *6.5.2.1 Comparison of experimental release to Peppas models (60% release)*

Similar to PLGA particles, the initial 60% release was characterized using Peppas and Peppas-Sahlin equations. Composite particles synthesized with 10 w/v % PLGA and 3 w/v % chitosan when added together and when added separately were used to characterize the release profiles of Ad-eGFP and Ad-flu. The values of diffusion rate constants and release exponents for the composite particles are given in **Table 6-3.** Adjusted $R^2$ values are reported to take into account the number of parameters used to fit the model.

Note, the adjusted $R^2$ for Ad-flu encapsulated in composite particles were less than 0.45 or negative and hence the Peppas and Peppas-Sahlin models were not used to compare the release profile of Ad-flu encapsulated in the composite particles.

**Table 6-3:** Values of rate constant and release exponent for Ad-eGFP encapsulated in composites

**Particle synthesized with 10 w/v % PLGA and 3 w/v % chitosan**

| | **Peppas** | | | **Peppas-Sahlin** | | | |
|---|---|---|---|---|---|---|---|
| | **n** | **$k_k$** | **Adjusted $R^2$** | **$k_{1s}$** | **$k_{2s}$** | **m** | **Adjusted $R^2$** |
| **Both polymers added together** | 1.687 | 0.0007 | 0.9978 | 0.002 | 9.3E-05 | 0.050 | 0.998 |
| **Both polymers added separately** | 2.642 | 0.0001 | 0.9912 | -90.62 | 156.6 | -14.5 | -5.103 |

As n > 0.85, it can be concluded (as mentioned in **Table 6-1**) that Ad-eGFP release from the composite particles as well follows a super Case II Non-Fickian transport and therefore the release in this period might be controlled by the relaxational stresses and swelling of the polymer. Therefore, we also used the Peppas-Sahlin model which takes into account the diffusional as well as the swelling of the polymer in order to characterize the release from the particles. The release profile in this initial period, when compared to Peppas and Peppas-Sahlin model, is given in **Figure 6-3**. As can be seen in **Table 6-2**, Peppas-Sahlin model is not a good fit to characterize the release profile from the composites when polymers are added separately.

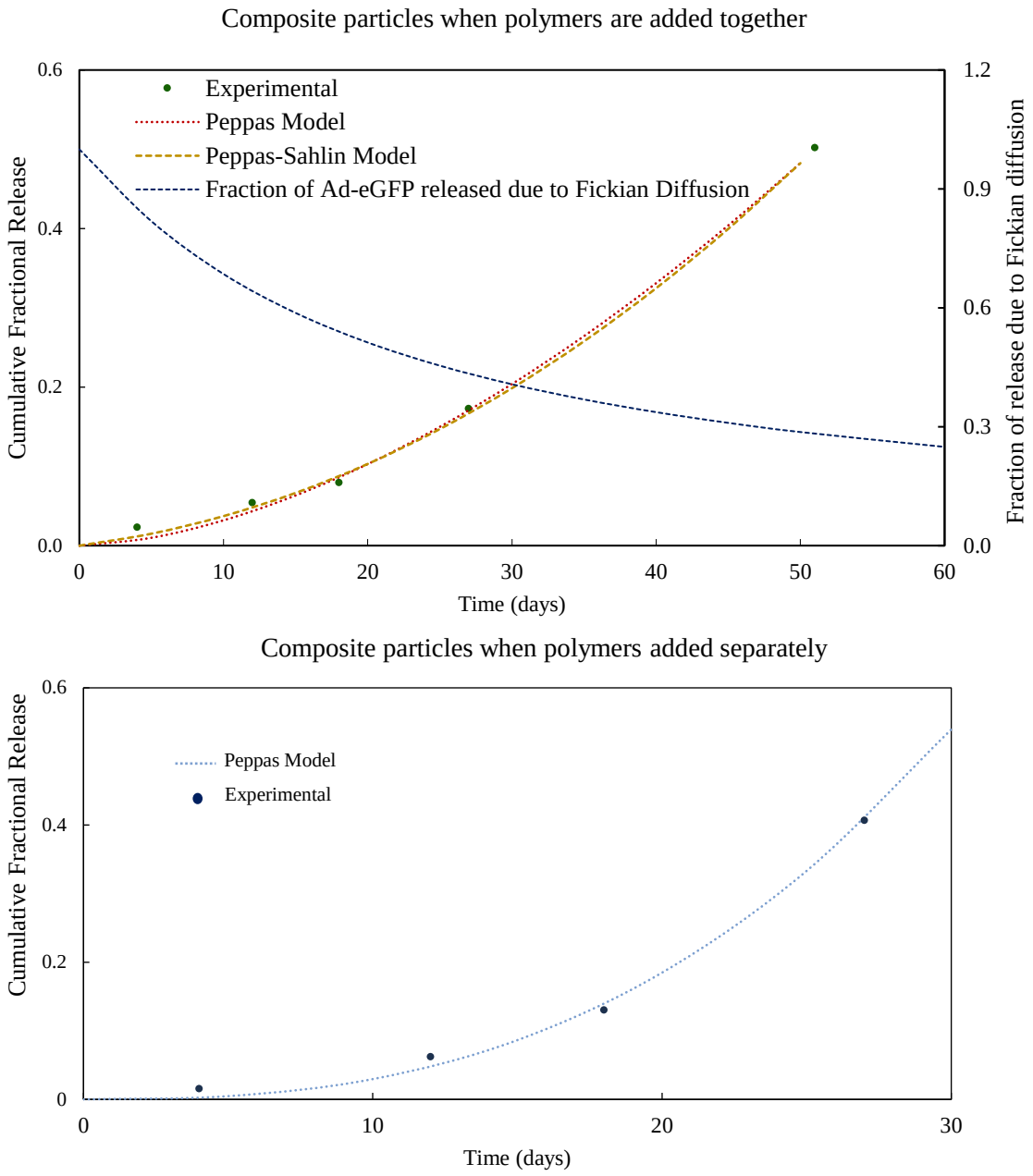


**Figure 6-3:** Release of Ad-eGFP from composite particles compared to theoretical release as calculated using Korsmeyer-Peppas and Peppas-Sahlin equations. The secondary axis represents the fractional release of Ad-eGFP due to Fickian diffusion calculated using Peppas-Sahlin equation. This model can be utilized to calculate fraction of Ad-eGFP released due to Fickian diffusion from the composites at a certain time.

### *6.5.2.2 Comparison of experimental release to Autocatalytic and Hopfenberg models*

The release of Ad-eGFP and Ad-flu over the entire duration of the degradation was modeled using Hopfenberg model and autocatalytic model. The release Ad-eGFP and Ad-flu from the composites

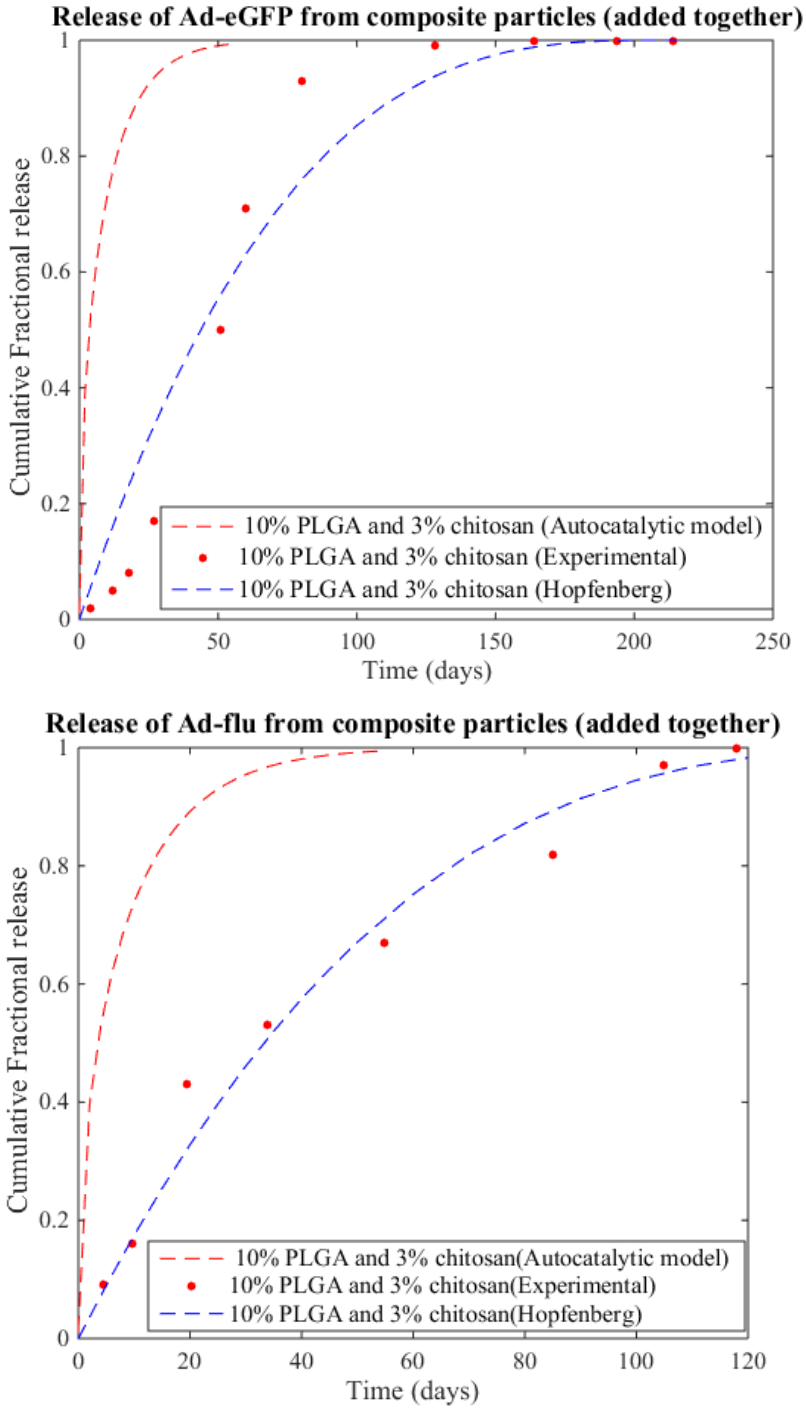


**Figure 6-4**: Release of Ad-eGFP and Ad-flu compared with surface eroding and autocatalytic model**.**

synthesized with 10% PLGA and 3% chitosan added together are represented in **Figure 6-4,** and the release of Ad-eGFP and Ad-flu from the composites synthesized with 10% PLGA and 3% chitosan added separately are represented in **Figure 6-5**.

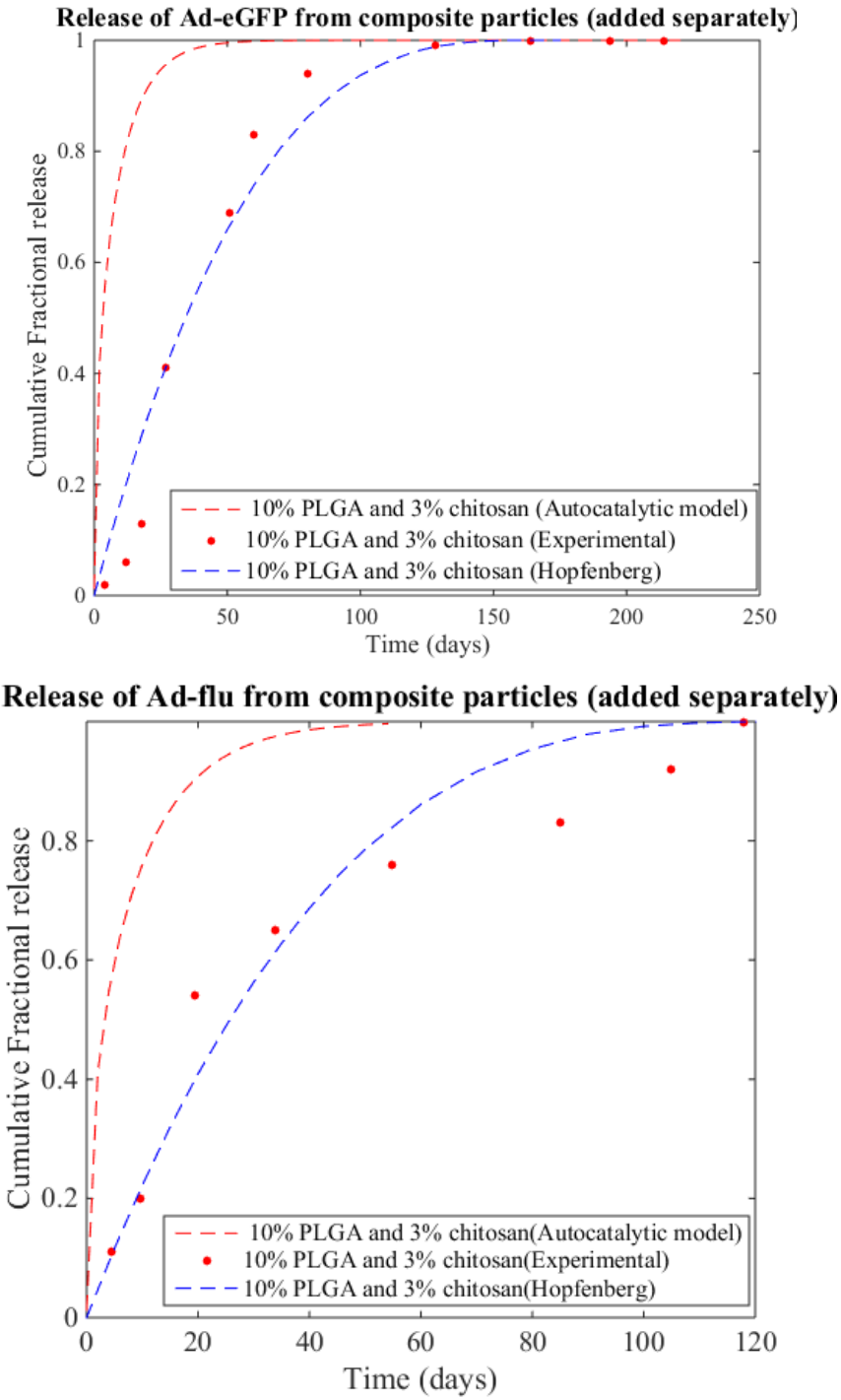


**Figure 6-5:** Release of Ad-eGFP and Ad-flu compared with surface eroding and autocatalytic model.

We can see that Ad-eGFP release when modeled using the Hopfenberg model shows better agreement as compared to the autocatalytic model. Moreover, if we compare the process of addition of polymers, the release of Ad-eGFP when both polymers (PLGA and chitosan) are added separately is in better agreement with the Hopfenberg model as compared to the release when both polymers are added together. It is likely due to the inherent structures of both types of composites produced when we change the sequence of addition. When we synthesize the composite particle, by addition of both polymers together PLGA and chitosan get incorporated into each other and when the composite particles are synthesized with different sequence of addition it produces core-shell structure with Ad-eGFP encapsulated in PLGA with layer of chitosan on the outside (for more information regarding discussion on the synthesis parameters refer to **section 3.2.3** and **section 3.3.1**). Moreover, the model indicates that the release of Ad-eGFP from the composites is in good agreement from the composites during phase II of the release, i.e., during the slow release of Ad-eGFP from the composite particles. This is not observed in pure PLGA particles (**Figure 6-2**) as well as composites when both polymers are added together (**Figure 6-4**).

It is also observed that the release of Ad-flu from both types of composites is partially in agreement with the Hopfenberg model and the release behavior is not captured by the autocatalytic model. In the autocatalytic, the diffusivity of the molecule is assumed to be constant over the release period and is assumed to depend only on the radius of the particle. This model does not take into consideration the formation of pores and change in diffusivity as the particles start degrading. It might be a limitation of the autocatalytic model which is a good agreement for larger particles[132].

## 6.6 Conclusions

Using the composite particles complicates the understanding of the release mechanism as there are very few models available to model the release from the composites. We used four different models to characterize the release kinetics. It could be concluded from the Korsmeyer-Peppas model for pure PLGA particles as well as composite particles produced with 10% PLGA and 3% chitosan that the release mechanism of the Ad-eGFP encapsulated follows non-Fickian diffusion kinetics. In case of non-Fickian

diffusion kinetics, the time required to form a sharp boundary between the highly swollen region and the glassy dry region is called as the initial induction time. Until this induction time the release of the adenovirus Fickian diffusion kinetics; beyond this time the swelling of the polymer controls the rate of the release. The initial slow release of adenovirus from the particles produced here could be due to Fickian diffusion kinetics followed later by non-Fickian. It seems an increase in the induction time could lead to the slower release of adenovirus encapsulated initially which could help us modulate the burst we hope to achieve for the use of a single dose vaccine. In order to quantify the fraction of adenovirus released by Fickian diffusion kinetics, we used the Peppas-Sahlin model, but this model does not accurately capture the behavior of the system. Therefore, models which take into account one or more than one of the phenomena out of bulk erosion, tortuosity of the particles, surface porosity, surface erosion and autocatalytic effects need to be taken into consideration.

Biodegradable particles undergo both surface and bulk erosion, and therefore the Hopfenberg model can be a starting point to give us an idea on which type of erosion dominates in the composite particles. We found that the Hopfenberg model can help us understand the release kinetics but does not accurately explain the behavior of the system. Additionally, the surface erosion model seems to characterize the release from the core-shell composite particles more accurately than for the other particles. Hence surface erosion seems to dominate the degradation of chitosan. The model used here to incorporate the autocatalysis effect due to acidic products of PLGA depends on the size of the particles. The model is in good agreement with large particles[132] but falls short when we use to understand the release kinetics of small particles produced in this study. The residence time of the acidic products in large particles is higher as compared to smaller particles which might be a reason why the autocatalysis effects dominate in bigger particles[119].

These classical models help us in understanding the release mechanism of Ad-eGFP and Ad-flu from pure PLGA and composite particles. But it should be noted that the semi-empirical models assume only one of the degradation parameter controls the overall drug release, which is usually not the case in biodegradable particles. Therefore, mechanistic models which consider specific physicochemical

phenomena like a change in diffusivity, change in size of the particles over the release period, effect of pore formation should be considered for a more detailed understanding of the release mechanism of molecules. The release of molecules from PLGA particles is very widely understood, and there are a lot of different models which explain the release of molecules from pure PLGA particles, but all these models are developed for the release of small molecules from the particles. Hence, there is a need for the development of models to understand the release of macromolecules. Furthermore, the release mechanism of macromolecules from the composite particles should be modeled using a combination of different theories like bulk erosion, surface erosion, diffusional resistances, osmotic pressure, pore formation and closure.

# Chapter 7: Future directions

## 7.1 Optimization of the release of macromolecule

It was observed that the composite particles gave controlled release of the Ad-vectors encapsulated in the interior more than replicating the pulsed system as we had hoped. Some of the other parameters that can help in optimizing this release of macromolecules are the varying the molecular weight of PLGA and chitosan, varying the DD of chitosan, varying lactic: glycolic ratio in PLGA. The chitosan used in this study is 75% deacetylated which has a very high half-life of degradation whereas PLGA 50:50 used here degrades faster. Due to this, the PLGA hydrolyzes faster than chitosan crumbling the structure of the particles. Degradation time of chitosan reduces with decreasing DD; therefore if we use a lower DD which can maintain the spherical structure of the composites while sustaining the osmotic pressure inside the particles, it can give us the pulsed release as explained in **Figure 2-5.** With DD decreased to 52 %, chitosan degraded to 10% of its weight in 20 days, and with 93 % DD chitosan does not degrade even after 90 days[199]. This can give us better control over controlling the release of the macromolecule and obtaining a pulsed release.

Release from PLGA particles also depends on the average molecular weight of polymer[78,200]. Polymers with higher molecular weights require longer durations to degrade than low molecular weight polymers, thereby causing slower release rate[58,155]. Therefore, depending on the release profile required molecular weight of the polymer molecular weight should be adjusted. On the other hand, end moieties of PLGA polymers affect the water absorption and subsequently the degradation rate of particles. It is reported that modification with hydroxyl end groups resulted in slower degradation than unmodified carboxylic group[12,81,105].

The copolymer ratio of lactic-to-glycolic acid was observed to have a greater relative effect on degradation and release kinetics than polymer molecular weight[16]. It has been seen that the higher the lactide content, the more hydrophobic the polymer. This has an ardent effect on the encapsulation efficiency as well as the degradation kinetics of the composites. It is found that using higher lactide to glycolide ratio has

shown higher entrapment efiiciencies[78,154,177,201] with larger particles formed. PLGA (75:25) has a higher glass transition temperature (Tg) as well as is more hydrophobic as compared to PLGA (50:50). Higher glass transition temperature (Tg) is expected to slow down drug diffusion through the polymer matrix[201]. The higher hydrophobicity will help in the slower diffusion of aqueous media leading to slow degradation of polymer bonds in PLGA.

Varying all these parameters is a very long and expensive study. There are many mathematical models available that can be used to tune the release of molecules from PLGA particles. Some of these mathematical models are compared in Chapter 5. But these models only take into account the PLGA particles; further mathematical models can be developed to take into account the degradation of chitosan and physical properties of this polymer and a new mathematical model can be developed for this composite particle[125] which will help us in better understanding the release mechanism.

### 7.2 Use for delivery of cancer vaccines

In spite the development of more efficacious cytotoxic drugs and improvements in surgical and radiotherapy, cancer is still a leading cause of mortality [22]. In general, the keystones of cancer therapy are surgery, chemotherapy, radiotherapy and, more recently, monoclonal antibody (mAb) mediated therapies. Scientists have studied the interactions between the immune system and cancer cells so that anti-tumor immunity could be amplified as a means of cancer therapy[21,22,202–205]. A vaccine can be defined as a biological preparation that provides active acquired immunity to a particular disease. Cancer vaccines have been proposed as therapy that is designed to elicit and/or boost antitumor immunity in patients, thereby preventing or prolonging the time to recurrence[21]. The fact that eight therapeutic antibodies are currently approved by the FDA for sale in the United States illustrates that antibodies which target tumor-associated surface proteins are effective in the treatment of cancer and thus exemplifies the cancer vaccine approach. More than 50 vaccines are tested clinically, and over 400 cancer vaccine studies have been undertaken[206]. Some of the key advantages of viral vaccines over existing cancer therapies are their excellent safety profile,

low incidence of adverse events which may impact on a patient's quality of life and the ease with which the vaccine is administered[21,22,202,203].

In the various clinical studies conducted, cancer vaccines are usually administered as multiple injections weeks apart. Out of this plethora of vaccines tested, some examples of the clinical studies are as follows. Prostate-specific antigen with vaccinia virus which was administered to 42 patients as three injections in 4-week intervals to see an enhanced T-cell response[207]. Phase I trials of recombinant canarypox vectors delivering the carcinoembryonic tumor antigen (CEA) have been undertaken in >100 patients[208,209] who were administered with homologous prime-boost over the period of 8 weeks. Enhanced cellular and humoral immune responses were observed simultaneously detecting CEA specific antibodies[210]. There are plenty of other examples with adenovirus[22,211], fowlpox virus[22,208,212]. One of the potential ways in which cancer vaccines can be optimized is through the use of different viral vectors to deliver the same tumor antigen (heterologous prime-boost)[21,22,203,204]. The use of one viral vector to prime an immune response and a different viral vector to boost the response should, theoretically, skew the expansion of immune cells in favor of the target antigen rather than the viral proteins[213,214].

### 7.3 Surface Modification of Particles to improve stability and targeting

In order for a delivery device to achieve the desired benefits of the particles, they must be present in the circulation long enough to reach or identify its therapeutic site of action. However, the opsonization or removal of nanoparticulate carriers from the body by the mononuclear phagocytic system (MPS), also known as the reticuloendothelial system (RES), is a major obstacle to the realization of this goal[215]. The macrophages of the MPS have the ability to remove unprotected nanoparticles from the bloodstream very quickly, rendering them ineffective as site-specific drug delivery devices[215]. These macrophages, which are typically Kupffer cells, or macrophages of the liver, cannot directly identify the nanoparticles themselves, but rather recognize specific opsonin proteins bound to the surface of the particles[141,216]. Broadly speaking, opsonins are any blood serum component that aids in the process of phagocytic recognition, but complement proteins such as C3, C4 and C5 and immunoglobulins are the most common. The process of

activation is very complex and not yet fully understood, but the important components involved are, for the most part, well known. The preferred method of imparting stealth or sterically stabilized properties to nanoparticles is by the PEGylation of these particles.

Modification of a particle surface by the covalently attaching, entrapping, or adsorbing of PEG chains in known as PEGylation. It is the process of covalent and non-covalent attachment of polyethylene glycol (PEG) polymer chains to molecules and particles, such as a drug, therapeutic protein or vesicle. Polyethylene glycol (PEG) is amphiphilic, chemically inert polymer consists of repeating units of ethylene oxide, which is arranged in either linear or branched conformations, creating a series of compounds of different molecular weights with distinct properties. Also, in the case of biodegradable nanoparticles, PEG chains can be incorporated as copolymers throughout the particle so that some surface. PEG is approved by the Food and Drug Administration (FDA) for use in drugs (parenteral, topicals, suppositories, nasal sprays), foods, and cosmetics. PEGylation is a well-established technique and is termed as conjugation of PEG to therapeutic peptides and proteins. Some researchers have directly shown that particles with covalently bound PEG chains achieve longer blood circulation half-lives than similar particles with the only surface adsorbed PEG[217,218]. It will also help in increasing the stability of the particles in media or serum as it was observed during the *in vivo* studies that the particles stayed in suspension only for a short period of time. Along with PEG various targeting ligands, proteins, antibodies, peptides can be attached to the surfaces of the nanoparticles by chemical coupling to achieve targeted delivery. Some of the targeting ligands studies are shown in **Table 7.1**. The use of small peptides may avoid these shortcomings because they are typically non-immunogenic and combine high affinity and selectivity with more desirable pharmacokinetic properties. Furthermore, specific targeting of tumor cells using high-affinity and highly selective peptides conjugated to conventional chemotherapeutics enables the use of small doses, reducing the toxic effects of chemotherapeutics[138,219,220].

**Table 7-1:** Examples of different ligands used for targeted delivery to various types of cells

| Ligands | Activity |
|---|---|
| Transferrin | Active targeting of anticancer agents and genes via transferrin receptors[11,221,222] |
| Lactoferrin | Anti-infective agent, immune-regulatory protein[223,224] |
| RPMReI | Specific to colorectal cancer cells[219] |
| Tat-peptide | Enhanced intracellular delivery[225,226] |
| Pullulan | No toxicity, non-immunogenic and non-antigenic properties[227,228] |

## Chapter 8: Summary and Significance

World Health Organization (WHO) states that vaccines help save billions of lives annually, but we still utilize a slight modification of vaccination principles that were developed by Edward Jenner in 1800s. Over the past three decades, there has been a continuous stream of freshly identified pathogens that have received increasing attention. In the present day, in order to develop long-term immunity, we still need to go multiple times to the hospital to receive our booster dosages. Due to this dosage system, one in six infants stay unimmunized every year[16]; additionally routinely vaccinating animals is more affordable than paying for the treatment of sick animals and it reduces transmission of microorganisms in the animal population reducing animal suffering. WHO also states that 1.5 million deaths can be avoided every year if global vaccine coverage is provided. Single Dose Vaccines can help us improve this global vaccine coverage and help us eradicate diseases.

The main goal of this work was to develop a pulsed delivery system which can be further utilized as a single dose vaccine. The controlled release of adenoviral vectors in pharmaceutical applications can be achieved by the microencapsulation using double emulsion technique. The properties of materials and the process engineering aspects strongly influence the properties of microspheres and the resultant controlled release rate. We have successfully developed a simple method to synthesize a novel composite, comprising of two different polymers poly-lactic-glycolic acid (PLGA) and chitosan, for controlled vaccine delivery. Overall particle size could be modulated from 300 nm to 4 μm with a positive surface charge by varying different parameters like emulsifier concentration, chitosan concentration, PLGA concentration and distribution of chitosan. Minimum energy input is used in order to maintain the activity of the adenoviral vector encapsulated. We found that the composite particles were spherical in shape and had a smooth surface, which would prevent leaching of any drug encapsulated within the particle. In general, it was found that the pure PLGA particles were mechanically “weak” as compared to the composite particles, which might be due to the presence of chitosan. PLGA and chitosan have different degradation kinetics and therefore results in different release mechanisms when a composite particle might be used as compared to

pure polymer particles. The modulation of the release kinetics of the adenoviral vector is also studied by varying the process parameters mentioned. It is observed that PLGA concentration and process of addition of the polymers affect the release kinetics significantly. It was demonstrated that using the PLGA-Chitosan composite particles could delay the release of Ad-eGFP followed by an increase in the rate of release to mimic the boost injection.

The activity of the viral vector encapsulated is seen to be maintained during the synthesis procedure. Additionally, successful encapsulation of Ad-flu was demonstrated in the composites with a particle size varying between 1.5 μm to 4 μm by varying synthesis parameters. These particles were also generally spherical in shape with a smooth surface. In vitro release of Ad-flu from PLGA gave a higher burst in the initial 4 days as compared to the composite particles. *In vivo* antibody response did not show a boost in the antibody levels after 20 days; several parameters like PLGA concentration, DD of chitosan, the molecular weight of polymers and energy input can be optimized further to modulate the release kinetics of the Ad-flu vaccine. Non-Fickian diffusion kinetics are observed for the release of the adenoviral vectors which was validated using the Korsmeyer-Peppas model. The release of encapsulated adenovirus from the composite is a combined effect of both Fickian and Non-Fickian diffusion kinetics; the fraction of release of adenovirus due to Fickian diffusion can be calculated using Peppas-Sahlin equation. It is observed using the Peppas-Sahlin model that Fickian diffusion kinetics control the rate of release from pure PLGA particles as opposed to composite particles.

## References


1. Wagner, V., Dullaart, A., Bock, A. K. & Zweck, A. The emerging nanomedicine landscape. *Nature Biotechnology* **24,** 1211–1217 (2006).
2. Riehemann, K. *et al.* Nanomedicine - Challenge and perspectives. *Angewandte Chemie - International Edition* **48,** 872–897 (2009).
3. Jatzkewitz, H. Incorporation of physiologically-active substances into a colloidal blood plasma substitute. I. Incorporation of mescaline peptide into polyvinylpyrrolidone. *Hoppe. Seylers. Z. Physiol. Chem.* **297,** 149–56 (1954).
4. Jatzkewitz, H. An ein kolloidales Blutplasma-Ersatzmittel (Polyvinylpyrrolidon) gebundenes Peptamin (Glycyl-L-leucyl-mezcalin) als neuartige Depotform für biologisch aktive primäre Amine (Mezcalin). *Zeitschrift fur Naturforsch. - Sect. B J. Chem. Sci.* **10,** 27–31 (1955).
5. Petros, R. a & DeSimone, J. M. Strategies in the design of nanoparticles for therapeutic applications. *Nat. Rev. Drug Discov.* **9,** 615–627 (2010).
6. Kumari, A., Yadav, S. K. & Yadav, S. C. Biodegradable polymeric nanoparticles based drug delivery systems. *Colloids Surfaces B Biointerfaces* **75,** 1–18 (2010).
7. Siepmann, J., Faisant, N. & Benoit, J. A new mathematical model quantifying drug release from bioerodible microparticles using Monte Carlo simulations. *Pharm. Res.* **19,** (2002).
8. Tobío, M., Nolley, J., Guo, Y., McIver, J. & Alonso, M. J. A novel system based on a poloxamer/PLGA blend as a tetanus toxoid delivery vehicle. *Pharm. Res.* **16,** 682–688 (1999).
9. Ganta, S., Devalapally, H., Shahiwala, A. & Amiji, M. A review of stimuli-responsive nanocarriers for drug and gene delivery. *Journal of Controlled Release* **126,** 187–204 (2008).
10. Imler, J. L. Adenovirus vectors as recombinant viral vaccines. *Vaccine* **13,** 1143–1151 (1995).
11. Curiel, D. T., Agarwal, S., Wagner, E. & Cotten, M. Adenovirus enhancement of transferrin-polylysine-mediated gene delivery. *Proc. Natl. Acad. Sci.* **88,** 8850–8854 (1991).
12. Cleland, J. L. *et al.* Development of poly-(D,L-lactide-coglycolide) microsphere formulations containing recombinant human vascular endothelial growth factor to promote local angiogenesis. *J. Control. Release* **72,** 13–24 (2001).
13. Sheng, Y. *et al.* In vitro macrophage uptake and in vivo biodistribution of PLA-PEG nanoparticles loaded with hemoglobin as blood substitutes: Effect of PEG content. *J. Mater. Sci. Mater. Med.* **20,** 1881–1891 (2009).
14. Harris, J. M., Martin, N. E. & Modi, M. Pegylation A Novel Process for Modifying Pharmacokinetics.
15. Turgeon, S. L., Beaulieu, M., Schmitt, C. & Sanchez, C. Protein-polysaccharide interactions: Phase-ordering kinetics, thermodynamic and structural aspects. *Current Opinion in Colloid and Interface Science* **8,** 401–414 (2003).
16. McHugh, K. J., Guarecuco, R., Langer, R. & Jaklenec, A. Single-injection vaccines: Progress, challenges, and opportunities. *J. Control. Release* **219,** 596–609 (2015).
17. Leader, B., Baca, Q. J. & Golan, D. E. Protein therapeutics: A summary and pharmacological classification. *Nature Reviews Drug Discovery* **7,** 21–39 (2008).
18. Tibbitt, M. W., Dahlman, J. E. & Langer, R. Emerging Frontiers in Drug Delivery. *Journal of the American Chemical Society* **138,** 704–717 (2016).

19. Langer, R. & Peppas, N. A. Advances in Biomaterials, Drug Delivery, and Bionanotechnology. in *AIChE Journal* **49,** 2990–3006 (Wiley-Blackwell, 2003).

20. Mitragotri, S., Burke, P. A. & Langer, R. Overcoming the challenges in administering biopharmaceuticals: Formulation and delivery strategies. *Nature Reviews Drug Discovery* **13,** 655–672 (2014).

21. Pardoll, D. M. Cancer vaccines. *Nature* **4,** 623–6 (1998).

22. Harrop, R., John, J. & Carroll, M. W. Recombinant viral vectors: Cancer vaccines. *Advanced Drug Delivery Reviews* **58,** 931–947 (2006).

23. Smith, D. M., Simon, J. K. & Baker, J. R. Applications of nanotechnology for immunology. *Nat. Rev. Immunol.* **13,** 592–605 (2013).

24. Waehler, R., Russell, S. J. & Curiel, D. T. Engineering targeted viral vectors for gene therapy. *Nat. Rev. Genet.* **8,** 573–587 (2007).

25. Santosuosso, M., McCormick, S. & Xing, Z. Adenoviral vectors for mucosal vaccination against infectious diseases. *Viral Immunol.* **18,** 283–291 (2005).

26. Thomas, C. E., Ehrhardt, A. & Kay, M. A. Progress and problems with the use of viral vectors for gene therapy. *Nat Rev Genet* **4,** 346–358 (2003).

27. Pillai, O. & Panchagnula, R. Polymers in drug delivery. *Current Opinion in Chemical Biology* **5,** 447–451 (2001).

28. Samad, A., Sultana, Y. & Aqil, M. Liposomal Drug Delivery Systems: An Update Review. *Curr. Drug Deliv.* **4,** 297–305 (2007).

29. Plotkin S, Offit P, O. W. A short history of vaccination | Vaccines. *The Lancet* 1–16 (2008). Available at: https://illiad.lib.auburn.edu/illiad.dll?Action=10&Form=75&Value=701179. (Accessed: 24th April 2017)

30. Clem, A. S. Fundamentals of vaccine immunology. *J. Glob. Infect. Dis.* **3,** 73–78 (2011).

31. Van Reeth, K. *et al.* Heterologous prime-boost vaccination with H3N2 influenza viruses of swine favors cross-clade antibody responses and protection. *npj Vaccines* **2,** (2017).

32. Fenner, F. *et al. Smallpox and its eradication*. *History of international public health ; no. 6* (World Health Organization, 1988).

33. Smith, J., Leke, R., Adams, A. & Tangermann, R. H. Certification of polio eradication: Process and lessons learned. *Bulletin of the World Health Organization* **82,** 24–30 (2004).

34. Correia-Pinto, J. F., Csaba, N. & Alonso, M. J. Vaccine delivery carriers: Insights and future perspectives. *Int. J. Pharm.* **440,** 27–38 (2013).

35. Siegrist, C.-A. in *Vaccine immunology* **2,** 17–36 (2008).

36. Zazo, H., Colino, C. I. & Lanao, J. M. Current applications of nanoparticles in infectious diseases. *Journal of Controlled Release* **224,** 86–102 (2016).

37. Medzhitov, R. & Janeway, C. A. J. Innate immunity: Minireview the virtues of a nonclonal system of recognition. *Cell* **91,** 295–298 (1997).

38. Preis, I. & Langer, R. S. A single-step immunization by sustained antigen release. *J. Immunol. Methods* **28,** 193–197 (1979).

39. Vila, A., Sánchez, A., Tobío, M., Calvo, P. & Alonso, M. J. Design of biodegradable particles for protein delivery. *J. Control. Release* **78,** 15–24 (2002).

40. Peek, L. J., Middaugh, C. R. & Berkland, C. Nanotechnology in vaccine delivery. *Adv. Drug Deliv. Rev.* **60,** 915–928 (2008).

41. Banchereau, J. & Steinman, R. M. Dendritic cells and the control of immunity. *Nature* **392,** 245–252 (1998).

42. Bjorkman, P. J. & Parham, P. Structure, Function, and Diversity of Class I Major Histocompatibility Complex Molecules. *Annu. Rev. Biochem.* **59,** 253–288 (1990).

43. Gorry, P. R. *et al.* Pathogenicity and immunogenicity of attenuated, nef-deleted HIV-1 strains in vivo. *Retrovirology* **4,** 66 (2007).

44. Wack, A. & Rappuoli, R. Vaccinology at the beginning of the 21st century. *Curr. Opin. Immunol.* **17,** 411–418 (2005).

45. Jaganathan, K. S., Singh, P., Prabakaran, D., Mishra, V. & Vyas, S. P. Development of a single-dose stabilized poly(D,L-lactic-co-glycolic acid) microspheres-based vaccine against hepatitis B. *J. Pharm. Pharmacol.* **56,** 1243–1250 (2004).

46. Singh, M. *et al.* Controlled release microparticles as a single dose diphtheria toxoid vaccine immunogenicity in small animal models. *Vaccine* **16,** 346–352 (1998).

47. Johansen, P. *et al.* Immunogenicity of single-dose diphtheria vaccines based on PLA/PLGA microspheres in guinea pigs. in *Vaccine* **18,** 209–215 (1999).

48. Lü, J.-M. *et al.* Current advances in research and clinical applications of PLGA-based nanotechnology. *Expert Rev. Mol. Diagn.* **9,** 325–41 (2009).

49. Patil, S. D., Rhodes, D. G. & Burgess, D. J. DNA-based therapeutics and DNA delivery systems: a comprehensive review. *AAPS J.* **7,** E61–E77 (2005).

50. O'Riordan, C. R. *et al.* PEGylation of adenovirus with retention of infectivity and protection from neutralizing antibody in vitro and in vivo. *Hum. Gene Ther.* **10,** 1349–1358 (1999).

51. Vemula, S. V & Mittal, S. K. Production of adenovirus vectors and their use as a delivery system for influenza vaccines. *Expert Opin. Biol. Ther.* **10,** 1469–1487 (2010).

52. Danthinne, X. & Imperiale, M. J. Production of first generation adenovirus vectors: a review. *Gene Ther.* **7,** 1707–1714 (2000).

53. Draper, S. J. *et al.* Effective induction of high-titer antibodies by viral vector vaccines. *Nat. Med.* **14,** 819–821 (2008).

54. Liu, M. DNA Vaccines : A Review. *J. Intern. Med.* **253,** 402–410 (2003).

55. Shi, Z. *et al.* Protection against Tetanus by Needle-Free Inoculation of Adenovirus-Vectored Nasal and Epicutaneous Vaccines. *J. Virol.* **75,** 11474–11482 (2001).

56. Van Kampen, K. R. *et al.* Safety and immunogenicity of adenovirus-vectored nasal and epicutaneous influenza vaccines in humans. *Vaccine* **23,** 1029–1036 (2005).

57. Danhier, F. *et al.* PLGA-based nanoparticles: An overview of biomedical applications. *Journal of Controlled Release* **161,** 505–522 (2012).

58. Ding, D. & Zhu, Q. Recent advances of PLGA micro/nanoparticles for the delivery of biomacromolecular therapeutics. *Mater. Sci. Eng. C* (2018). doi:10.1016/j.msec.2017.12.036

59. Copland, M. J., Rades, T., Davies, N. M. & Baird, M. A. Lipid based particulate formulations for the delivery of antigen. *Immunology and Cell Biology* **83,** 97–105 (2005).

60. O'Hagan, D. T. & Singh, M. Microparticles as vaccine adjuvants and delivery systems. *Expert Rev.*

*Vaccines* **2,** 269–283 (2003).

61. Zheng, X., Huang, Y., Zheng, C., Dong, S. & Liang, W. Alginate-chitosan-PLGA composite microspheres enabling single-shot hepatitis B vaccination. *AAPS J.* **12,** 519–524 (2010).

62. Borges, O., Borchard, G., Verhoef, J. C., De Sousa, A. & Junginger, H. E. Preparation of coated nanoparticles for a new mucosal vaccine delivery system. *Int. J. Pharm.* **299,** 155–166 (2005).

63. Jones, L. S. *et al.* Effects of adsorption to aluminum salt adjuvants on the structure and stability of model protein antigens. *J. Biol. Chem.* **280,** 13406–14 (2005).

64. Jeffery, H., Davis, S. S. & O'Hagan, D. T. The preparation and characterisation of poly(lactide-co-glycolide) microparticles. I: Oil-in-water emulsion solvent evaporation. *Int. J. Pharm.* **77,** 169–175 (1991).

65. Gupta, R. K., Rost, B. E., Relyveld, E. & Siber, G. R. Adjuvant properties of aluminum and calcium compounds. *Pharm. Biotechnol.* **6,** 229–248 (1995).

66. Eldridge, J. H., Staas, J. K., Meulbroek, J. A., Tice, T. R. & Gilley, R. M. Biodegradable and biocompatible poly(DL-lactide-co-glycolide) microspheres as an adjuvant for staphylococcal enterotoxin B toxoid which enhances the level of toxin-neutralizing antibodies. *Infect. Immun.* **59,** 2978–2986 (1991).

67. Decuzzi, P. *et al.* Size and shape effects in the biodistribution of intravascularly injected particles. *J. Control. Release* **141,** 320–327 (2010).

68. Schwendener, R. A. Liposomes as vaccine delivery systems: a review of the recent advances. *Ther. Adv. Vaccines* **2,** 159–182 (2014).

69. Gregory, A. E., Titball, R. & Williamson, D. Vaccine delivery using nanoparticles. *Front. Cell. Infect. Microbiol.* **3,** 13 (2013).

70. Gradauer, K. *et al.* Liposomes coated with thiolated chitosan enhance oral peptide delivery to rats. *J. Control. Release* **172,** 872–878 (2013).

71. Felnerova, D., Viret, J.-F., Glück, R. & Moser, C. Liposomes and virosomes as delivery systems for antigens, nucleic acids and drugs. *Curr. Opin. Biotechnol.* **15,** 518–529 (2004).

72. Kim, M.-G. & Joo Yeon Park, Yuna Shon, Gunwoo Kim, Gayong Shim, Y.-K. O. Nanotechnology and vaccine development. *Asian J. Pharm. Sci.* **9,** 227–235 (2014).

73. Wang, A. Z., Langer, R. & Farokhzad, O. C. Nanoparticle Delivery of Cancer Drugs. *Annu. Rev. Med.* **63,** 185–198 (2012).

74. Mountain, A. Gene therapy: The first decade. *Trends in Biotechnology* **18,** 119–128 (2000).

75. Slütter, B. *et al.* Nasal vaccination with N-trimethyl chitosan and PLGA based nanoparticles: Nanoparticle characteristics determine quality and strength of the antibody response in mice against the encapsulated antigen. *Vaccine* **28,** 6282–6291 (2010).

76. Cleland, J. L. Solvent evaporation processes for the production of controlled release biodegradable microsphere formulations for therapeutics and vaccines. *Biotechnol. Prog.* **14,** 102–107 (1998).

77. Jaganathan, K. S. *et al.* Development of a single dose tetanus toxoid formulation based on polymeric microspheres: A comparative study of poly(D,L-lactic-co-glycolic acid) versus chitosan microspheres. *Int. J. Pharm.* **294,** 23–32 (2005).

78. Wischke, C. & Schwendeman, S. P. Principles of encapsulating hydrophobic drugs in PLA/PLGA microparticles. *Int. J. Pharm.* **364,** 298–327 (2008).

79. Cleland, J. L., Lim, A., Barrón, L., Duenas, E. T. & Powell, M. F. Development of a single-shot

subunit vaccine for HIV-I: Part 4. Optimizing microencapsulation and pulsatile release of MN rgp120 from biodegradable microspheres. *J. Control. Release* **47,** 135–150 (1997).

80. Kamaly, N., Yameen, B., Wu, J. & Farokhzad, O. C. Degradable Controlled-Release Polymers and Polymeric Nanoparticles: Mechanisms of Controlling Drug Release. *Chem. Rev.* **116,** 2602–2663 (2016).

81. Park, T. G. Degradation of poly(lactic-co-glycolic acid) microspheres: effect of copolymer composition. *Biomaterials* **16,** 1123–1130 (1995).

82. Goldberg, M. & Gomez-Orellana, I. Challenges for the oral delivery of macromolecules. *Nat. Rev. Drug Discov.* **2,** 289–295 (2003).

83. Kratz, F. & Beyer, U. Serum proteins as drug carriers of anticancer agents: a review. *Drug Deliv.* **5,** 281–99 (1998).

84. Makadia, H. K. & Siegel, S. J. Poly Lactic-co-Glycolic Acid (PLGA) as biodegradable controlled drug delivery carrier. *Polymers (Basel).* **3,** 1377–1397 (2011).

85. Wang, H. *et al.* PLGA/polymeric liposome for targeted drug and gene co-delivery. *Biomaterials* **31,** 8741–8748 (2010).

86. Amidi, M. *et al.* N-Trimethyl chitosan (TMC) nanoparticles loaded with influenza subunit antigen for intranasal vaccination: Biological properties and immunogenicity in a mouse model. *Vaccine* **25,** 144–153 (2007).

87. Ramya, R. *et al.* Poly(lactide-co-glycolide) microspheres: A potent oral delivery system to elicit systemic immune response against inactivated rabies virus. *Vaccine* **27,** 2138–2143 (2009).

88. Carcaboso, A. M. *et al.* Immune response after oral administration of the encapsulated malaria synthetic peptide SPf66. *Int. J. Pharm.* **260,** 273–282 (2003).

89. Feng, L. *et al.* Pharmaceutical and immunological evaluation of a single-dose hepatitis B vaccine using PLGA microspheres. *J. Control. Release* **112,** 35–42 (2006).

90. Saini, V. *et al.* Comparison of humoral and cell-mediated immune responses to cationic PLGA microspheres containing recombinant hepatitis B antigen. *Int. J. Pharm.* **408,** 50–57 (2011).

91. Gómez, S. *et al.* Nanoparticles as an adjuvant for oral immunotherapy with allergens. *Vaccine* **25,** 5263–5271 (2007).

92. Mokarram, R. & Alonso, M. J. Preparation and evaluation of chitosan nanoparticles containing Diphtheria toxoid as new carriers for nasal vaccine delivery in mice. *Arch. Razi Inst.* **61,** 13–25 (2006).

93. Singh, J., Pandit, S., Bramwell, V. W. & Alpar, H. O. Diphtheria toxoid loaded poly-(ε-caprolactone) nanoparticles as mucosal vaccine delivery systems. *Methods* **38,** 96–105 (2006).

94. Jain, R. A. The manufacturing techniques of various drug loaded biodegradable poly(lactide-co-glycolide) (PLGA) devices. *Biomaterials* **21,** 2475–2490 (2000).

95. Dang, J. M. & Leong, K. W. Natural polymers for gene delivery and tissue engineering. *Advanced Drug Delivery Reviews* **58,** 487–499 (2006).

96. Zhao, L. *et al.* Nanoparticle vaccines. *Vaccine* **32,** 327–337 (2014).

97. Das, R. K., Kasoju, N. & Bora, U. Encapsulation of curcumin in alginate-chitosan-pluronic composite nanoparticles for delivery to cancer cells. *Nanomedicine Nanotechnology, Biol. Med.* **6,** 153–160 (2010).

98. Das, S., Chaudhury, A. & Ng, K.-Y. Preparation and evaluation of zinc–pectin–chitosan composite

particles for drug delivery to the colon: Role of chitosan in modifying in vitro and in vivo drug release. *Int. J. Pharm.* **406,** 11–20 (2011).

99. Jeong, Y.-I., Choi, K.-C. & Song, C.-E. Doxorubicin release from core-shell type nanoparticles of poly(DL-lactide-co-glycolide)-grafted dextran. *Arch. Pharm. Res.* **29,** 712–719 (2006).

100. Levy, R. J. *et al.* Gene delivery from a DNA controlled-release stent in porcine coronaryarteries. *Nat. Biotechnol.* **18,** 1181–1184 (2000).

101. Zhi, J., Wang, Y., Lu, Y., Ma, J. & Luo, G. In situ preparation of magnetic chitosan/Fe3O4 composite nanoparticles in tiny pools of water-in-oil microemulsion. *React. Funct. Polym.* **66,** 1552–1558 (2006).

102. Sanchez, A., Gupta, R. K., Alonso, M. J., Siber, G. R. & Langer, R. Pulsed controlled-released system for potential use in vaccine delivery. *J Pharm Sci* **85,** 547–52. (1996).

103. Nair, L. S. & Laurencin, C. T. Biodegradable polymers as biomaterials. *Progress in Polymer Science (Oxford)* **32,** 762–798 (2007).

104. Han, F. Y., Thurecht, K. J., Whittaker, A. K. & Smith, M. T. Bioerodable PLGA-based microparticles for producing sustained-release drug formulations and strategies for improving drug loading. *Frontiers in Pharmacology* **7,** (2016).

105. Weiss, B. *et al.* Nanoparticles made of fluorescence-labelled Poly(L-lactide-co-glycolide): preparation, stability, and biocompatibility. *J. Nanosci. Nanotechnol.* **6,** 3048–3056 (2006).

106. Tobío, M. & Alonso, M. J. Study of the inactivation process of the tetanus toxoid in contact with poly(lactic/glycolic acid) degrading microspheres. *S.T.P. Pharma Sci.* **8,** 303–310 (1998).

107. Sahoo, S. K., Panyam, J., Prabha, S. & Labhasetwar, V. Residual polyvinyl alcohol associated with poly (D,L-lactide-co-glycolide) nanoparticles affects their physical properties and cellular uptake. *J. Control. Release* **82,** 105–114 (2002).

108. Kean, T. & Thanou, M. in *Renewable Resources for Functional Polymers and Biomaterials: Polysaccharides{,} Proteins and Polyesters* 292–318 (2011). doi:10.1039/9781849733519-00292

109. Kumar, M. A review of chitin and chitosan applications. *React. Funct. Polym.* **46,** 1–27 (2000).

110. Khor, E. & Lim, L. Y. Implantable applications of chitin and chitosan. *Biomaterials* **24,** 2339–2349 (2003).

111. Blackwell, J. Physical methods for the determination of chitin structure and conformation. *Methods Enzymol.* **161,** 435–442 (1988).

112. Gorzelanny, C., Pöppelmann, B., Pappelbaum, K., Moerschbacher, B. M. & Schneider, S. W. Human macrophage activation triggered by chitotriosidase-mediated chitin and chitosan degradation. *Biomaterials* **31,** 8556–8563 (2010).

113. Prabaharan, M. & Mano, J. F. Chitosan-based particles as controlled drug delivery systems. *Drug Deliv. J. Deliv. Target. Ther. Agents* **12,** 41–57 (2005).

114. Desai, K. G. H. Chitosan Nanoparticles Prepared by Ionotropic Gelation : An Overview of Recent Advances. **33,** 107–158 (2016).

115. Şenel, S. & McClure, S. J. Potential applications of chitosan in veterinary medicine. *Advanced Drug Delivery Reviews* **56,** 1467–1480 (2004).

116. Nishimura, K. *et al.* Adjuvant activity of chitin derivatives in mice and guinea-pigs. *Vaccine* **3,** 379–384 (1985).

117. Seferian, P. G. & Martinez, M. L. Immune stimulating activity of two new chitosan containing

adjuvant formulations. *Vaccine* **19,** 661–668 (2000).

118. Fredenberg, S., Wahlgren, M., Reslow, M. & Axelsson, A. The mechanisms of drug release in poly(lactic-co-glycolic acid)-based drug delivery systems--a review. *Int. J. Pharm.* **415,** 34–52 (2011).

119. Ding, D. & Zhu, Q. Recent advances of PLGA micro/nanoparticles for the delivery of biomacromolecular therapeutics. *Materials Science and Engineering C* (2018). doi:10.1016/j.msec.2017.12.036

120. Siepmann, J. & Peppas, N. A. Modeling of drug release from delivery systems based on hydroxypropyl methylcellulose (HPMC). *Adv. Drug Deliv. Rev.* **64,** 163–174 (2012).

121. Agnihotri, S. A., Mallikarjuna, N. N. & Aminabhavi, T. M. Recent advances on chitosan-based micro- and nanoparticles in drug delivery. *Journal of Controlled Release* **100,** 5–28 (2004).

122. Grassi, M. & Grassi, G. Mathematical modelling and controlled drug delivery: matrix systems. *Curr. Drug Deliv.* **2,** 97–116 (2005).

123. Tabata, Y. & Langer, R. Polyanhydride Mierospheres that Display Near-Constant Release of Water-Soluble Model Drug Compounds. *Pharm. Res.* **10,** 391–399 (1993).

124. Tabata, Y., Gutta, S. & Langer, R. Controlled Delivery Systems for Proteins Using Polyanhydride Microspheres. *Pharm. Res. An Off. J. Am. Assoc. Pharm. Sci.* **10,** 487–496 (1993).

125. Lao, L. L., Venkatraman, S. S. & Peppas, N. A. Modeling of drug release from biodegradable polymer blends. *Eur. J. Pharm. Biopharm.* **70,** 796–803 (2008).

126. Faisant, N., Siepmann, J. & Benoit, J. P. PLGA-based microparticles: elucidation of mechanisms and a new, simple mathematical model quantifying drug release. *Eur. J. Pharm. Sci.* **15,** 355–366 (2002).

127. Fonte, P., Reis, S. & Sarmento, B. Facts and evidences on the lyophilization of polymeric nanoparticles for drug delivery. *Journal of Controlled Release* **225,** 75–86 (2016).

128. Kim, H. K., Chung, H. J. & Park, T. G. Biodegradable polymeric microspheres with "open/closed" pores for sustained release of human growth hormone. *J. Control. Release* **112,** 167–174 (2006).

129. Costa, P. & Sousa Lobo, J. M. Modeling and comparison of dissolution profiles. *European Journal of Pharmaceutical Sciences* **13,** 123–133 (2001).

130. Peppas, N. A. & Sahlin, J. J. A simple equation for the description of solute release. III. Coupling of diffusion and relaxation. *Int. J. Pharm.* **57,** 169–172 (1989).

131. Grassi, M. & Grassi, G. Mathematical modelling and controlled drug delivery: matrix systems. *Curr. Drug Deliv.* **2,** 97–116 (2005).

132. Siepmann, J., Elkharraz, K., Siepmann, F. & Klose, D. How autocatalysis accelerates drug release from PLGA-based microparticles: A quantitative treatment. *Biomacromolecules* **6,** 2312–2319 (2005).

133. Kean, T. & Thanou, M. Biodegradation, biodistribution and toxicity of chitosan. *Adv. Drug Deliv. Rev.* **62,** 3–11 (2010).

134. Hill, C. *et al.* Efficient Delivery of Genome-Editing Proteins In Vitro and In Vivo. *Proc. SPIE--the Int. Soc. Opt. Eng.* **73,** 389–400 (2015).

135. Yu, M., Wu, J., Shi, J. & Farokhzad, O. C. Nanotechnology for protein delivery: Overview and perspectives. *J. Control. Release* **240,** 24–37 (2016).

136. Mok, H., Park, J. W. & Park, T. G. Microencapsulation of PEGylated adenovirus within PLGA

microspheres for enhanced stability and gene transfection efficiency. *Pharm. Res.* **24,** 2263–2269 (2007).

137. Ghosh, S. S., Gopinath, P. & Ramesh, A. Adenoviral vectors: A promising tool for gene therapy. *Applied Biochemistry and Biotechnology* **133,** 9–29 (2006).

138. Xie, J., Lee, S. & Chen, X. Nanoparticle-based theranostic agents. *Advanced Drug Delivery Reviews* **62,** 1064–1079 (2010).

139. Zborowski, M., Häfeli, U., Schütt, W. & Teller, J. *Scientific and Clinical Applications of Magnetic Carriers*. (1997).

140. Chertok, B. *et al.* Iron oxide nanoparticles as a drug delivery vehicle for MRI monitored magnetic targeting of brain tumors. *Biomaterials* **29,** 487–496 (2008).

141. Ruxandra Gref, Yoshiharu Minamitake, Maria Teresa Peracchia, Vladimir Trubetskoy, Vladimir Torchilin, R. L. Biodegradable Long-CirculatingPolymeric Nanospheres. *Science (80-. ).* **263,** 1600–1603 (1994).

142. Cleland, J. L. Protein Delivery from Biodegradable Microspheres.

143. Gregoriadis, G. Engineering liposomes for drug delivery: progress and problems. *Trends in Biotechnology* **13,** 527–537 (1995).

144. Lian, T. & Ho, R. J. Y. Trends and developments in liposome drug delivery systems. *Journal of Pharmaceutical Sciences* **90,** 667–680 (2001).

145. Li, J. *et al.* Self-assembled supramolecular hydrogels formed by biodegradable PEO-PHB-PEO triblock copolymers and α-cyclodextrin for controlled drug delivery. *Biomaterials* **27,** 4132–4140 (2006).

146. Yan, Q. & Hoffman, A. S. Synthesis of macroporous hydrogels with rapid swelling and deswelling properties for delivery of macromolecules. *Polymer (Guildf).* **36,** 887–889 (1995).

147. Wagner, A. M., Spencer, D. S. & Peppas, N. A. Advanced architectures in the design of responsive polymers for cancer nanomedicine. *J. Appl. Polym. Sci.* **135,** 1–17 (2018).

148. De La Rica, R., Aili, D. & Stevens, M. M. Enzyme-responsive nanoparticles for drug release and diagnostics ☆. *Adv. Drug Deliv. Rev.* **64,** 967–978 (2012).

149. Andresen, T. L., Thompson, D. H. & Kaasgaard, T. Enzyme-triggered nanomedicine: drug release strategies in cancer therapy. *Mol. Membr. Biol.* **27,** 353–63 (2010).

150. Gupta, P. K. & Hung, C. T. Minireview Magnetically controlled targeted micro-carrier systems. *Life Sci.* **44,** 175–186 (1989).

151. Mura, S., Nicolas, J. & Couvreur, P. Stimuli-responsive nanocarriers for drug delivery. *Nat. Mater.* **12,** 991–1003 (2013).

152. Bhattacharjee, S. DLS and zeta potential - What they are and what they are not? *Journal of Controlled Release* **235,** 337–351 (2016).

153. Onishi, H. & Machida, Y. Biodegradation and distribution of water-soluble chitosan in mice. *Biomaterials* **20,** 175–182 (1999).

154. MJ Alonso, S Cohen, TG Park, RK Gupta, G. S. and R. L. Determinants of Release Rate of Tetanus Vaccine from Polyester Microspheres. *Pharm. Res.* **10,** 945–953 (1993).

155. Shi, L. *et al.* Pharmaceutical and immunological evaluation of a single-shot Hepatitis B vaccine formulated with PLGA microspheres. *J. Pharm. Sci.* **91,** 1019–1035 (2002).

156. Kissel, T., Koneberg, R., Hilbert, A. K. & Hungerer, K. D. Microencapsulation of antigens using biodegradable polyesters: facts and phantasies. *Behring Inst Mitt* 172–183 (1997).

157. Mao, S. *et al.* Effects of process and formulation parameters on characteristics and internal morphology of poly(d,l-lactide-co-glycolide) microspheres formed by the solvent evaporation method. *Eur. J. Pharm. Biopharm.* **68,** 214–223 (2008).

158. Anton, N., Benoit, J. P. & Saulnier, P. Design and production of nanoparticles formulated from nano-emulsion templates-A review. *Journal of Controlled Release* **128,** 185–199 (2008).

159. Yang, Y. Y., Chung, T. S. & Ping Ng, N. Morphology, drug distribution, and in vitro release profiles of biodegradable polymeric microspheres containing protein fabricated by double-emulsion solvent extraction/evaporation method. *Biomaterials* **22,** 231–241 (2001).

160. Paragkumar N, T., Edith, D. & Six, J.-L. Surface characteristics of PLA and PLGA films. *Appl. Surf. Sci.* **253,** 2758–2764 (2006).

161. Ren, D., Yi, H., Wang, W. & Ma, X. The enzymatic degradation and swelling properties of chitosan matrices with different degrees of N-acetylation. *Carbohydr. Res.* **340,** 2403–2410 (2005).

162. Bustin, S. A. Why the need for qPCR publication guidelines?-The case for MIQE. *Methods* **50,** 217–226 (2010).

163. Gupta, R. K. *et al.* Determination of protein loading in biodegradable polymer microspheres containing tetanus toxoid. *Vaccine* **15,** 672–8 (1997).

164. Sánchez, A., Villamayor, B., Guo, Y., McIver, J. & Alonso, M. J. Formulation strategies for the stabilization of tetanus toxoid in poly(lactide-co-glycolide) microspheres. *Int. J. Pharm.* **185,** 255–266 (1999).

165. Shenderova, A., Burke, T. G. & Schwendeman, S. P. The Acidic Microclimate in Poly(lactide-co-glycolide) Microspheres Stabilizes Camptothecins. *Pharm. Res.* **16,** 241–248 (1999).

166. Mäder, K., Bittner, B., Li, Y., Wohlauf, W. & Kissel, T. Monitoring microviscosity and microacidity of the albumin microenvironment inside degrading microparticles from poly(lactide-co- glycolide) (PLG) or ABA-triblock polymers containing hydrophobic poly(lactide-co-glycolide) A blocks and hydrophilic poly(ethy. *Pharm. Res.* **15,** 787–793 (1998).

167. Fu, K., Pack, D. W., Klibanov, A. M. & Langer, R. Visual Evidence of Acidic Environment Within Degrading Poly(lactic-co-glycolic acid) (PLGA) Microspheres. *Pharm. Res.* **17,** 100–106 (2000).

168. Rampino, A., Borgogna, M., Blasi, P., Bellich, B. & Cesàro, A. Chitosan nanoparticles: Preparation, size evolution and stability. *Int. J. Pharm.* **455,** 219–228 (2013).

169. Mao, H. Q. *et al.* Chitosan-DNA nanoparticles as gene carriers: Synthesis, characterization and transfection efficiency. *J. Control. Release* **70,** 399–421 (2001).

170. Sameti, M. *et al.* Stabilisation by freeze-drying of cationically modified silica nanoparticles for gene delivery. *Int. J. Pharm.* **266,** 51–60 (2003).

171. Abdelwahed, W., Degobert, G., Stainmesse, S. & Fessi, H. Freeze-drying of nanoparticles: Formulation, process and storage considerations. *Advanced Drug Delivery Reviews* **58,** 1688–1713 (2006).

172. Fonte, P. *et al.* Effect of cryoprotectants on the porosity and stability of insulin-loaded PLGA nanoparticles after freeze-drying. *Biomatter* **2,** 329–339 (2012).

173. del Pozo-Rodríguez, A., Solinís, M. A., Gascón, A. R. & Pedraz, J. L. Short- and long-term stability study of lyophilized solid lipid nanoparticles for gene therapy. *Eur. J. Pharm. Biopharm.* **71,** 181–189 (2009).

174. Fasbender, A. *et al.* Complexes of adenovirus with polycationic polymers and cationic lipids increase the efficiency of gene transfer in vitro and in vivo. *J. Biol. Chem.* **272,** 6479–6489 (1997).

175. Pawar, D., Mangal, S., Goswami, R. & Jaganathan, K. S. Development and characterization of surface modified PLGA nanoparticles for nasal vaccine delivery: Effect of mucoadhesive coating on antigen uptake and immune adjuvant activity. *Eur. J. Pharm. Biopharm.* **85,** 550–559 (2013).

176. Medlicott, N. J. & Tucker, I. G. Pulsatile release from subcutaneous implants. *Advanced Drug Delivery Reviews* **38,** 139–149 (1999).

177. Cleland, J. L. in *Vaccine design* 439–462 (Springer, 1995).

178. Rothstein, S. N., Federspiel, W. J. & Little, S. R. A simple model framework for the prediction of controlled release from bulk eroding polymer matrices. *J. Mater. Chem.* **18,** 1873–1880 (2008).

179. Arifin, D. Y., Lee, L. Y. & Wang, C. H. Mathematical modeling and simulation of drug release from microspheres: Implications to drug delivery systems. *Advanced Drug Delivery Reviews* **58,** 1274–1325 (2006).

180. Yao, F. & Weiyuan, J. K. Drug Release Kinetics and Transport Mechanisms of Non- degradable and Degradable Polymeric Delivery Systems. *Expert Opin. Drug Deliv.* **7,** 429–444 (2010).

181. Rothstein, S. N., Federspiel, W. J. & Little, S. R. A unified mathematical model for the prediction of controlled release from surface and bulk eroding polymer matrices. *Biomaterials* **30,** 1657–1664 (2009).

182. Comunian, T. A. *et al.* Microencapsulation of ascorbic acid by complex coacervation: Protection and controlled release. *Food Res. Int.* **52,** 373–379 (2013).

183. Santos, M. G., Bozza, F. T., Thomazini, M. & Favaro-Trindade, C. S. Microencapsulation of xylitol by double emulsion followed by complex coacervation. *Food Chem.* **171,** 32–39 (2015).

184. Bachelder, E. M. *et al.* In Vitro Analysis of Acetalated Dextran Microparticles as a Potent Delivery Platform for Vaccine Adjuvants. doi:10.1021/mp900311x

185. Wonganan, P. & Croyle, M. A. *PEGylated adenoviruses: From mice to monkeys*. *Viruses* **2,** (2010).

186. Gao, J. Q. *et al.* Effective tumor targeted gene transfer using PEGylated adenovirus vector via systemic administration. *J. Control. Release* **122,** 102–110 (2007).

187. Azevedo, H. S. & Reis, R. R. L. Understanding the enzymatic degradation of biodegradable polymers and strategies to control their degradation rate. *Biodegrad. Syst. tissue* 177–202 (2005). doi:10.1201/9780203491232.ch12

188. Corrigan, O. I. & Li, X. Quantifying drug release from PLGA nanoparticulates. *Eur. J. Pharm. Sci.* **37,** 477–485 (2009).

189. Choi, H. S., Seo, S.-A., Khang, G., Rhee, J. M. & Lee, H. B. Preparation and characterization of fentanyl-loaded PLGA microspheres: in vitro release profiles. *Int. J. Pharm.* **234,** 195–203 (2002).

190. Yang, Y., Li, Q., Ertl, H. C. & Wilson, J. M. Cellular and humoral immune responses to viral antigens create barriers to lung-directed gene therapy with recombinant adenoviruses. *J. Virol.* **69,** 2004–15 (1995).

191. Yang, Y., Jooss, K. U., Su, Q., Ertl, H. C. & Wilson, J. M. Immune responses to viral antigens versus transgene product in the elimination of recombinant adenovirus-infected hepatocytes in vivo. *Gene Ther.* **3,** 137–144 (1996).

192. Koppolu, B. & Zaharoff, D. A. The effect of antigen encapsulation in chitosan particles on uptake, activation, and presentation by antigen presenting cells. *Biomaterials* **34,** 2359–2369 (2013).

193. Banchereau, J. & Palucka, K. Immunotherapy: Cancer vaccines on the move. *Nat. Rev. Clin. Oncol.* **15,** 9–10 (2017).

194. Hamburg, M. A. & Collins, F. S. The Path to Personalized Medicine. *N. Engl. J. Med.* **363,** 301–304 (2010).

195. Ford Versypt, A. N., Pack, D. W. & Braatz, R. D. Mathematical modeling of drug delivery from autocatalytically degradable PLGA microspheres - A review. *Journal of Controlled Release* **165,** 29–37 (2013).

196. Peppas, N. A. & Narasimhan, B. Mathematical models in drug delivery: How modeling has shaped the way we design new drug delivery systems. *J. Control. Release* **190,** 75–81 (2014).

197. Costa, P. & Sousa Lobo, J. M. Modeling and comparison of dissolution profiles. *Eur. J. Pharm. Sci.* **13,** 123–133 (2001).

198. Ritger, P. L. & Peppas, N. A. A simple equation for description of solute release I. Fickian and non-fickian release from non-swellable devices in the form of slabs, spheres, cylinders or discs. *J. Control. Release* **5,** 23–36 (1987).

199. Ren, D., Yi, H., Wang, W. & Ma, X. The enzymatic degradation and swelling properties of chitosan matrices with different degrees of N-acetylation. *Carbohydr. Res.* **340,** 2403–2410 (2005).

200. Li, M., Rouaud, O. & Poncelet, D. Microencapsulation by solvent evaporation: State of the art for process engineering approaches. *International Journal of Pharmaceutics* **363,** 26–39 (2008).

201. Janoria, K. G. & Mitra, A. K. Effect of lactide/glycolide ratio on the in vitro release of ganciclovir and its lipophilic prodrug (GCV-monobutyrate) from PLGA microspheres. *Int. J. Pharm.* **338,** 133–141 (2007).

202. Haber, D. a & Fearon, E. R. The promise of cancer genetics. *Lancet* **351 Suppl,** SII1-I8 (1998).

203. Finn, O. J. Cancer vaccines: between the idea and the reality. *Nat. Rev. Immunol.* **3,** 630–641 (2003).

204. Gilboa, E. DC-based cancer vaccines. *Journal of Clinical Investigation* **117,** 1195–1203 (2007).

205. Rosenberg, S. A., Yang, J. C. & Restifo, N. P. Cancer immunotherapy: moving beyond current vaccines. *Nat. Med.* **10,** 909–915 (2004).

206. Lage, A., Perez, R. & Fernandez, L. Therapeutic Cancer Vaccines: At Midway Between Immunology and Pharmacology. *Curr. Cancer Drug Targets* **5,** 611–627 (2005).

207. Gulley, J. *et al.* Phase I study of a vaccine using recombinant vaccinia virus expressing PSA (rV-PSA) in patients with metastatic androgen-independent prostate cancer. *Prostate* **53,** 109–117 (2002).

208. von Mehren, M. *et al.* Pilot Study of a Dual Gene Recombinant Avipox Vaccine Containing Both Carcinoembryonic Antigen (CEA) and B7.1 Transgenes in Patients with Recurrent CEA-expressing Adenocarcinomas. *Clin. Cancer Res.* **6,** (2000).

209. Marshall, J. L. *et al.* Phase I study in cancer patients of a replication-defective avipox recombinant vaccine that expresses human carcinoembryonic antigen. *J. Clin. Oncol.* **17,** 332–7 (1999).

210. Tukhvatulin, A. *et al.* Powerful complex immunoadjuvant based on synergistic effect of combined TLR4 and NOD2 activation significantly enhances magnitude of humoral and cellular adaptive immune responses. *PLoS One* **11,** e0155650 (2016).

211. Rosenberg, S. A. *et al.* Immunizing patients with metastatic melanoma using recombinant adenoviruses encoding MART-1 or gp100 melanoma antigens. *J. Natl. Cancer Inst.* **90,** 1894–900 (1998).

212. Marshall, J. L. *et al.* Phase I study of sequential vaccinations with fowlpox-CEA(6D)-TRICOM alone and sequentially with vaccinia-CEA(6D)-TRICOM, with and without granulocyte-macrophage colony-stimulating factor, in patients with carcinoembryonic antigen-expressing carcinomas. *J. Clin. Oncol.* **23,** 720–31 (2005).

213. Hodge, J. W., McLaughlin, J. P., Kantor, J. A. & Schlom, J. Diversified prime and boost protocols using recombinant vaccinia virus and recombinant non-replicating avian pox virus to enhance T-cell immunity and antitumor responses. *Vaccine* **15,** 759–768 (1997).

214. Hodge, J. W. *et al.* Modified Vaccinia Virus Ankara Recombinants Are as Potent as Vaccinia Recombinants in Diversified Prime and Boost Vaccine Regimens to Elicit Therapeutic Antitumor Responses. *Cancer Res.* **63,** (2003).

215. Owens, D. E. & Peppas, N. A. Opsonization, biodistribution, and pharmacokinetics of polymeric nanoparticles. *International Journal of Pharmaceutics* **307,** 93–102 (2006).

216. Frank, M. M. & Fries, L. F. The role of complement in inflammation and phagocytosis. *Immunol. Today* **12,** 322–326 (1991).

217. Bazile, D. *et al.* Stealth Me.PEG-PLA nanoparticles avoid uptake by the mononuclear phagocytes system. *J. Pharm. Sci.* **84,** 493–498 (1995).

218. Harper, G. R. *et al.* Sterie stabilization of microspheres with grafted polyethylene oxide reduces phagocytosis by rat Kupffer cells in vitro. *Biomaterials* **12,** 695–700 (1991).

219. Kelly, K. A. & Jones, D. A. Isolation of a Colon Tumor Specific Binding Peptide Using Phage Display Selection. *Neoplasia* **5,** 437–444 (2003).

220. Kim, S. M., Faix, P. H. & Schnitzer, J. E. Overcoming key biological barriers to cancer drug delivery and efficacy. *J. Control. Release* **267,** 15–30 (2017).

221. Moore, A., Basilion, J. P., Chiocca, E. A. & Weissleder, R. Measuring transferrin receptor gene expression by NMR imaging. *Biochim. Biophys. Acta - Mol. Cell Res.* **1402,** 239–249 (1998).

222. Berry, C. C., Charles, S., Wells, S., Dalby, M. J. & Curtis, A. S. . The influence of transferrin stabilized magnetic nanoparticles on human dermal fibroblasts in culture. *Int. J. Pharm.* **269,** 211–225 (2004).

223. Gupta, A. K. & Curtis, A. S. . Lactoferrin and ceruloplasmin derivatized superparamagnetic iron oxide nanoparticles for targeting cell surface receptors. *Biomaterials* **25,** 3029–3040 (2004).

224. Biology, C., Darwin, C. & Wyhe, J. Van. The International Journal of Biochemistry. *Int. J. Biochem.* **41,** 251–253 (2009).

225. Lee Josephson, Ching-Hsuan Tung, Anna Moore, and & Weissleder*, R. High-Efficiency Intracellular Magnetic Labeling with Novel Superparamagnetic-Tat Peptide Conjugates. (1999). doi:10.1021/BC980125H

226. Lewin, M. *et al.* Tat peptide-derivatized magnetic nanoparticles allow in vivo tracking and recovery of progenitor cells. *Nat. Biotechnol.* **18,** 410–414 (2000).

227. S., Y. Pullulan and its applications. *Process Biochem.* (1974).

228. Kaneo, Y., Tanaka, T., Nakano, T. & Yamaguchi, Y. Evidence for receptor-mediated hepatic uptake of pullulan in rats. *J. Control. Release* **70,** 365–373 (2001).

229. Fanger, G. O. in *Microencapsulation* 1–20 (Springer US, 1974). doi:10.1007/978-1-4684-0739-6_1

230. Mainardes, R. M. & Evangelista, R. C. PLGA nanoparticles containing praziquantel: Effect of formulation variables on size distribution. *Int. J. Pharm.* **290,** 137–144 (2005).

231. Gryparis, E. C., Mattheolabakis, G., Bikiaris, D. & Avgoustakis, K. Effect of Conditions of Preparation on the Size and Encapsulation Properties of PLGA-mPEG Nanoparticles of Cisplatin. *Drug Deliv.* **14,** 371–380 (2007).

232. Polysciences Inc. *PLGA ( Poly Lactic co-Glycolic Acid ) Uniform Dry Microspheres*. **1,** (2013).

233. Turgeon, S. L., Schmitt, C. & Sanchez, C. Protein-polysaccharide complexes and coacervates. *Current Opinion in Colloid and Interface Science* **12,** 166–178 (2007).

234. Sánchez, A., Villamayor, B., Guo, Y., McIver, J. & Alonso, M. J. Formulation strategies for the stabilization of tetanus toxoid in poly(lactide-co-glycolide) microspheres. *Int. J. Pharm.* **185,** 255–266 (1999).

## Appendix 1 : Production of PLGA with varying process parameters

### A 1.1 Introduction

Encapsulation of small molecules has been proven to be a critical formulation strategy since its initiation in the 1930s. This idea has expanded from its primary aim of protection of vitamins from oxidation[229] to a state of art technology which can encapsulate small as well as macromolecules and control their delivery to target sites. However, even today, about 40% of drugs in the pipeline of pharmaceutical companies belong to a class called 'brickdust candidates'[1]. Modulating release of the drugs, increasing their bioavailability, decreasing toxicity, overcoming the barriers encountered in the body, improving pharmacokinetics and pharmacodynamics of these drugs are just some of the ways biodegradable PLGA particles can offer solutions to using these 'brickdust' drugs. PLGA has shown immense potential as a drug delivery carrier and is FDA approved for use in sutures[84]. The release kinetics of molecules encapsulated in PLGA particles depends on the size of the particles, polymer chain density, surface properties of the particles. This study presents a modulation of the size of the particles by varying process parameters.

### A 1.2 Materials and methods

Materials:

All materials were purchased from commercial suppliers and used without further modification unless noted otherwise. Poly-lactic glycolic acid (PLGA) with lactide: glycolide ratio of 50:50 (MW 30 – 60 kDa) (inherent viscosity 0.55-0.75 dL/g), polyvinyl alcohol (PVA) (MW 30 – 70 kDa) (viscosity in water 4 - 6 cps) and dichloromethane (DCM) was of analytical grade. Deionized water used throughout the study was obtained from a Milli-Q Purelab Flex 2 water purification system (Elga LLC, Woodridge, IL).

Synthesis of PLGA particles:

PLGA particles were prepared by single emulsion method at room temperature. In brief, 2 ml solution of PLGA was added to 5 ml solution of PVA. This mixture was vortexed and sonicated to create an oil-in-

water (o/w) emulsion. This mixture was then added to 25 ml PVA in round bottom flask to keep water to oil ratio constant at 1:15. This mixture was stirred to let the DCM evaporate and harden the nanoparticles. After the stirring was completed, the particles were centrifuged at 10,000 rpm for 20 min and given four washes with DI water. The particles were suspended in 1 ml DI water and frozen at -80$^0$C overnight; then lyophilized overnight at a temperature of -105$^0$C and pressure of 0.01 mbar using a Labconco FreeZone-4.5 lyophilizer (purchased from Labconco Corporation, Kansas City, MO). These lyophilized particles were stored at -80$^0$C until further use. **Table A-1** summarizes the initial process parameters that were studied.

**Table A-1:** Process parameters used to study the size distribution of PLGA particles

| Time of reaction | Sonication amplitude | PLGA concentration | PVA concentration |
|---|---|---|---|
| 4 hours | 0 % | 1 w/v % | 0.1 w/v % |
| 72 hours | 40 % | 3 w/v % | 1 w/v % |
| | | 5 w/v % | 3 w/v % |
| | | | 5 w/v % |

Measurement of size and size distribution of PLGA particles:

The hydrodynamic diameter, polydispersity index (PDI) and surface charge (zeta potential) of composite particles are analyzed by dynamic light scattering and laser Doppler electrophoresis using Zetasizer Nano ZS (Malvern Instruments Inc., UK). The size of PLGA particles is characterized by backscatter detection (173°. Measurements were performed with particles collected after the 4$^{th}$ wash in DI water.

## A 1.3 Results

Effect of time of reaction

The effect of time of evaporation of the solvent is studied to see the result on the size of the particles. The size of the particles did not change significantly after 4 hours indicating that the solvent evaporation process is almost completed in 4 hours (**Figure A1-1**). Therefore, we used 4 hours as out time for all other synthesis' of particles.

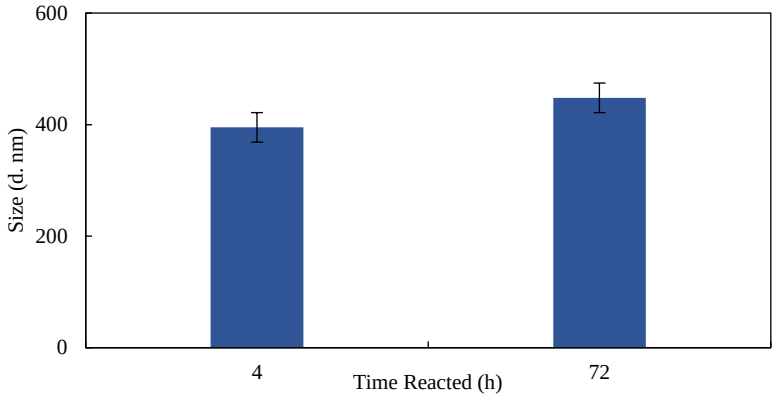


**Figure A1-1:** Effect of solvent evaporation time on size of particles

Effect of sonication amplitude

Sonication is used in this study as an energy input to create small emulsion droplets. Sonication amplitude will decide the size and size distribution of the emulsion droplets formed and optimizing this parameter is very important. Increase in energy input will lead to smaller emulsion droplets, therefore, smaller particles[230,231]. It can be seen that with no sonication we get very large particles with a wide size distribution which is likely due to the inefficient dispersion of oil and water phases (**Figure A1-2**). Additionally, it can be seen that increasing sonication amplitude resulted in small particles as well as a narrow size distribution of the particles. It should be noted that though increasing the energy input will result in the smaller size of the particles, the bioactivity/structure of the molecule to be encapsulated might get hampered due to the higher energy input. Moreover, the glass transition temperature of 50:50 PLGA is

44-55$^{0}$C[232]; using higher sonication amplitudes for longer times increases the temperature of the system which might affect the nature of the polymer.

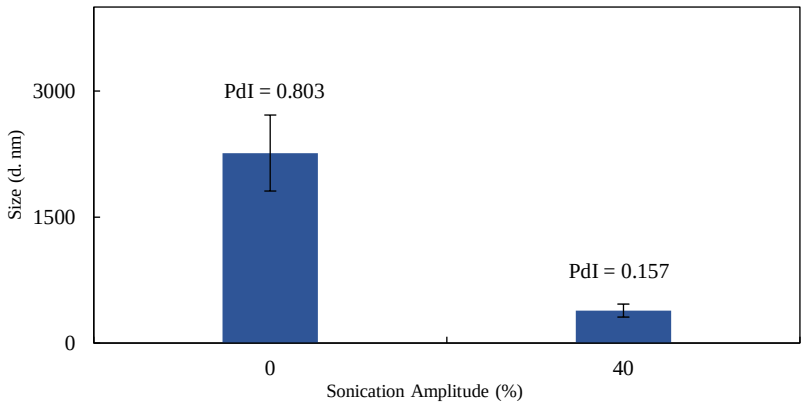


**Figure A1-2:** Effect of sonication amplitude on size and size distribution of particles.

Effect of varying polymer concentration (oil phase)

Polymer concentration has an effect on the viscosity of the oil phase and also the internal tortuosity of the PLGA particles[129,159]. Increasing the PLGA concentration increases the viscosity of o-phase, and therefore higher energy is required to break this oil phase into small emulsion droplets. Therefore, at the same energy input to the system, an increase in viscosity will lead to an increase in the size of the emulsion droplets and hence increase in the size of the particles[64,157,159]. This increase in polymer concentration also leads to an increase in internal density of the particles and high tortuosity[159]. It was observed that an increase in polymer concentration leads to the larger size of the particles (**Figure A1-3**). This increase in tortuosity will lead to higher resistance for diffusion of encapsulated molecules in these particles possibly leading to slow release[129,196,233].

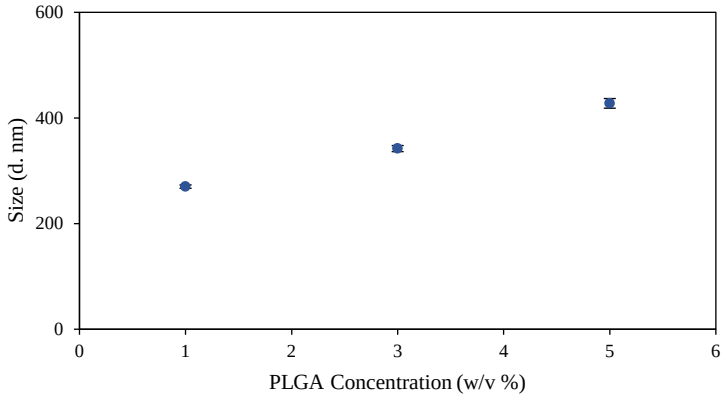


**Figure A1-3:** Effect of PLGA concentration on size of the particles

Effect of changing surfactant concentration (water phase)

Once the water in oil emulsion is formed, its tendency towards coalescence depends on efficiency of stabilizing mechanisms such as (i) static stabilization, i.e., electrostatic forces due to the droplets surface charge (by adsorbed ions, ionic surfactants, or polymer carboxylate groups introduced in the water phase) and/or steric repulsion due to adsorbed surface-active polymers (e.g., PVA) or solid particles that theoretically form a mechanic barrier prohibiting droplet approaching[78]. Increasing the PVA concentration is known to result in smaller particles due to low interfacial tension at the surface of the emulsion droplets[78,234]. It was observed that increasing PVA concentration led to the production of smaller particles (**Figure A1-4**). But when the PVA concentration is increased beyond 6 w/v%, it results in larger particles. This could be due to the residual PVA left on the particles or due to the high viscosity of the surfactant that causes the emulsion droplets to aggregate giving us larger particles[107].

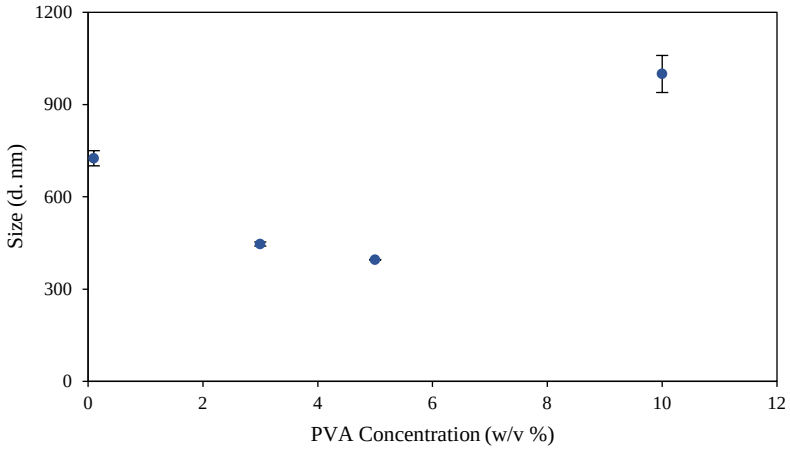


**Figure A1-4:** Effect of surfactant concentration on the size of particles

## Appendix 2 : Standard Curves for qPCR

Specific primer finding tool developed by NIH (Bethesda, MD) is utilized to confirm alignment and length of product formed between Ad-eGFP and Ad-flu primers with the respective adenoviral vector. The primers are found to be specific to the adenoviral sequences using the NIH tool. For Ad-eGFP, the length of the final product formed is 292 nucleotides whereas for Ad-flu it is 144 nucleotides. The standard curves developed are shown in **Figure A2-1** and **Figure A2-2**.

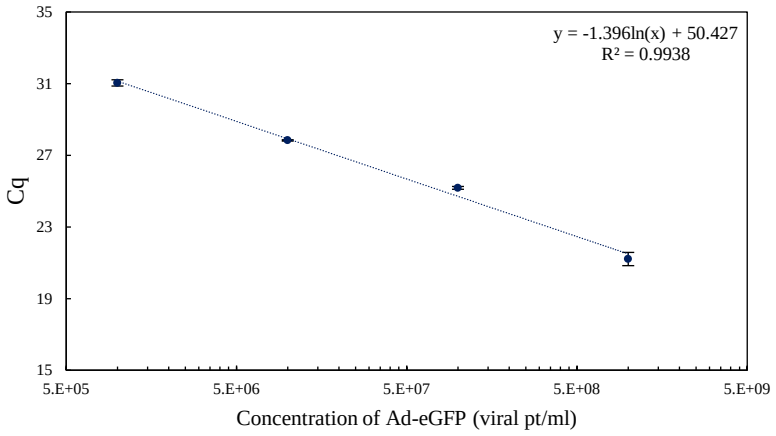


**Figure A2-2:** Ad-eGFP standard curve

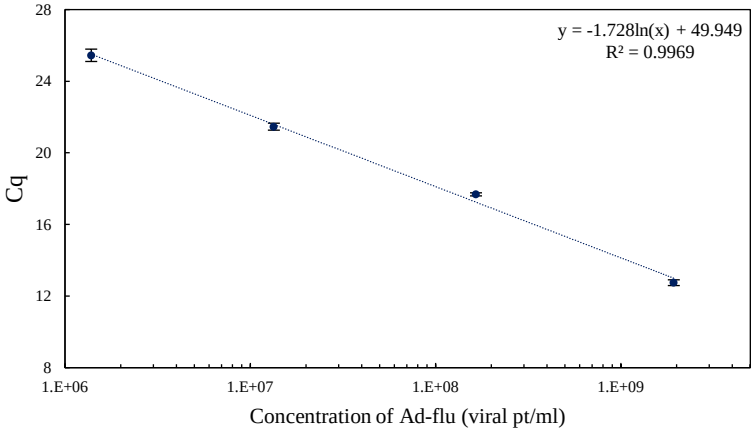


**Figure A2-2:** Ad-flu standard curve